Wildfire effects on net precipitation, streamflow regime and rainfall-runoff events in northern Rocky Mountain watersheds

by

Christopher Hart Stanley Williams

A thesis submitted in partial fulfillment of the requirements for the degree of

Doctor of Philosophy

in

Water and Land Resources

Department of Renewable Resources
University of Alberta

Abstract

In recent decades, severe wildfire in western North America has increased in frequency as a result of a warming climate and historical fire suppression, impacting an increasing amount of forested area. Reduced forest canopy interception and storage combined with soil water repellency and altered soil structure after wildfire can lead to greater runoff responses than in unburned forests. This has led to a proliferation of post-wildfire hydrological studies, mostly at the plot and hillslope scales, and mainly located in heavily impacted regions of the USA (e.g. Colorado, New Mexico, California). However, the more northern Rocky Mountain regions have also been subjected to warming and increased risk of wildfire. The eastern slopes of the Canadian Rocky Mountains provide a disproportionate amount of vital surface water supplies to the Prairie Provinces largely owing to high overwinter snow accumulation. Much less is known about post-wildfire hydrology and runoff response in these more northern, snow-dominated mountain regions. This study examined impacts from the 2003 Lost Creek wildfire on net precipitation, flow regimes, and storm rainfall-runoff events in Rocky Mountain watersheds in the Crowsnest Pass, Alberta, Canada.

Net precipitation was studied in subalpine forest stands while flow regimes and storms were studied at the watershed scale. Four subalpine forest stands (two burned and two unburned reference) were used to measure rainfall interception and snow accumulation (SWE); net precipitation was derived from these measurements for the study period (2005-2014). Mean net precipitation was 274 mm (51%) greater in burned than in unburned reference forest stands. Greater mean snow accumulation (SWE) and net rainfall, respectively, constituted 152 and 122 mm of this total. Studies focused on post-wildfire flow regimes at varying time intervals (annual, monthly, weekly) were conducted

during the 2^{nd} to 11^{th} years (2005-2014) after the wildfire. Streamflow and precipitation were measured in three burned and two unburned reference watersheds in a replicated post-hoc study design to enable comparisons. Flow regime studies highlighted greater magnitude and earlier timing of snowmelt runoff in wildfire-affected watersheds – April and May water yields were 100-200% and 40-50% higher, respectively, and half-flow dates arrived approximately 7-10 days earlier in burned compared to reference watersheds. The effects of wildfire on storm runoff during the snow-free season (late June to late September) was more ambiguous but flow responses in burned watersheds were proportionally greater, in general, than those in reference watersheds. However, post-wildfire storm runoff was surprisingly muted compared to that from other wildfire-affected regions and multiple regression analysis suggested fire accounted for <4% of the overall variability in runoff response. Despite greater net rainfall and snow accumulation at the forest stand level, effects to components of the flow regime and to storm runoff in burned watersheds were not large in comparison to results from studies in other regions.

Preface

This thesis is original work by Christopher Williams and was completed under the supervision of Dr. Uldis Silins. Research conducted for this thesis is part of the Southern Rockies Watershed Project (SRWP), an international collaboration led by Dr. Silins.

For Chapter 2, Dr. Silins led conceptualization of the study design and assisted with field data collection, data analysis, writing and editing. Michael Wagner assisted with study design conceptualization, field data collection, data analysis and editing. Dr. Sheena Spencer assisted with data analysis, writing and editing. SRWP field crews helped with field data collection during 2006-2008. Drs. Micheal Stone and Monica Emelko helped secure funding for the research and provided editorial feedback. I led field data collection, data analysis, writing, revisions and assisted with study design conceptualization.

Chapter 2 of this thesis has been published as ‘Williams, C. H. S., Silins, U., Spencer, S. A., Wagner, M. J., Stone, M., & Emelko, M. B. (2019). Net precipitation in burned and unburned subalpine forest stands after wildfire in the northern Rocky Mountains. *International Journal of Wildland Fire*, *28*(10), 750-760’

Dedication

This thesis is dedicated to my grandparents – Guy & Marie Williams and Stanley & Marjorie Therou. Their acreages were my introduction to trees and water, and their natural inclination to conserve resources was a vital lesson. Their kindness and patience will always be remembered.

Acknowledgements

This thesis represents the culmination of a nearly two-decade journey for me, personally, but its completion would not have been possible without determined efforts from many organizations and individuals. I gratefully acknowledge the funding sources for this research: Alberta Agriculture and Forestry, Alberta Innovates Bio Solutions, Alberta Innovates Energy and Environment Solutions, and the Foothills Research Institute. I owe a debt of gratitude to my long-time supervisor and friend, Uldis Silins, for his years of mentorship, kindness, patience, and enthusiasm for the science of forest hydrology. It was a pleasure working with Uldis and given the inertia of big ideas like the Southern Rockies Watershed Project (SRWP), I hope our collaborative efforts continue to move more scientific contributions through to the finish line. I would also like to thank the other members of my supervisory committee, Rita Winkler and Axel Anderson, for their critical input to this work. Additionally, I'd like to acknowledge Dave Scott and Carl Mendoza, my external examiners, for their keen insights during my thesis defence. I'd also like to thank Kevin Bladon, Mike Stone and Monica Emelko for their many years of support, encouragement, friendship and their contributions to both my work and SRWP.

I must also thank the legions of SRWP technicians with whom I've worked shoulder-to-shoulder from 2006-2022. It was a pleasure to do fieldwork, cook and head to the Rum Runner with these folks and some have become lifelong friends. In particular, I'd like to acknowledge Michael Wagner, Ian Tichkowsky, Jeremy Fitzpatrick, Eddie Noton, Amanda Martens, Kirk Hawthorn, Evan Esch, Kalli Herlein, Mike Pekrul, Erin Cherlet and Paul Leonard. I've spent many, many hours with this stand-up cast of characters talking hydrology, grinding out miles on backcountry trails, and/or slugging pints at the Empress Ale House (rest in peace friendly neighbourhood pub).

Finally, I would like to thank my family for all their love and support during this long endeavour, particularly my partner Sheena who not only provided critical input at every stage of this process, but she also endured a fair bit of thesis-related ranting, raving and procrastination. Mom, Dad, Michelle (sis), and Aaron (bro) have been the bedrock underlying my journey along with Jerry, Wayne, Kelty, Zac, Olive and several very supportive aunts, uncles and cousins – a heartfelt thanks to all of you.

Table of Contents

Abstract ii

Preface iv

Dedication v

Acknowledgements vi

Table of Contents vii

List of Tables xi

List of Figures xii

Chapter 1. Introduction 1

1.1. Rainfall Interception and Snow Accumulation 1

1.2. Streamflow Regime 2

1.3. Post-wildfire recovery 5

1.4. Wildfire and Hydrologic Change Detection 5

1.5. Wildfire research in the northern Rocky Mountains 8

1.6. Study Objectives 8

1.7. Figures 11

Chapter 2. Net precipitation in burned and unburned subalpine forest stands after wildfire in the northern Rocky Mountains 12

2.1. Introduction 12

2.2. Materials and Methods 14

2.2.1. Study Site Description 14

2.2.2. Study approach 16

2.2.3. Throughfall (2006-2008) 16

2.2.4. Stemflow (2006-2008) 16

2.2.5. Net rainfall (2005-2014) 17

2.2.6. Snow Accumulation 17

2.2.7. Net Precipitation 18

2.3. Results 18

2.3.1. Net Rainfall 2006-2008 18

2.3.2. Net rainfall (2005-2014) 19

2.3.3. Net Snow Accumulation (2005-2014) 19

2.3.4. Net precipitation (2005-2014) 20

2.4. Discussion 20

2.4.1. Net rainfall and throughfall 21

2.4.2. Stemflow 22

2.4.3. Snow Accumulation 22

2.4.4. Net Precipitation 24

2.5. Tables 26

2.6. Figures 29

Chapter 3. Investigation of Flow Regime for a Decade Following Wildfire in Rocky Mountain Watersheds, Alberta, Canada. 35

3.1. Introduction 35

3.2. Methods and Materials 38

3.2.1. Study Site Characteristics 38

3.1.1. The Lost Creek Wildfire and Study Design 39

3.1.2. Streamflow 40

3.1.3. Precipitation 41

3.1.4. Water Quality 41

3.1.5. Data Analysis 42

3.3. Results 43

3.3.1. Climate Across Study Period 43

3.3.2. Annual Precipitation-Runoff Relationships and Water Yield 44

3.3.3. Streamflow Magnitude During Snowmelt (Apr.-Jun.) and Low Flow (Jul.-Sept.) Periods 45

3.3.3.1. Snowmelt Water Yield (April to June) 45

3.3.3.2. Low Flow Water Yield (July to September) 46

3.3.4. Streamflow Timing 46

3.3.5. Evidence of Hydrologic Recovery? 48

3.4. Discussion 50

3.4.1. Annual Water Yield: Muted Effects of Wildfire 50

3.4.2. Snowmelt (Apr. to Jun.) Magnitude and Timing 52

3.4.3. Low Flow Period (Jul. to Sept.) 53

3.4.4. Hydrologic Recovery 54

3.4.5. Uncertainty Within LP and HP Watershed Groups 55

3.5. Key Findings 57

3.6. Tables 59

3.7. Figures 62

Chapter 4. Rainfall – storm runoff relationships after wildfire over a 10-year period in Rocky Mountain watersheds, Alberta, Canada 71

4.1. Introduction 71

4.2. Methods and Materials 73

4.2.1. Study Site 73

4.2.2. Precipitation 74

4.2.3. Streamflow 74

4.2.4. Rainfall and Runoff Variables 75

4.2.5. Data Analysis 76

4.2.6. Multiple Linear Regression 77

4.3. Results 77

4.3.1. Rainfall 77
4.3.2. Quickflow, Event Rise and Runoff Coefficients (2005-2014) 77
4.3.3. Runoff Response Early After Wildfire 78
4.3.4. Rainfall Intensity (I30) 79
4.3.5. Basin Lag and Rise Time 80
4.3.6. Factors Explaining Post-Wildfire Stormflow Response 80
4.4. Discussion 81
4.4.1. Near-surface versus Deeper Hydrologic Pathways 81
4.4.2. Runoff Magnitude During Rain Storms and Comparison with Previous Studies 82
4.4.3. Diminished Importance of Rainfall Intensity ($I30_{max}$) During Dry Season 84
4.4.4. Antecedent Watershed Conditions 85
4.4.5. Timing Metrics 86
4.5. Conclusions 87
4.6. Tables 88
4.7. Figures 93
Chapter 5. Synthesis 100
5.1. Summary of Key Findings 100
5.2. Implications 101
5.3. Limitations 103
5.4. Recommendations for Future Research 103
References 106

List of Tables

Table 2.1. Stand attributes in rainfall and snow measurement sites. Plots were measured after the wildfire. Area of fixed plots varied (63-314 m^2) with the objective of including a minimum of 40 sampled trees. Trees ≥1.3 m in height were included in fixed area plot surveys. [A]Upper quartile range. [B]Gap Light Analyzer version 2.0 (Frazer et al. 1999). 26

Table 2.2. Rainfall and snowfall in burned and reference stands. Gross and net a) rainfall (R_N), and b) snowfall and SWE (S_A) in burned and reference stands during 2005-2014. R_N calculated using the event-based relations developed during 2006-2008 measurement period. 27

Table 2.3. Difference in net precipitation. Gross precipitation (P_g) and surplus in net precipitation (P_N) in burned stands compared to reference stands (2005-2014). 28

Table 3.1. Watershed characteristics. "Alpine Area" includes exposed bedrock, talus, open meadow and shrubland. Aspect information pertains, conceptually, to low (N; North), neutral (E+W; East + West), and high (S; South) solar energy inputs. Low precipitation (LP) and high precipitation (HP) watershed groups indicated in Watershed column. 59

Table 3.2. Water year (Oct 1 – Sept 30) precipitation (P), water yield (Q) and runoff coefficient (C_R) for the study watersheds. Drum streamflow data were not available for 2007 because of stage sensor malfunction. Runoff ratios equal to or >1 likely contain relatively large errors and are highlighted in red. Low precipitation (LP) and high precipitation (HP) watershed groups indicated above stream names. 60

Table 3.3. Daily flow exceedance values (mm) at the 10%, 25%, and 50% thresholds during April-September for the study watersheds across the study period. Values come from flow duration curves produced for 2005-2014 study period (Figure 3.7). Low precipitation (LP) and high precipitation (HP) watershed groups indicated in Stream column. 61

Table 4.1. Predictor (P) and response (R) variables for precipitation and runoff calculated for each storm event. 88

Table 4.2. Median (range) of rainfall and runoff variables across all five watersheds (2005-2014). The variables are: total event precipitation (P_{tot}), maximum 30-minute rainfall intensity ($I30_{max}$), precipitation event duration (P_{dur}), event quickflow (Q_e), event rise (Q_Δ), runoff coefficient (C_r), basin lag (T_{lag}), and rise time (T_r). 89

Table 4.3. Rainfall-runoff variables for a >20 mm event in August, 2005 for the high precipitation (HP) watersheds. 90

Table 4.4. Results of multiple regression model predicting the transformed runoff response variables. Predictors are total event precipitation (P_{tot}), 30-minute maximum rainfall intensity ($I30_{max}$), pre-event streamflow (Q_{pre}), and a dummy variable (FIRE) indicating burned or reference watershed. Significance codes: *** (p=0 – 0.001), ** (p=0.001 – 0.01), * (p=0.01 – 0.05). 91

Table 4.5. ANOVA tables for each of the runoff variables used in multiple regression analysis. Top: runoff coefficient (C_r); middle: quickflow (Q_e); bottom: event rise (Q_Δ). 92

List of Figures

Figure 1.1. Schematic overview of Chapters 2 to 4. Studies for Chapter 2 were completed at the stand scale in burned and unburned subalpine forest while those for Chapters 3 and 4 were done at the watershed scale and included insights from three burned and two unburned reference watersheds. Studies for Chapter 3 focused on potential wildfire effects across the seasonal flow regime while those for Chapter 4 focused specifically on rainfall-runoff (storm) events during the snow-free part of the year. 11

Figure 2.1. Main image: Rainfall interception and snow accumulation stands shown on orthophoto of the study area. Thick black line shows burn boundary at northern edge of Lost Creek wildfire. Middle-left inset: Larger unburned watershed is North York while the smaller wildfire-impacted watershed is South York. Hatched box shows the study site area depicted in the orthophoto. 29

Figure 2.2. Typical hemispherical photographs showing canopy structure in burned and reference stands. (a) reference snow course, (b) burned snow course, (c) reference throughfall trough and (d) burned throughfall trough. 30

Figure 2.3. Average monthly precipitation and air temperature during period of study (2005-2014) measured at South York climate station. 31

Figure 2.4. Relationships between throughfall (T_f), stemflow (S_f) and canopy interception (I_C) in the reference stand (left) and burned stand (right) with gross rainfall (R_G) during the three-year measurement period (2006-2008). 32

Figure 2.5. Relationship between gross rainfall (R_G) and canopy interception (I_C) in burned and reference stands during the three-year measurement period (2006-2008). 33

Figure 2.6. Snow accumulation (S_A) on the snow courses from 2005-2014. Top: Average snow depth at time of measurement indicated by dark grey (burned) and open (reference) circles. Continuous snow depth (recorded in clearing at North York station) indicated by the light grey line. Bottom: Boxplots of annual snow water equivalent near date of peak SWE. Median indicated by the solid line in the boxplots. Box represents 25th and 75th percentiles, whiskers represent 10th and 90th percentiles, and dots are outliers. 34

Figure 3.1. Map of study watersheds situated near the northern extent of the 2003 Lost Creek wildfire. Star Ck. (reference) and Drum Ck. (burned) represent the low precipitation (LP) group. North York Ck. (reference), South York Ck. (burned) and Lynx Ck. (burned) represent the high precipitation (HP) group. 62

Figure 3.2. Water year precipitation (a) and water yield (b) for each of the study watersheds. In the legend, "R" indicates unburned reference watersheds and "B" indicates burned watersheds. Triangles are used for "high precipitation" (HP) watershed group and circles for "low precipitation" (LP) watershed group in figures. 63

Figure 3.3. Left panel (a): Water year (Oct. 1 – Sept. 30) runoff coefficients (C_r) for reference (R) and burned (B) watersheds across the study period (2005-2014). Right panel (b): Half flow dates for each stream across the study period. The half flow date is defined as the Julian day upon which half

of the calendar-year streamflow has passed the gauging station. Low precipitation (LP) and high precipitation (HP) watershed groups indicated below each boxplot. Median indicated by horizontal line inside each box. Upper and lower hinges indicate 25th and 75th percentiles. Upper and lower whiskers extend to the highest (or lowest) value that is within 1.5 * IQR of the hinge. Outliers indicated by black points. 64

Figure 3.4. Relationship between water year (Oct. 1 – Sept. 30) precipitation and water yield for all watersheds across a) all study years (2005-2014); b) the first 5 years of study (2005-2009); c) the last 5 years of study (2010-2014). Circles indicate low precipitation (LP) watershed group and triangles indicate high precipitation (HP) group........ 65

Figure 3.5. Water yield from burned watersheds in comparison with that from unburned reference watersheds for the snowmelt (April to June) and low flow (July to September) periods across the study (2005-2014). Left-hand plots show relationships during the snowmelt period for: a) high precipitation (HP) watersheds using North York Ck. as reference and; b) low precipitation (LP) watersheds using Star Ck. as reference. Right-hand panels show relationships during the low flow period for: c) HP watersheds and d) LP watersheds using same references as snowmelt period. Red dashed line is the 1:1 relation for comparison. 66

Figure 3.6. Mean monthly water yield during ice-free season (Apr. – Oct.) in the five study watersheds: a) low precipitation (LP) watershed group during first 5 years (2005-2009); b) high precipitation (HP) watershed group during first 5 years (2005-2009); c) low precipitation (LP) watershed group during last 5 years (2010-2014); d) high precipitation (HP) watershed group during last 5 years (2010-2014). In legend, (R) and (B) symbolize reference and burned watersheds, respectively. Error bars indicate standard deviation. 67

Figure 3.7. Flow duration curves for daily water yield (Apr. to Sept) for reference and burned watersheds across the study period (2005-2014). Low precipitation (LP) group on left, high precipitation (HP) group on right........ 68

Figure 3.8. Bottom graphs: Mean weekly water yield over the ten years of study (2005-2014) during the ice-free part of the year, generally encompassing week 14 (Apr. 2-8) through week 42 (Oct. 16-22). Top graphs: Residual differences in mean weekly water yield between burned and reference catchments of similar annual precipitation (values >0 indicate more yield in burned relative to reference watershed). Low precipitation (LP) watershed group on the left, high precipitation (HP) group on the right. Error bars indicate standard deviation........ 69

Figure 3.9. Potassium:Silica (KSi) ratios for each stream during the first 5 years (2005-2009; top panels a-c) and last 5 years (2010-2014; bottom panels d-f) of data collection following the wildfire (2003). Median indicated by horizontal line inside each box. Upper and lower hinges indicate 25th and 75th percentiles. Upper and lower whiskers extend to the highest (or lowest) value that is within 1.5 * IQR of the hinge. Outliers indicated by black points. In legend, reference streams indicated with (R) and burned with (B). “LP group” indicates low-precipitation watersheds and “HP group” indicates high-precipitation watersheds. Uppercase letters (A-D) above boxplots indicate statistical significance – streams with identical letters (within same panel) are not significantly different from one another. Columns (left, middle, right, respectively) depict 1) all data for snowmelt and low flow period combined; 2) snowmelt (Apr. to Jun.); 3) low flow period (Jul. to Sept.)........ 70

Figure 4.1. Schematic depiction of hydrograph separation for a rainfall-runoff event showing the main streamflow variables; Q_Δ (event rise) and Q_e (quickflow). The constant slope (CS) line was derived using the baseflow separation method of Hewlett and Hibbert (1967). 93

Figure 4.2. Regression relationship between log10 total event precipitation (P_{tot}) and log10 quickflow (Q_e) during summer rain storms across complete study period (2005-2014). Top plot shows low precipitation (LP) group and bottom plot shows high precipitation (HP) watershed group. Reference and burned watersheds indicated by (R) and (B) in legend, respectively. 94

Figure 4.3. Regression relationship between log10 total event precipitation (P_{tot}) and log10 event rise (Q_Δ) during summer rain storms across complete study period (2005-2014). Top plot shows low precipitation (LP) group and bottom plot shows high precipitation (HP) watershed group. Reference and burned watersheds indicated by (R) and (B) in legend, respectively. 95

Figure 4.4. Boxplots for each watershed across the study period (2005-2014) showing a) the runoff coefficient (C_r), b) basin lag (T_{lag}), and c) rise time (T_r). Low (LP) and high (HP) precipitation groups indicated below panels. The boundary of the box closest to zero indicates the 25th percentile, a line within the box marks the median, and the boundary of the box farthest from zero indicates the 75th percentile. Whiskers (error bars) above and below the box indicate the 90th and 10th percentiles. ... 96

Figure 4.5. A comparison of matched post-wildfire rainfall-runoff events during an early period (2005) and later period (2011-2012) for the high precipitation (HP) watersheds: North York Ck. (reference), Lynx Ck. (burned), and South York Ck. (burned). Solid regression lines are for 2005 and dashed lines are for 2011-2012. 97

Figure 4.6. Runoff responses for a >20 mm rainfall event which occurred August 11-12, 2005 (2nd year after wildfire) in the high precipitation (HP) study watersheds. Rainfall and runoff variables are detailed in Table 4.3 for this storm. Sloping dotted lines represent the constant-slope baseflow separation line (Hewlett and Hibbert 1967). 98

Figure 4.7. Relationship between rainfall intensity (I30max) and runoff event rise (Q_Δ). The three HP watersheds are shown in the left panels and the two LP watersheds are shown in the right panels. 99

Chapter 1. Introduction

Wildfire is a common natural disturbance agent in western North America and one of the main drivers of changes to forest cover. In recent decades, however, wildfire frequency, annual area burned and fire season length have increased across large areas (Hanes et al. 2019; Westerling et al. 2016). The effects of wildfire on water supplies, particularly from mountain headwaters, can be profound. Many changes to hydrology and water quality can occur including increased annual water yield and storm flows, shifts in aquatic ecology (e.g. algae, invertebrates, fish), increased stream temperature and nutrient exports, and degraded water quality which can lead to drinking water treatment challenges (Helvey 1980; Moreno et al. 2020; Wagner et al. 2014; Silins et al. 2014; Martens et al. 2019; Schindler et al. 1980; Bladon et al. 2008; Emelko et al. 2011). The Rocky Mountain headwaters are also home to threatened species such as Westslope Cutthroat Trout (*Oncorhynchus clarkii lewisi*) (Fisheries and Oceans Canada 2014) and changes in streamflow could have negative consequences on these, and other, fish species. These pressures are driving a need to better understand hydrological changes after wildfire in mountainous, snow-dominated systems.

Research on the hydrological effects of wildfire started over 80 years ago, but began to proliferate in the early 2000s in response to an increasing frequency of severe wildfires in several parts of the world, particularly the western USA and Australia (Westerling et al. 2006; Adams 2013; Moody et al. 2013; Dennison et al. 2014; Fairman et al. 2016). However, while snow-dominated and mountainous regions such as western Canada have experienced similarly aggressive wildfires over the past two decades (Coogan et al. 2019), there remains a paucity of basic post-wildfire hydrologic research in these environments at all spatial scales.

1.1. Rainfall Interception and Snow Accumulation

Previous research has shown that wildfire can affect several hydrologic processes in forested regions such as precipitation interception, evapotranspiration, and infiltration (Onodera and Van Stan 2011), which can contribute to higher streamflow in burned watersheds. Large reductions in understory and litter interception of precipitation can occur depending on the severity of the wildfire (Neary et al. 2005; Moody et al. 2013). Fire effects on forest canopies can range from the scorching of tree needles, which may turn red and eventually fall to the ground, to complete removal of foliage and branches over hundreds of square kilometres (Neary et al. 2005). The reduced interception associated with tree loss can allow much more precipitation to reach the forest floor than prior to the disturbance

(Moore et al. 2008; Burles and Boon 2011). Particularly severe fire can also burn much of the organic layer from the forest floor, leaving widespread areas of bare rock or mineral soil, reducing surface roughness and opportunities for depression storage (Moody et al. 2013).

While mountainous regions often receive very high annual precipitation, a large proportion can be intercepted by forest canopies and lost from the water budget because much of it evaporates before reaching the forest floor (Carlyle-Moses and Gash 2011). Interception efficiency largely depends on forest attributes such as leaf area index, canopy closure, and forest structure (Hedstrom and Pomeroy 1998; Llorens and Gallart 2000). Forest canopies in the higher elevation regions of the Canadian Rockies are predominantly coniferous or needleleaf, which have been shown to intercept 20-45% of season-long or annual rainfall (Carlyle-Moses and Gash 2011). Thus, more severe crown fires can potentially cause large increases in precipitation reaching the forest floor. Despite this, the author is aware of only two previous studies that have measured rainfall interception in burned forests (Mitsudera et al. 1984; Moore et al. 2008). Similarly, healthy forest canopies play a key role in regulating both snow accumulation and ablation (Varhola et al. 2010) where sublimation of intercepted snow can account for 10 to 45% of seasonal snowfall (Pomeroy and Gray 1995). The interception of snowfall by forest canopies is more difficult to measure than rainfall; snow interception losses are usually inferred from differences in snowpack accumulation or snow water equivalent (SWE) under forest canopies to those in nearby clearings or openings (Boon 2009; Winkler 2011). Measurements of snow accumulation in wildfire-affected forests are more common than those for rainfall. For example, Winkler (2011) observed 25% greater 5-year mean SWE in a burned stand (170 mm SWE) compared to a mature mixed lodgepole pine/Engelmann spruce/subalpine fir reference stand (136 mm SWE) in interior British Columbia. Overall, however, there have been exceedingly few studies on rainfall interception and snow accumulation in burned forests. Given the high potential for wildfire to increase net precipitation and subsequent hydrologic forcing in Rocky Mountain settings, a much better understanding of fire effects on on these important hydrologic processes is needed.

1.2. Streamflow Regime

Potential changes in net precipitation could impact the broader post-wildfire flow regime at the watershed scale. Impacted elements of the flow regime could include annual water yield, snowmelt magnitude and timing, the summer low flow period, and storm runoff. Many forest harvesting studies have repeatedly shown loss of forest cover increases annual water yields but the magnitude of change is highly variable (Bosch and Hewlett 1982; Stednick 1996). For example, forest harvesting has been shown to increase annual water yield from 0.25 mm to over 3 mm for every percent of area harvested in a watershed (Moore and Wondzell 2005). While there are far fewer studies on water yield from wildfire-impacted watersheds, changes have also been shown to be extremely variable with some examples of pronounced change. For example, three watersheds (4.7 to 5.6 km^2) impacted by wildfire in Washington in 1970 experienced increases in annual runoff of 150-202% during the first 7 post-fire years (Helvey 1980; Niemeyer et al. 2020). Most studies have been done in small to medium sized watersheds, but one study also showed elevated post-wildfire water yield in a relatively large basin (~4800 km2) (Wine and Cadol 2016). Two Canadian studies in similar environments have suggested relatively subdued increases in annual streamflow after wildfire (Owens et al. 2013; Pomeroy et al. 2012). Another previous study found larger increases, but acknowledged precipitation differences complicated analysis (Mahat et al. 2016). Thus, the effects of wildfire on annual water yield in northern Rocky Mountain systems are still far from being well-understood. Additionally, even if very little water yield change appears to have occurred at the annual time step, it is possible for significant changes to occur during key parts of the flow regime as seen after forest harvesting (Winkler et al. 2017). However, these changes in flow regime have not been extensively addressed in wildfire affected snow-dominated watersheds.

The snowmelt period is an extremely important element of the flow regime in snow-dominated regions. While greater snowpack has been observed in burned forests, increased shortwave radiation because of the loss of canopy cover and lower albedo, owing to charred, black surfaces can cause faster melting (Burles and Boon 2011; Gleason et al. 2013). These changes suggest a larger snowpack at the watershed scale could melt quicker in burned forests which could affect the magnitude of snowmelt runoff during the spring period. Pomeroy et al. (2012) modeled an approximate 45% increase in streamflow during the snowmelt period after simulation of wildfire in a Rocky Mountain watershed. Earlier snowmelt also suggests a potential shift in the seasonal hydrograph to earlier in the season. This is consistent with observations of 1-2 week earlier arrival of peak flows in the burned Fishtrap Creek watershed in British Columbia in comparison to an unburned reference watershed (Owens et al. 2013). However, there remains very little information on effects to the snowmelt period associated with wildfire in snow dominated areas.

Following forest disturbance, summer low flows are frequently observed to be higher in the subsequent years. However, both the direction and magnitude of change are highly variable (Goeking and Tarboton 2020). To the author's knowledge, no post-wildfire evidence on the summer low flow period exists for Canadian Rocky Mountain watersheds. However, clear-cutting 20% of the Rocky Mountain Cabin Creek watershed suggested 10-15% greater low flows during August, September and October, though this was not statistically significant (Swanson et al. 1986). In contrast, post-wildfire low flow volume in southern California watersheds increased dramatically from pre-fire values (Kinoshita and Hogue 2015). Given the importance of summer low flows in southern Alberta rivers for values such as agricultural irrigation, human consumption, and environmental flow needs, fundamental information is needed on the low-flow period after wildfire.

The potential for post-wildfire increases in the magnitude of peak flows and floods has been documented since at least as far back as the 1930s and 1940s (Rowe et al. 1949). In addition to reductions in canopy interception, wildfire causes several changes to the forest floor and soil surface which can enable these effects to storm runoff. Very early after fire, an ash layer often exists across the burned landscape which can be effective at absorbing and storing rainfall (Ebel et al. 2012). However, precipitation and wind generally diminish this layer quickly, leaving bare mineral soil and rock. Further, infiltration can be hampered by soil water repellency (SWR) and changes to soil structural properties (Benavides-Solario and MacDonald 2005; Larsen et al. 2009). These changes can cause increased infiltration-excess overland flow which can, in turn, lead to substantial increases in storm runoff (Scott and Van Wyk 1990; Moody and Martin 2001). SWR, in particular, is widely thought to be one of the primary causes of short-term increases in surface runoff in burned areas. However, predicting the effects of SWR remains very difficult because high natural (unburned) levels of water repellency exist in some regions (Doerr et al. 2009). Moreover, extreme high temperatures associated with wildfire can actually destroy rather than cause SWR (Debano 2000). In extreme cases, the combined fire effects to land surface cover can cause flash flooding and debris flows which can have serious implications for human life and property (Cannon et al. 2008; Jordan 2015). Often, rainfall-runoff studies have been undertaken at the plot or hillslope scale (Moreno et al. 2020) at least in part because watershed scale studies are resource-intensive and difficult to set up and maintain. Existing watershed-scale studies show peak flow, quickflow and runoff ratios can increase significantly in post-wildfire landscapes because of the aforementioned effects to hydrologic processes (e.g. Campbell et al. 1977; Scott and Van Wyk 1990; Moreno et al. 2020). The timing of rainfall-runoff event water has also been shown to be affected following both harvesting and wildfire, generally reaching streams faster (i.e. decreasing lag times) (Wright et al. 1990; Neary et al. 2005; Cydzik and Hogue 2009). However, most of the studies examining post-wildfire storm runoff focus on the first 1-2 years after fire because this period often encapsulates some of the largest post-fire effects.

1.3. Post-wildfire recovery

Recovery of post-wildfire runoff depends strongly on the regrowth of vegetation which aids the restoration of interception and infiltration properties (Cerda and Doerr 2005). Thus, depending on local climate and plant species, recovery timelines likely vary considerably from region to region. Some recovery of short-term processes, such as SWR, can be expected during the first year or two after fire. However, others which are unlikely to recover quickly include canopy interception, transpiration and energy balance components which are largely governed by forest cover. The northern Rocky Mountains are known for colder climates and slow growth rates which suggests these processes could remain affected for many post-wildfire years. Moreover, the expectation of a return to pre-fire levels of forest density or tree species composition may not be reasonable because severe fire or erosive conditions (e.g. intense rain or wind) early after fire can destroy or remove seed banks, potentially setting a new trajectory toward more open-forest conditions (Stevens-Rumann and Morgan 2019). Thus, net precipitation could be affected for many years in wildfire-affected forest which eventually could increase soil and groundwater recharge. This would be expected to lead to wetter antecedent conditions until transpiration rates approached pre-fire levels. However, better penetration of shortwave radiation and substantial blackened surface area in burned forest could lead to higher evaporation rates. This could cause faster soil drying across burned landscapes. Thus, the magnitude and timing of runoff is dependent on the strength of recovery across an array of hydrologic processes, many of which are still not well understood. Because most studies have investigated only the initial post-fire period not much is known about longer term recovery of runoff, though recent studies are starting to focus on this in other environments (Niemeyer et al. 2020; Wagenbrenner et al. 2021). Recovery of watershed scale runoff remains a key question in many regions including the northern Rocky Mountains.

1.4. Wildfire and Hydrologic Change Detection

A common challenge associated with the detection of post-wildfire hydrologic change is a lack of control over the location and timing of wildfire which limits the ability to capture pre-disturbance data. Approaches to study design for hydrologic research include experimental plots, paired, single and replicated watershed designs, and methods based in remote sensing/GIS (Chang 2006). More recently, the use of modeling or simulation has increased as another tool for change detection. While most post-wildfire hydrologic studies have used experimental plots and/or hillslope scale designs to allow control over environmental factors (Moody et al. 2013) watershed-scale studies employ other approaches. The paired watershed approach, also known as the before-after control-impacted (BACI) study design relies on pre-disturbance "calibration" of response variables such as streamflow between at least two undisturbed watersheds until statistically significant relationships between "control" and "treated" watersheds are observed (generally for at least 7 years) prior to implementation of a treatment on one of the watersheds (Chang 2006). The approach has been used extensively over the last century in forest harvesting research (e.g. Bates 1921) and occasionally for prescribed burns (e.g. Britton 1991; Stoof et al. 2012) where there is a significant amount of researcher control over the location, timing, and magnitude of disturbance. A key benefit of the paired watershed design is some measure of control for climatic variability across the study period which generally is the dominant control over watershed behavior. However, limited (or no) spatial replication of treated and control watersheds strongly restricts the spatial inference space (generalizations concerning treatment effects) because only one treatment watershed is typically employed. Moreover, outside of a few rare cases where watersheds with active data collection programs have burned and nearby reference watersheds remained available (e.g. Helvey 1980; Scott 1993; Owens et al. 2013), post-wildfire hydrology research has typically not employed BACI-designed studies.

The single and replicated watershed designs are less well-equipped to parse treatment effects from natural climate variability, but both have been used to produce post-wildfire insights on runoff. The single watershed approach usually involves a watershed for which data collection was underway for several years before disturbance; it generally requires a longer calibration period than for paired watersheds (Chang 2006). The primary challenge with this approach is separating the hydrological impact of forest disturbance from that of normal climate variability. Recently, modeling or simulation efforts have sought to address this issue by using meteorological inputs and/or pre-disturbance streamflow to produce calibration datasets, then statistically assess differences in observed post-disturbance streamflow or implement time trend analysis (Seibert et al. 2010; Zegre et al. 2010; Zhao et al. 2010). Others have used process-based models such as the Cold Regions Hydrological Model (CHRM) (Pomeroy et al. 2012) or the Soil and Water Assessment Tool (SWAT) (Havel et al. 2018) to simulate wildfire scenarios and assess changes to flow regimes. The replicated watershed design is purely post-hoc in nature and has been implemented when researchers have no pre-disturbance data (Campbell et al. 1977; Troendle and Bevenger 1996; Mayor et al. 2007; Mahat et al. 2016). In this design, at least one burned and one unburned control watershed with very similar physiography and meteorology are instrumented as soon as possible after wildfire to enable comparisons. However, the studies which have used this approach typically employ limited or no replication of disturbed and reference watersheds, and short study periods (< 5 years). This leads to considerable uncertainly owing to severely limited spatial and temporal inference space. While studies employing greater replication of both disturbed and reference watersheds would conceptually increase the strength of generalizations regarding disturbance effects, these would also rely on strong similarity in watershed characteristics that regulate higher-order controls on watershed response. Additional uncertainty regarding disturbance effects could be inherent, depending on the degree of variation in elevation, aspect, and other physiographic features among disturbed and reference watersheds and the influence of these factors on precipitation and temperature regimes.

Expanding technological capabilities in recent years have enabled the efficient collection and retrieval of considerable amounts of fine-resolution hydrometeorological and spatial data. This has increasingly allowed contemporary post-wildfire hydrology studies to: 1) analyze data from a large number of watersheds enabling increased statistical power, often including pre- and post-disturbance data; 2) easily relate numerous spatial and meteorological characteristics to watershed runoff; 3) increase the scale at which insights are generated (e.g. Wine et al. 2018). For example, Saxe et al. (2018) examined streamflow records from 82 fire-affected western US watersheds making use of several independent predictor variables including topographic, vegetation, climate, burn severity, percent area burned and soils data. Similarly, Beyene et al. (2021) used a quantile-based analytical framework to examine the hydrologic effects of wildfire in 44 western US watersheds. Other studies have focused on fewer watersheds using remote sensing to assess post-wildfire recovery of vegetation as a key determinant of streamflow through its effects on interception and evapotranspiration. Wine and Cadol (2016) used over 30 years of streamflow and geospatial data, modeling and an enhanced vegetation index (EVI) to assess the hydrologic impacts of several wildfires on three large (191 - 4807 km2) watersheds in New Mexico, USA. Moreno et al. (2020) used Normalized Burn Ratio (NBR) and both pre- and post-disturbance relations with an unburned control watershed to assess the effects of the Waldo Canyon fire on streamflow from Camp Creek in Colorado, USA. Key data requirements for these studies were pre- and post-disturbance data with long records, the availability of data from a large number of watersheds, and/or high quality GIS or remote sensing data.

1.5. Wildfire research in the northern Rocky Mountains

Despite the apparent potential for dramatic hydrologic change following severe forest disturbance, multiple studies have indicated a certain level of hydrologic resilience in northern Rocky Mountain regions (Harder et al. 2015; Spencer et al. 2019). These responses may be largely explained by the complex geology and subsurface flowpaths in these systems which have permeable sedimentary bedrock overlain by deep glacial tills (Spencer et al. 2019). However, most post-wildfire research on hydrological response has come from a handful of well-studied regions such as the US Midwest, the European Mediterranean, and Australia (e.g. Hallema et al. 2017; Shakesby 2011; Lane et al. 2006). Highlighting this, a recent review found only 19 studies over the past 40 years have been conducted on streamflow changes after wildfire across the entirety of Canada and Alaska with only a small subset of these in the Rocky Mountains (Robinne et al. 2020). Available information is particularly sparse for rainfall interception, snow accumulation and impacts to the post-fire flow regime. Moreover, the broader body of post-wildfire literature still lacks research after the initial post-wildfire years. These research gaps need to be addressed because the Canadian Rocky Mountains are a critical source of water not only for human use but aquatic life. Therefore, the objective of this thesis is to better understand how much precipitation reaches the forest floor in these vital forests and how streamflow responds to both fast (e.g. rain storms) and slower (e.g. snowmelt) hydrologic processes in the recovery phase following initial impacts. Figure 1.1 presents a conceptual framework the thesis which is separated into three components as follows:

1.6. Study Objectives

Study 1: Net precipitation in burned and unburned subalpine forest stands after wildfire in the northern Rocky Mountains

The first study (Chapter 2) focuses on net precipitation in subalpine forest stands during the decade following wildfire (Figure 1.1). This study addresses three key questions: 1) Were there differences in net rainfall and its components, throughfall and stemflow, between burned and unburned subalpine forest stands?; 2) Were there differences in snow accumulation between burned and unburned subalpine forest stands?; 3) Were there differences in net precipitation (net rainfall + snow accumulation) between burned and unburned subalpine forest stands?

Study 2: Investigation of Flow Regime for a Decade Following Wildfire in Rocky Mountain Watersheds, Alberta, Canada

The second study (Chapter 3) makes use of multiple lines of evidence to investigate potential wildfire-induced impacts to the flow regime at various time steps in three burned watersheds in the northern Rocky Mountains (Figure 1.1). Two additional watersheds serve as unburned references against which data from the burned watersheds can be compared. Four specific questions are examined in this chapter: 1) How did the wildfire affect annual precipitation-runoff relationships and water yield?; 2) Did the wildfire alter streamflow magnitude during: a) the peak snowmelt runoff period, or b) during the late summer low flow period?; 3) How did the fire affect seasonal timing of flows, and lastly; 4) Is there any evidence of recovery from wildfire effects on flow a decade after the fire?

Study 3: Rainfall – storm runoff relationships after wildfire over a 10-year period in Canada's southern Rocky Mountains

The third study (Chapter 4) investigates rainfall-storm runoff relationships in the same five watersheds as the previous study (Figure 1.1). However, this study focuses on the snow-free season in an attempt to examine rainfall-runoff relationships in isolation from the influence of snowmelt. Questions examined in this study are: 1) Did wildfire affect the magnitude of runoff during rain storms? 2) Did wildfire influence the timing of the delivery of storm water during rainfall-runoff events? 3) Which factors are most important in determining runoff response?

For Studies 2 and 3, a 10-year window of streamflow and precipitation data was collected beginning in the second year after wildfire. The objective was to use multiple lines of evidence and an intensive, field data-driven approach to reveal large differences in post-wildfire streamflow between burned and unburned reference watersheds beyond potential differences caused by watershed structure. The replicated post-hoc design was employed with two unburned reference and three burned watersheds reflecting both greater watershed-scale replication (capturing greater directly-measured variability among disturbed and reference watersheds), and a robust period of hydro-climatic measurement which collectively support stronger spatial and temporal inferences than past replicated watershed-scale wildfire studies.

Chapters 2, 3, and 4 detail the aforementioned studies which address the research questions. For Chapter 2, field research was completed at four forest stands within the larger watershed study. As such, it has its own study site description, while the watershed characteristics described in Chapter 3 also serve as the site description for Chapter 4. Chapter 5 synthesizes the key findings from the study and makes recommendations for future research.

1.7. Figures

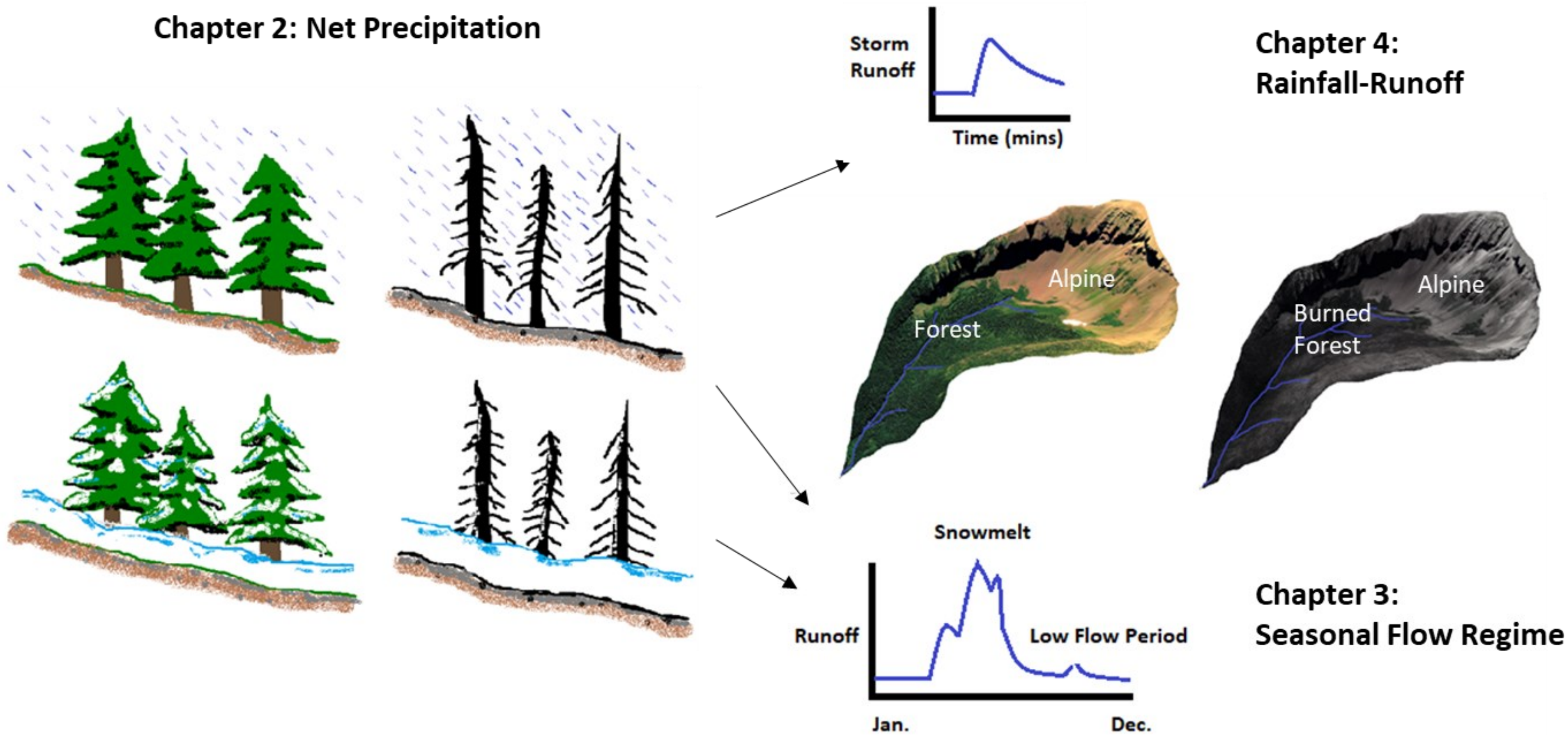

Figure 1.1. *Schematic overview of Chapters 2 to 4. Studies for Chapter 2 were completed at the stand scale in burned and unburned subalpine forest while those for Chapters 3 and 4 were done at the watershed scale and included insights from three burned and two unburned reference watersheds. Studies for Chapter 3 focused on potential wildfire effects across the seasonal flow regime while those for Chapter 4 focused specifically on rainfall-runoff (storm) events during the snow-free part of the year.*

Chapter 2. Net precipitation in burned and unburned subalpine forest stands after wildfire in the northern Rocky Mountains[1]

2.1. Introduction

Large wildfires in the western US have increased in frequency since the 1980s (Westerling et al. 2006), a trend which has been linked to a warming climate (Harvey 2016). Across Canada, annual area burned is projected to increase significantly (Flannigan et al. 2005); similarly, fire frequency in western Canada is projected to rise 21-190% by the end of the 21st century (Wotton et al. 2010). Consistent with these expectations, area burned in the 2017 and 2018 fire seasons far exceeded that in the previous record year (1958), burning more forests than the previous 28 years combined (pers. comm. M. Flannigan 2018). Over the past two decades, a broad range of wildfire impacts on watersheds have been reported including changes in soil water repellency (Debano 2000), infiltration (Ebel and Moody 2013), and rainfall-runoff relationships (Moody and Martin 2001). These altered watershed characteristics and processes can increase risks to communities from mass erosion, debris flows, and flooding (Shakesby and Doerr 2006; Cannon et al. 2008) and may have implications for ecosystem health (Silins et al. 2014) and human use of water (Emelko et al. 2011).

Precipitation intercepted by forest canopies is lost to evaporation or sublimation (Carlyle-Moses and Gash 2011); moreover, its intensity as it passes through the canopy is dampened, reducing splash erosion and the potential for landslides (Keim and Skaugset 2003). While significantly reduced interception after wildfire is often acknowledged, wildfire effects on net rainfall (R_N) and snow accumulation (S_A) have not been extensively documented. Interception losses can be high in some forests (e.g. Rutter et al. 1975; Pomeroy and Schmidt 1993); thus, reduced canopy cover resulting from severe crown fires could substantially increase the amount of precipitation reaching forest floors (net precipitation, P_N) potentially affecting post-fire hydrologic responses. Several studies have attempted to simulate these effects through hydrologic modelling (Seibert et al. 2010; Pomeroy et al. 2012); however, fire effects on P_N, which includes both R_N and S_A, have not been quantified in mixed rain/snow precipitation regimes.

[1] A version of this chapter has been published as: Williams, C. H. S., Silins, U., Spencer, S. A., Wagner, M. J., Stone, M., & Emelko, M. B. (2019). Net precipitation in burned and unburned subalpine forest stands after wildfire in the northern Rocky Mountains. *International Journal of Wildland Fire*, *28*(10), 750-760.

R_N is the sum of throughfall (T_f) and stemflow (S_f) falling through the canopy:

$$R_N = T_f + S_f \tag{2-1}$$

while interception is generally measured from T_f and S_f indirectly (Carlyle-Moses and Gash 2011) as:

$$I_C = R_G - (T_f + S_f) \tag{2-2}$$

where I_C is rainfall interception, and R_G is gross rainfall measured above or outside of the canopy. S_A is commonly directly characterized from measurement of snowpack depth and density to determine snow water equivalent (SWE) along snow courses near the date of peak SWE. Peak SWE represents maximum seasonal S_A because significant losses occur due to I_C and ablation prior to the time of peak SWE.

I_C is controlled by the distribution of rainfall event size in relation to the storage capacity of forest canopies; thus, both climate and canopy characteristics govern I_C (Carlyle-Moses and Gash 2011). During small storms, a large fraction of R_G is typically intercepted by the canopy, whereas I_C represents a smaller fraction of R_G during large storms because of canopy saturation. The temporal distribution of rainfall event magnitude is a key factor regulating I_C (Spittlehouse 1998). While I_C as a percent of R_G can vary substantially among forest types, high seasonal I_C has been reported for several conifer species including pure stands of Norway spruce (48%, Rutter et al. 1975), Balsam fir (38%, Plamondon et al. 1984), Douglas fir (24%, Rothacher 1963), and mixed stands of subalpine fir/Engelmann spruce (41%, Carlyle-Moses et al. 2014).

Snow interception can similarly result in large losses of precipitation. Greater than 40% of annual snowfall can be intercepted by coniferous forest canopies (Pomeroy et al. 1998), exposing it to sublimation rates potentially greater than 0.3 mm hr^{-1} (Lundberg and Halldin 1994). Changes in forest cover are a primary driver of snowpack dynamics (Varhola et al. 2010). While loss of canopy cover generally increases S_A, increased wind redistribution, radiation and sublimation losses after canopy disturbance can also reduce S_A creating significant challenges in predicting disturbance effects on snowpacks (Pomeroy et al. 2002).

Few studies have reported impacts of wildfire to R_N or S_A. For R_N, only two studies in burned shrublands in Spain and Portugal (Soto and Diaz-Fierros 1997; Stoof et al. 2012) and two studies in burned conifer forests have been conducted. A 12% increase in R_N in burned red pine forests with lower I_C capacity (unburned I_C =14% of R_G) was observed in western Japan (Mitsudera et al. 1984), while a 21% increase in R_N after fire in a mixed conifer stand with much greater I_C (31%) was reported in south-central British Columbia, Canada (Moore et al. 2008). Increases in S_A (peak SWE) are variable after wildfire and range from <10% to >50% in magnitude (Skidmore 1994; Winkler 2011; Burles and Boon 2011; Maxwell et al. 2019). Decreased peak SWE was observed in one study in a semi-arid conifer ecosystem in New Mexico and attributed to higher post-fire ablation (Harpold et al. 2014). From these studies, it appears increases in post-fire snowpack are more common than decreases, especially in northern latitude forests with high annual precipitation and snow accumulation (e.g. Winkler 2011; Gleason et al. 2013). More studies are needed to predict trends in post-wildfire S_A and its potential effects on spring runoff in snowmelt-dominated regions.

The fraction of annual precipitation from rainfall or snowfall is highly variable, spatially and temporally in mountainous terrain (Rolland 2003; Lehning et al. 2008; Kienzle 2008). Thus, wildfire has the potential to produce a wide range of effects on R_N and S_A in the Canadian Rocky Mountains. Here, the effects of severe wildfire on net precipitation (P_N) were evaluated over a 10 year period in a subalpine watershed in the eastern slopes of the Rocky Mountains—a key water-producing region of Alberta, Canada. This included characterization of a) T_f, S_f, I_C, and R_N, and b) S_A (snowpack depth, density, and peak SWE) in burned and unburned forest stands. This study combines post-wildfire rainfall measurements from one pair of burned and unburned stands with snow accumulation measurements from another pair. Though not replicated across multiple fire-impacted and unburned stands, sites were generally representative of mixed conifer subalpine stands in the study region. Within-stand replication of I_C, R_N and S_A measurements were used to characterize temporal variability in P_N during the first decade after the fire.

2.2. Materials and Methods

2.2.1. Study Site Description

This study was conducted in the Front Range Rocky Mountains in southwestern Alberta, Canada (Figure 2.1**)** as part of the Southern Rockies Watershed Project (SRWP; Silins et al. 2016). Sites were selected in the South York and North York Creek watersheds near the northern boundary of the 2003

Lost Creek wildfire, a near-contiguous crown fire that burned 15,369 ha of forest (Peddle et al. 2007). The watersheds span upper montane, subalpine, and alpine ecological sub-regions (Downing and Pettapiece 2006) with subalpine forests comprising 50% of the combined watershed area. A pair of stands (one burned, one unburned reference) was selected for snow measurements; another pair of stands was selected for rainfall measurements (Figure 2.1) with each stand covering an area of approximately 0.5-1 ha. Forests were dominated by subalpine fir (*Abies lasiocarpa* (Hook.) Nutt.) with lower proportions of Engelmann spruce (*Picea engelmanii*) and lodgepole pine (*Pinus contorta* Dougl. ex Loud. var. latifolia Engelm.). Stand characteristics were measured in randomly located fixed area survey plots in each of the burned/reference stands. Canopy closure was determined using hemispherical photographs captured in October, 2007 on clear days shortly after sunset (Figure 2.2). Photos were taken at 90 cm above ground, over throughfall troughs and at SWE points, providing 21 photos from the rainfall interception stands and 20 from snow accumulation stands. Hemispherical photographs were analyzed using Gap Light Analyzer Version 2.0 software to calculate the gap fraction (ratio of open sky pixels to total pixels; Frazer et al. 1999). Stand attributes are detailed in Table 2.1. Differences in species proportion, height and stem density were observed between study stands. However, all trees in burned stands were fire-killed and all foliage and fire branches were consumed. Thus, while there was a higher proportion of lodgepole pine in the burned R_N stand than the reference stand, species composition would have little discernable effect on interception. Diameter-height relationships were produced using measurements from 120 burned and 145 unburned trees to estimate if mean tree characteristics were affected by the fire. These relationships indicated that tree height was marginally lower in burned stands for similar diameters, likely a result of the fire consuming tree leaders and bark. This could account for some of the difference in overstory height shown in Table 2.1. While tree density was greater in the S_A compared to R_N stands, leaf area, crown bulk density and canopy closure regulate snow and rain interception losses (Hedstrom and Pomeroy 1998; Llorens and Gallart 2000) and canopy closure was comparable among the pairs of study stands.

Long-term continuous precipitation data (2004-2014) were collected at 10-minute intervals with a Jarek tipping bucket gauge (Geoscientific, Vancouver, Canada) fitted with an antifreeze overflow system for winter collection. This gauge was located less than 450 m from the study stands at the South York climate station (~1700 masl; Figure 2.1). Snow comprised approximately 53% of the average annual precipitation (1137 mm) over the study period (Figure 2.3). Separation of rain and snow precipitation was based on air temperature after Kienzle (2008). Average daily air temperatures at the South York climate station ranged from -9.1 C° in December to 14.2 C° in July (annual average = 1.6 C°).

2.2.2. *Study approach*

The broad study approach involved separate characterization of R_N and S_A from 2005-2014. R_N was calculated from measurements of T_f and S_f in 2006-2008. Relationships between R_G and I_C were subsequently used to project R_N over the broader distribution of rainfall events from the 2005-2014 period. In contrast, S_A was measured directly from 2005-2014. Seasonal total R_N and S_A were combined to characterize P_N over the 10-year period.

2.2.3. *Throughfall (2006-2008)*

T_f was measured during the snow free period from June to September for three years using trough collectors. Three trough collectors constructed from vinyl drainage pipe (6 m long x 4.3 cm wide; collection area = 0.26 m^2) were installed in one burned and one unburned reference stand. Troughs were attached to wooden stakes 70 cm above the forest floor and gently angled to allow rain water to drain through a hose into covered Davis tipping bucket rain gauges (Davis Instruments Corp. model 7852, Hayward, CA, USA) connected to HOBO event data loggers (Onset Computer Corporation, Pocasset, MA USA). Two additional trough collectors were situated in a cleared area within the burned stand to measure R_G. Mean T_f for burned and reference plots was calculated for each individual rainfall event from the three troughs in the plots. Individual rainfall events were identified from trough gauges in the clearing (R_G), using a minimum of 6 h with no rain to separate rainfall events (Valente et al.1997; Link et al. 2004).

2.2.4. *Stemflow (2006-2008)*

S_f was measured for four fir trees in the reference stand and three trees (two fir and one pine) in the burned stand during the same snow free periods as T_f. Trees were selected for a representative range of diameters (9.4 cm to 42 cm diameter at breast height, DBH) within each stand. A 1-cm deep groove was shaved in a spiral orientation around each tree trunk at 1.3 m height and a 19 mm garden hose (spilt open lengthwise) was stapled into the groove and caulked on one edge to produce a watertight seal. S_f running down the boles was captured by the hose and routed into a covered Davis tipping bucket gauge wired to a HOBO event logger at the base of each tree. Linear relationships between R_G and S_f volume (ml) were developed for each instrumented tree. S_f volumes were converted to equivalent depths (mm) for all trees in the fixed area plots by regressing the slopes and intercepts from these relationships against tree stem surface area of all instrumented trees in each stand (calculated from tree diameter and height, assuming trees represented cones). Slopes and intercepts from these latter regressions were used to predict total volume of S_f (mL) for all trees in the fixed area plots for each rainfall event based on measured DBH and heights of the trees. This is a more robust approach to scaling S_f up to the full distribution of tree sizes at the stand scale than simply averaging S_f from multiple trees. S_f depth (mm) for each event was calculated from R_G and total S_f volume standardized to the plot area.

2.2.5. Net rainfall (2005-2014)

R_G over the broader distribution of rainfall events occurring at the South York climate station was used to project R_N over the 2005-2014 period based on relationships between R_G and I_C (Equation 2-2) for reference and burned sites measured during 2006-2008. Power functions were developed to describe I_C (Figure 2.5). I_C was calculated from 10 min R_G data using a 6 h minimum period without rain to separate individual rainfall events. R_N was aggregated by water year (2005-2014) based on the date when a continuous snowpack began to accumulate near the study sites to partition the "rain season" and "snow season". This date was established using continuously measured snow depth measured at the nearby North York climate station (1.9 km north and 145 m lower elevation than the R_N plots) using an SR50 ultrasonic snow depth sensor (Campbell Scientific, Logan, UT, USA).

2.2.6. Snow Accumulation

S_A was measured in burned and unburned reference stands. Five snow courses, each 100 m in length, were established in each stand type and surveyed every year (2005-2014) in late February/early March. Snow depth was measured each 10 m along transects using graduated avalanche probes, while depth and snow density were measured at each end of the 100 m transects using a Federal Snow Tube and field scale. Thus, snow measurements from each snow course consisted of 50 depths and 10 densities for each stand type annually. Fewer snow density measurements are required than depths as density is less spatially variable than depth (Elder et al. 1998). Snow density measurements were corrected using a relationship between field measured SWE and snow samples weighed with a digital scale to account for overestimates at higher masses (Dixon and Boon 2012). Mean SWE for each snow course was calculated from mean density and depth for each of the remaining 40 depth measurements. While our snow surveys did not precisely correspond with the date of peak SWE prior to the onset of melt, they captured SWE close to the date of peak snow depth at the North York climate station.

2.2.7. Net Precipitation

The 10-year record of projected R_N was combined with the observations for S_A to estimate P_N for burned and reference sites across water years (2005-2014). Measured T_f, and R_N in burned and reference stands were compared using paired sample t-tests for the 49 rainfall events observed in 2006-2008. These data were normalized using the Box-Cox transformation prior to testing. S_f and I_C data could not be normalized; thus, the Wilcoxon Signed-Rank test was used to compare these parameters. Projected SWE and snowpack depth were normalized using the Box-Cox transformation, and mean annual measurements were evaluated using two sample t-tests across 2005-2014.

2.3. Results

2.3.1. Net Rainfall 2006-2008

The summers of 2006-2008 were relatively dry and did not produce any large (>25 mm) rainfall events. T_f and S_f observations were collected for 49 rainfall events during this period. R_N ranged from 0.1-21.5 mm where 47% (23 events) of all events were less than 2 mm and 78% (38 events) were <6 mm. Only 6 events exceeded 10 mm and only one event exceeded 20 mm.

Total R_N across the three rainfall seasons was 166 mm in the burned stand which represented 85% of R_G (195 mm). In contrast, total R_N in the reference stand was 112 mm, which represented only 58% of R_G ($p<0.001$). Significant differences were found between R_G and burned stand R_N ($p<0.0001$), as well as between burned and reference stand R_N ($p<0.0001$) using the Wilcoxon Rank-Sum non-parametric test (for non-normally distributed data). Asymptotic (positive) relationships were evident between T_f and R_G in both reference and burned stands; however, the proportion of R_G occurring as T_f was much greater in the burned compared to the reference stand (Figure 2.4). For the smallest events (<0.5 mm), T_f in the burned stand was generally >45% of R_G, increasing to >90% for the largest events, whereas in the reference stand T_f for the smaller events ranged between 5-20% of R_G and approached approximately 70% of R_G for the largest events (Figure 2.4). Total T_f during the three years of measurement in the burned stand was 162 mm (83% of R_G; standard error, SE = 7.48) compared to 112 mm (58% of R_G; SE = 19.4) in the unburned stand ($p<0.001$). Similarly, while S_f

was low in both stand types (Figure 2.4), total S_f was much greater in the burned stand (3.8 mm, 2% of R_G, $p<0.001$). Maximum S_f in the burned stand was just under 0.5 mm during the largest event and generally ranged from 0-2.3% of R_G. In contrast, S_f in the reference stand was negligible averaging 0.0011% of R_G and often not observed at all, except during the largest events.

Differences in T_f and S_f corresponded to differences in I_C among the stand types. While I_C of both stand types increased with event R_G, I_C of the burned stand was much lower than observed in the reference stand, particularly for larger rainfall events (Figure 2.5). Total I_C (2006-2008) in the burned stand was 29 mm (15% of R_G) compared to 83 mm (42% of R_G) in the reference stand ($p<0.001$).

2.3.2. Net rainfall (2005-2014)

From 2005-2014, 761 rainfall events larger than 0.25 mm occurred where 53% of the rainfall events were <2 mm, 73% were <6 mm, and 92% were < 22 mm. While the frequency distribution of rainfall events during the 10-year record was similar to that observed during the I_C measurements, 8% of the rainfall events exceeded the maximum R_G observed during 2006-2008 which required extrapolation of I_C relationships beyond the range of our observations.

Mean annual projected R_N was 454 mm (range 343-721 mm) in the burned stand compared to 328 mm (245-529 mm) in the unburned stand ($p<0.001$, Table 2.2a). These differences corresponded to a 36% increase (122 mm) in mean projected R_N and ranged from 28-46% (88-162 mm) over 10 years (Table 2.2a). While differences in R_N (mm) were strongly (positively) correlated with annual R_G (R^2=0.83, $p<0.001$) and frequency of rainfall events greater than 25 mm (R^2=0.43, $p<0.009$), the percent increases in R_N were negatively correlated with R_G (R^2=0.48, p=0.025) and frequency of rainfall events greater than 25 mm (R^2=0.43, $p<0.001$).

2.3.3. Net Snow Accumulation (2005-2014)

Mean annual SWE in the burned and unburned stands was 347 mm (213-479 mm; standard deviation, SD = 52.6 mm) and 195 mm (73-349 mm; SD = 54.3 mm), respectively, during the 10-year study ($p<0.001$, Figure 2.6). This corresponds to 78% (152 mm) more SWE, on average, in the burned stand ranging from 29-201% (81-190 mm) over 10 years (Table 2.2b). However, in contrast to R_N there was no relationship between cumulative annual snowfall and either mean SWE or percent increase in mean SWE (R^2=0.13) measured on the snow courses in each of the 10 years of study.

Differences in mean SWE between burned and reference stands largely reflected differences in snow depth, though small differences in snow density were evident between stand conditions.
Peak annual snow depth measured continuously in a clearing near the snow courses ranged from 72 cm (March 30, 2010) to 165 cm (March 31, 2014; Figure 2.6). Average annual peak snow depth (at the time of SWE measurements) in the burn was 132 cm (SD = 10.6 cm) across the entire period of study and ranged from 81 cm (2005) to 185 cm (2014), compared to a mean depth of 81 cm (SD = 17.6 cm) in the unburned stand ranging from 27 cm (2005) to 132 cm (2014) (Figure 2.6). The burned stand had 62% greater mean snow depth (50 cm) compared to the unburned stand ($p<0.001$). Snowpack density was also significantly higher ($p<0.001$) in the burned stand in 8 of 10 years (28 and 24% in burned and unburned, respectively).

2.3.4. Net precipitation (2005-2014)

Mean annual precipitation (water year) was 1137 mm during the study period (863-1469 mm; Table 2.3). Approximately 47% and 53% of total precipitation fell as rain and snow, respectively. Mean annual P_N was 812 mm (559-965 mm) in the burned stand and 538 mm (368-656 mm) in the unburned stand ($p<0.001$).

The combination of greater R_N and S_A resulted in 274 mm higher mean annual P_N in burned stands (range 191-344 mm). This represents an additional 51% P_N in the burned stand compared to the reference and approximately 24% of total gross annual precipitation measured in a clearing at the South York climate station. There was no relationship between wildfire effects on increased P_N (mm or percentage) and variation in annual total gross precipitation.

2.4. Discussion

This study suggests that wildfire can produce large and sustained increases in P_N in mixed conifer subalpine Rocky Mountain stands as we found no significant temporal trend over the study period ($p=0.28$). While extensive research has focused on soil and hillslope processes governing precipitation-runoff relationships in fire-affected landscapes, increased precipitation resulting from wildfire-associated canopy loss (leading to reduced rainfall and snow interception losses) has been largely overlooked. Here, burned stands had over 50% greater P_N, comprised of rain and snow, than reference stands over a 10-year period. Increases of this magnitude can represent a major shift in the dominant precipitation inputs that govern hydrologic responses in fire affected landscapes.

2.4.1. Net rainfall and throughfall

We observed 28-47% greater R_N in the burned stand during the study period. T_f comprised 98 and 100% of R_N in the burned and reference stands, respectively, while S_f was minimal (2.3 and 0% of R_N). The only other study in North American forests reported a 21% increase in R_N in a mixed lodgepole pine, Engelmann spruce and subalpine fir stand 4 years after the 2003 McClure wildfire in British Columbia (Moore et al. 2008). Both studies observed lower I_C, though we found twice the relative difference in our burned stand; I_C was 15% of R_G in our study compared to 8% reported after the McClure fire. There are notable differences in methodology and forest characteristics between the two studies. For example, Moore et al. (2008) evaluated I_C by combining rainfall interception data from two separate unburned stands measured in 1998-1999 and 2006-2007 (Upper Penticton Creek and Mayson Lake, respectively). Differences in species composition and canopy structure also likely contributed to different post-fire interception between the two studies. Unburned forests in our study area were dominated by fir and spruce (98%) with little pine (Table 2.1). In contrast, the British Columbia site had 17% pine (pers. comm. R.Winkler 2018). Engelmann spruce and subalpine fir have greater crown bulk density, leaf area, and I_C than lodgepole pine (Kaufmann et al. 1982; Plamondon et al. 1984; Brabender 2005). Furthermore, while stem density and canopy coverage were not reported by Moore et al. (2008), Winkler (2011) reported canopy coverage of 54% for a snow accumulation study at Mayson Lake compared to our reference canopy coverage of 74%. Our reference stand measurements are more similar to those of Carlyle-Moses et al. (2014), who measured I_C in a mature, declining spruce-fir-pine stand in British Columbia (also at Mayson Lake). T_f and I_C were 59.4% and 40.6% of total R_G, respectively, compared to our 58% and 42% suggesting R_N is 58-60% of R_g.

I_C is generally greater for smaller (<5 mm) rain storms (Carlyle Moses and Gash 2011); thus, wildfire effects on R_N are also greatest for smaller events. This trend is evident in Figure 2.4, where I_C in our reference stand represents, as a proportion of R_G, 0.65, 0.49 and 0.37 for 2 mm, 10 mm, and 25 mm rain storms, respectively; the same storm sizes in the burned stand produced proportional I_C of 0.22, 0.16 and 0.13. This suggests R_N was higher in the burned stand by 0.9 mm (123%), 3.3 mm (65%), and 6.0 mm (38%), respectively compared to our reference stand across the range of storm sizes. In contrast, the relationships reported in Moore et al. (2008) where pine was more abundant suggest R_N was 0.6 mm (51%), 1.7 mm (23%), and 3.0 mm (15%) greater in their burned stand for the same size storms, respectively. This illustrates that differences in storm magnitude and tree species composition among broadly similar stand types can result in meaningful differences in R_N.

2.4.2. Stemflow

While S_f was very low in both burned and reference stands (2% and ~0% of R_G, respectively), this study is the first to show the magnitude of change in a burned stand. Stand-scale funneling ratios, a measure of water input from stemflow compared to open-area rainfall (Carlyle-Moses et al. 2018), were 4.64 and 0.002 for burned and reference stands, respectively, a difference of three orders of magnitude. Wind-driven rainfall has been shown to be more susceptible to I_C due to lateral rain shadows produced by prominent tree crowns (Herwitz and Slye 1995). With rain shadows largely absent after the fire, exposure of tree bole surface area increased S_f catch efficiency and likely produced more S_f during rains driven by wind. Furthermore, photographs and site observations indicate bark burned or peeled away from many trees in the burned stand leaving smooth sapwood where textured bark existed pre-fire. The reduction in surface roughness and bark microrelief was likely an important factor increasing S_f (Van Stan and Levia 2010) in the burned stand. Large increases in stemflow after wildfire may have important ecological implications by focusing delivery of nutrients, leaf exudates and ions to the forest floor (Parker 1983; White 2015).

2.4.3. Snow Accumulation

The 78% higher mean peak SWE in the burned stand was considerably greater than we observed for R_N and it is higher than results from other studies of wildfire (Skidmore 1994; Winkler 2011; Gleason et al. 2013; Harpold et al. 2014; Maxwell et al. 2019), logging or insect infestation (Varhola 2010). Reported changes in peak SWE range from -10% in a burned subalpine forest in New Mexico (Harpold et al. 2014) to >50% in the Canadian Rockies (Burles and Boon 2011) in comparison to unburned reference stands. These differences are largely a result of the competing influences of canopy loss and energy regime which, respectively, reduce interception and increase ablation in burned stands. Maxwell et al. (2019) contrasted studies reporting fire effects on peak SWE in North America and suggest the possibility of a latitudinal effect, whereby the lower energy available in more northern sites may amplify S_A differences due to fire.

Among studies geographically closest to our study region, Skidmore (1994) observed a 9% increase in mean post-fire peak SWE in a mature lodgepole pine forest in southwestern Montana. Differences in tree species, canopy cover and basal area may explain the greater S_A in our burned stand as

Skidmore (1994) reported reference canopy coverage and basal area of 35% and 12.1 m^2/ha, respectively, to our 74% and 81.6 m^2/ha. Winkler (2011) reported a 25% increase in SWE in a mixed conifer (fir/spruce/pine) stand in British Columbia. While stand types and stem densities are similar to the present study, Winkler (2011) also reported less canopy cover (54%) in their unburned stand compared to ours which may have facilitated higher S_A in their reference stand, reducing the apparent change in the burned area. Not surprisingly, our results are most similar to those reported by Burles and Boon (2011) who observed 58% and 50% greater peak SWE in 2009 and 2010, respectively, in the same burned stand as our R_N study. We measured 61 and 88% higher SWE in our burned stand in those two years in comparison to our reference, highlighting variability in S_A even within the same small area. Timing of snow surveys may have contributed to this difference as Burles and Boon (2011) performed measurements on April 1 and March 31 for 2009 and 2010, respectively, while we surveyed on February 19 and March 1.

The two southern-most studies took place in subalpine forest stands in New Mexico and Utah, USA (Harpold et al. 2014; Maxwell et al. 2019). Harpold et al. (2014) showed that 25-45% of new snow was intercepted in unburned spruce-fir forest during a single event. Despite this, peak SWE during the study was 10% less in the burned area, a result the authors attributed to increased ablation and a shift from vegetative to topographic controls on S_A. In our study area, Burles and Boon (2011) found 30% more energy available for snowmelt in burned stands compared to unburned stands and the date of complete snowpack removal occurred 7 and 13 days earlier (2009 and 2010, respectively). Thus, as with Harpold et al. (2014), ablation increased significantly in our burned area, but the higher S_A in our study suggests energy is limited and increased ablation is unlikely to compensate for the additional snowpack resulting from loss of canopy interception. Maxwell et al. (2019) found no differences in peak SWE in burned and unburned subalpine forest stands in Utah. However, the snow-free date on north and south facing slopes in burned stands occurred 4 and 14.5 days earlier, respectively, than on similar slopes in unburned stands. This demonstrates differential strength of ablation due to aspect and may help explain why the northwest facing slope used for our study retained consistently larger snowpacks.

Event-scale meteorological conditions such as air temperature, wind and snow density can promote higher interception losses. Schmidt and Gluns (1991) measured snow interception on conifer branches of nearly 50% from a 10 mm storm (water equivalent) when the density of event snow was low (specific gravities of 0.04-0.07), while only 10% of the same size storm was intercepted at higher densities (specific gravity = 0.13). Snowfall events 3-4 mm in size with low densities displayed the highest interception efficiencies (Schmidt and Gluns 1991). Thus, both the density of the falling snow (often less at lower air temperatures) and event magnitude partially determine the amount intercepted. Low winter temperatures (Figure 2.3) and high percentage of snow events <5 mm (almost 70% of all events) are consistent with meteorological conditions promoting high annual snow interception and sublimation in the continental climate of our study region. This likely played a role in the magnitude of differences in S_A we observed between our burned and unburned stands in comparison to results reported in other regions.

Forest structure and climate characteristics were likely both important drivers of the 78% difference in peak SWE observed between our burned and reference stands. Consistent with previous work (e.g. Pomeroy and Schmidt 1993; Hedstrom and Pomeroy 1998), conifer tree species with dense foliage and high canopy coverage can efficiently intercept snow. Coupled with high annual snowfall (600 mm), frequent small (<5 mm) events, and relatively low air temperatures and ablative processes, this resulted in much higher S_A in our burned stand. Caution is advised in the extrapolation of our results to other forest types or climatic regions as this study was not replicated across multiple burned and unburned stands. Despite this, ten years of measurement enabled thorough assessment of temporal variation of S_A in the subalpine stands in our study area.

2.4.4. Net Precipitation

Though limited by our study design, results from multiple years of measurement suggest severe wildfire can have a significant effect on precipitation inputs in the subalpine forests of our study region. The 51% (274 mm) greater mean annual P_N in the burned stands resulted from the combination of 45% (122 mm) greater R_N and 55% (152 mm) greater S_A compared to the unburned stands. To our knowledge, no previous study has characterized wildfire effects on P_N in a mixed rain/snow precipitation regime. We speculate that the large increases in P_N observed here reflect conditions that may promote greater sensitivity of subalpine forests to these effects. Higher elevation forests in our region are typically dominated by subalpine fir/spruce with significant I_C efficiencies, and precipitation regimes driven by high lapse rates which promote frequent precipitation events. In combination with low winter energy inputs, large impacts to P_N are not surprising.

Our projection of R_N may slightly overestimate wildfire effects later in the study period as measurements were conducted in years 2 to 4 after the wildfire, prior to post-fire tree regeneration. However, this uncertainty is likely small as tree establishment was only evident in the latter 2-3 years of the study and low density, open-canopy conditions persisted longer. Forest recovery was equally slow in the burned S_A stand. The slow recovery of canopy leaf area and interception in these forests is likely to prolong wildfire effects on P_N for decades.

The higher summer and winter P_N observed in burned stands is likely to alter surface and subsurface flow pathways, groundwater recharge, and storage dynamics that regulate magnitude, timing, and variability of post-wildfire flows. Thus, these findings have several potentially critical implications for downstream communities including risks of flooding, erosion, debris flows, and transport of contaminants from the landscape (Shakesby and Doerr 2006; Cannon et al. 2008). These can impact water quality and its variability (Silins et al. 2009; Stone et al. 2011; Bladon et al. 2014), which can affect ecosystem health (Silins et al. 2014) and lead to more frequent drinking water treatment challenges (Emelko et al. 2011).

2.5. Tables

Table 2.1. *Stand attributes in rainfall and snow measurement sites.*
Plots were measured after the wildfire. Area of fixed plots varied (63-314 m^2) with the objective of including a minimum of 40 sampled trees. Trees ≥1.3 m in height were included in fixed area plot surveys. [A]Upper quartile range. [B]Gap Light Analyzer version 2.0 (Frazer et al. 1999).

	Rainfall plots		Snow plots	
	Reference	Burned	Reference	Burned
Fixed Area Plot Surveys (n)	1	1	2	2
Trees/Survery (n)	58	41	46.5	77.5
Species composition (%)				
Fir	95	63	84	94
Pine	0	29	1	4
Spruce	2	0	15	2
Dead Trees (%)	9	100	8	100
Density (stems/ha)	1719	1446	3486	3915
Overstory Ht. Range (m)[A]	17.4 - 24.2	17.6 - 20.9	18.3 - 22.0	12.3 - 15.5
Basal Area (m^2 ha^{-1})	52.8	43.1	81.6	53.2
Avg. DBH (cm)	17.6	16.6	14.7	11.5
DBH Range (cm)	5.2 - 44.8	4.5 - 32.9	1.3 - 47.8	3.2 - 28.5
Avg. Canopy Closure (% from GLA[B])	71	26	74	29
Height to Live Crown (m)	5.1	N/A	4.7	N/A
Stand elevation (m)	1680	1775	1680	1725
Stand aspect	neutral	neutral	NW	NW
Average age (years)	110	110	120	110

Table 2.2. *Rainfall and snowfall in burned and reference stands.*
Gross and net a) rainfall (R_N), and b) snowfall and SWE (S_A) in burned and reference stands during 2005-2014. R_N calculated using the event-based relations developed during 2006-2008 measurement period.

a) Rainfall

Water year	Gross rainfall (mm)	Net rainfall (R_N) Burned (mm)	Net rainfall (R_N) Reference (mm)	Difference in net rainfall (mm)	Difference in net rainfall (%)
2005	830	745	583	162	28
2006	387	342	254	88	35
2007	500	435	303	132	44
2008	453	400	290	109	38
2009	399	346	236	110	46
2010	599	529	389	140	36
2011	530	470	352	118	33
2012	423	368	250	117	47
2013	697	624	482	142	30
2014	441	390	291	99	34
10 yr. avg.	**526**	**465**	**343**	**122**	**36**

b) Snow accumulation

Water year	Gross snowfall (mm)	Snow accumulation (S_A; SWE) Burned (mm)	Snow accumulation (S_A; SWE) Reference (mm)	Difference in net SWE (mm)	Difference in net SWE (%)
2005	639	220	73	147	201
2006	476	410	175	235	134
2007	782	363	217	146	67
2008	505	427	237	190	80
2009	530	213	132	81	61
2010	437	224	119	105	88
2011	622	391	234	157	67
2012	617	479	252	227	90
2013	740	295	166	129	78
2014	766	450	349	101	29
10 yr. avg.	**611**	**347**	**195**	**152**	**78**

Table 2.3. *Difference in net precipitation.*

Gross precipitation (P_g) and surplus in net precipitation (P_N) in burned stands compared to reference stands (2005-2014).

Water year	P_g (mm)	Increase in P_N (mm)	(%)
2005	1469	309	47
2006	863	323	75
2007	1282	278	54
2008	958	299	57
2009	929	191	52
2010	1036	245	48
2011	1152	275	47
2012	1040	344	69
2013	1436	271	42
2014	1206	200	31
10 Yr. Avg.	**1137**	**274**	**51**

2.6. Figures

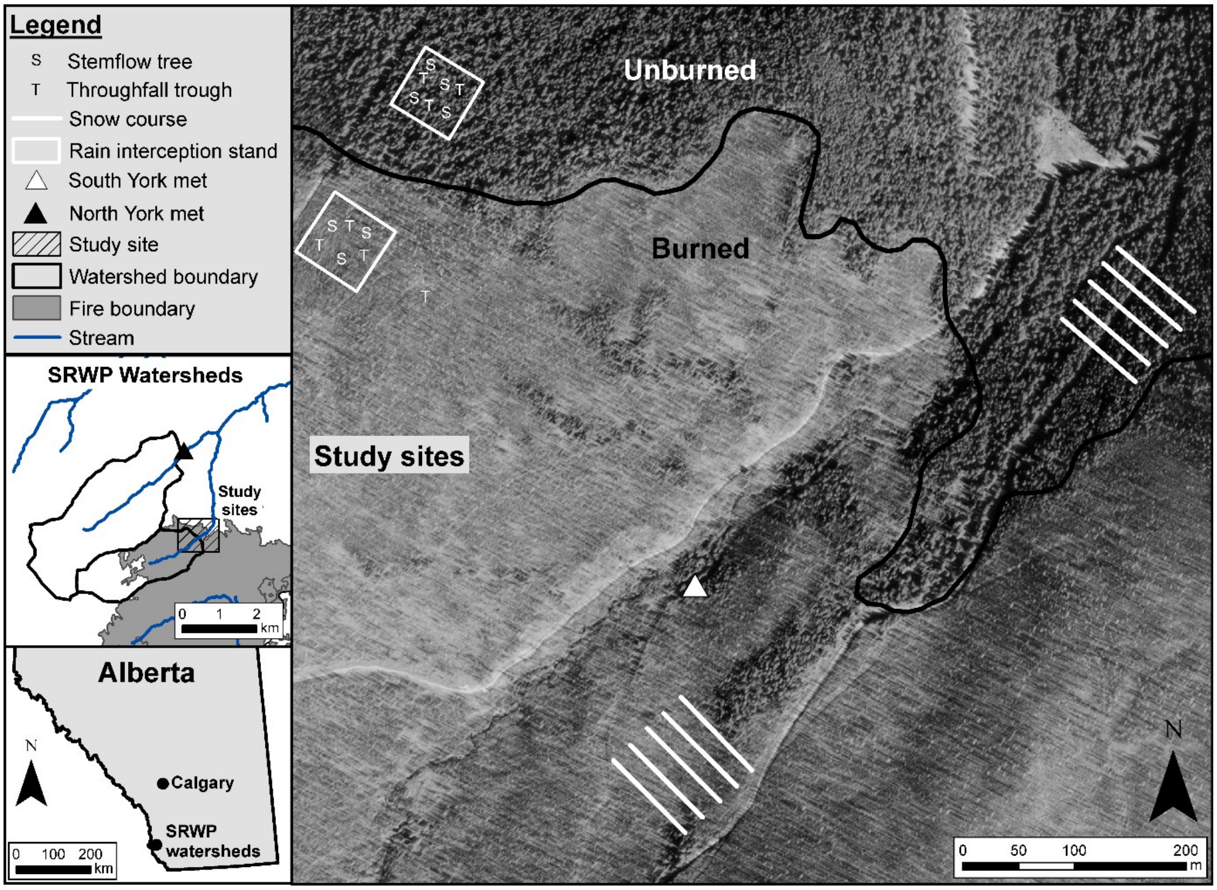

Figure 2.1. *Main image: Rainfall interception and snow accumulation stands shown on orthophoto of the study area. Thick black line shows burn boundary at northern edge of Lost Creek wildfire. Middle-left inset: Larger unburned watershed is North York while the smaller wildfire-impacted watershed is South York. Hatched box shows the study site area depicted in the orthophoto.*

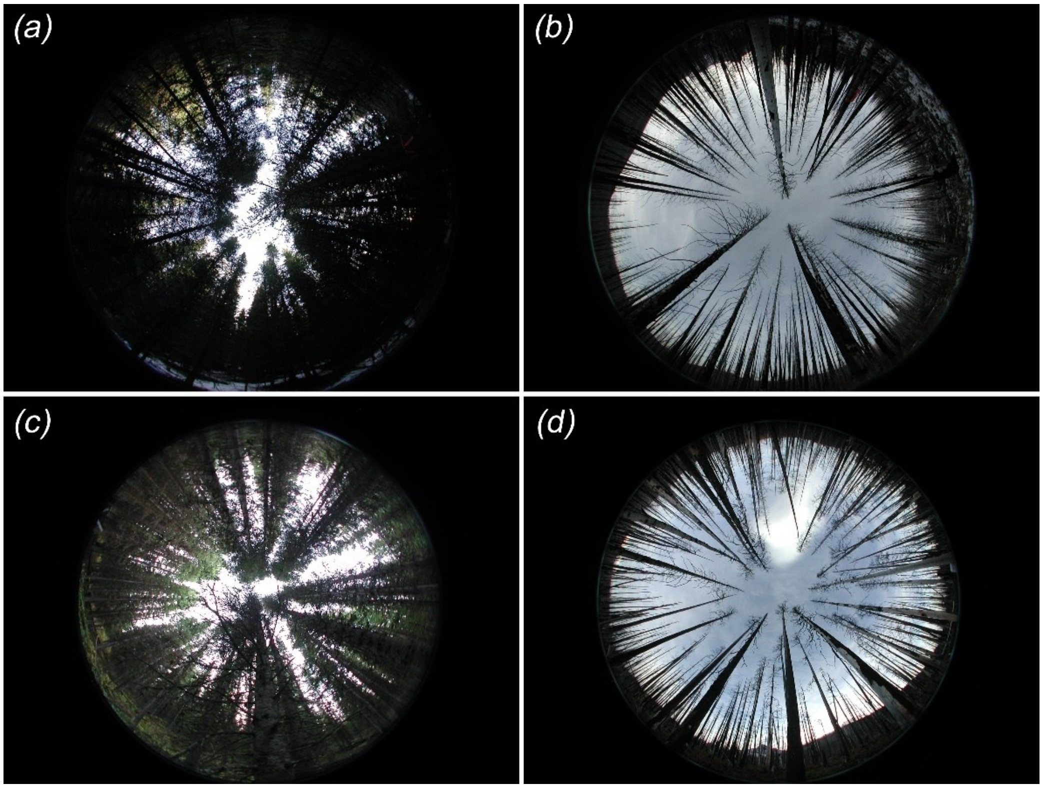

Figure 2.2. *Typical hemispherical photographs showing canopy structure in burned and reference stands. (a) reference snow course, (b) burned snow course, (c) reference throughfall trough and (d) burned throughfall trough.*

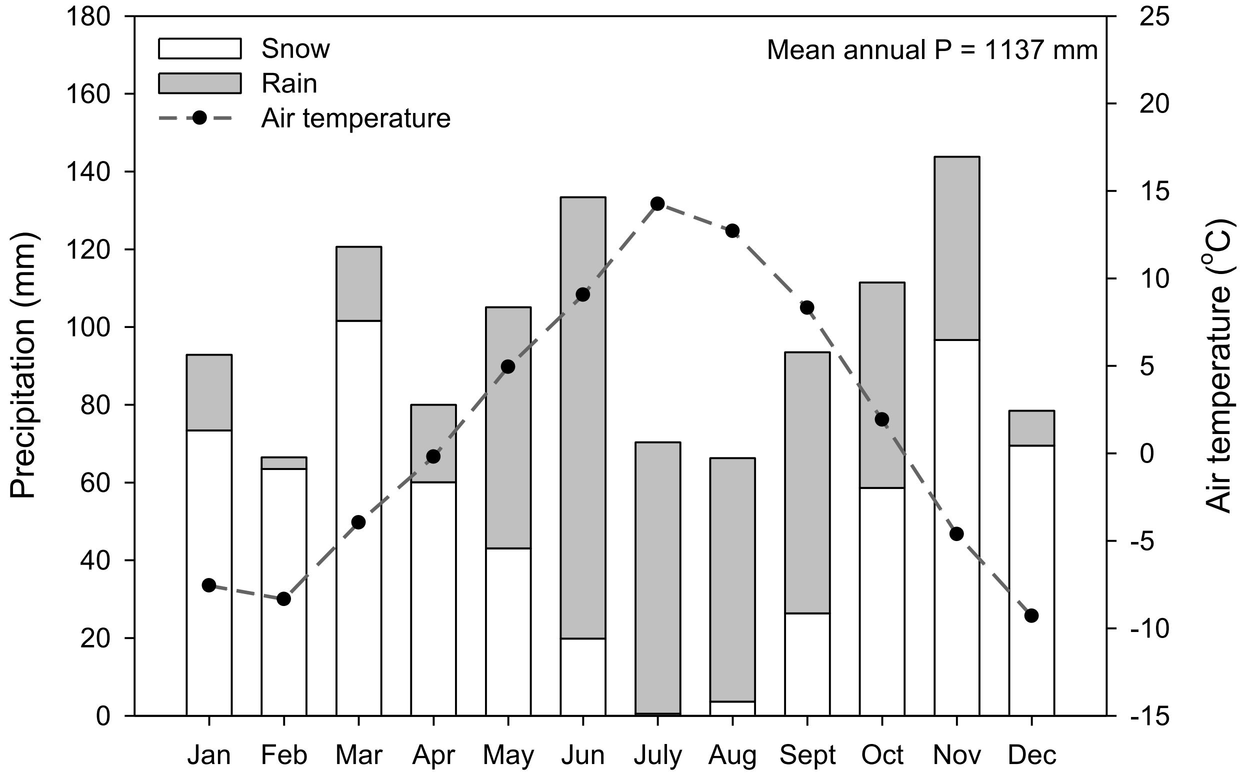

Figure 2.3. *Average monthly precipitation and air temperature during period of study (2005-2014) measured at South York climate station.*

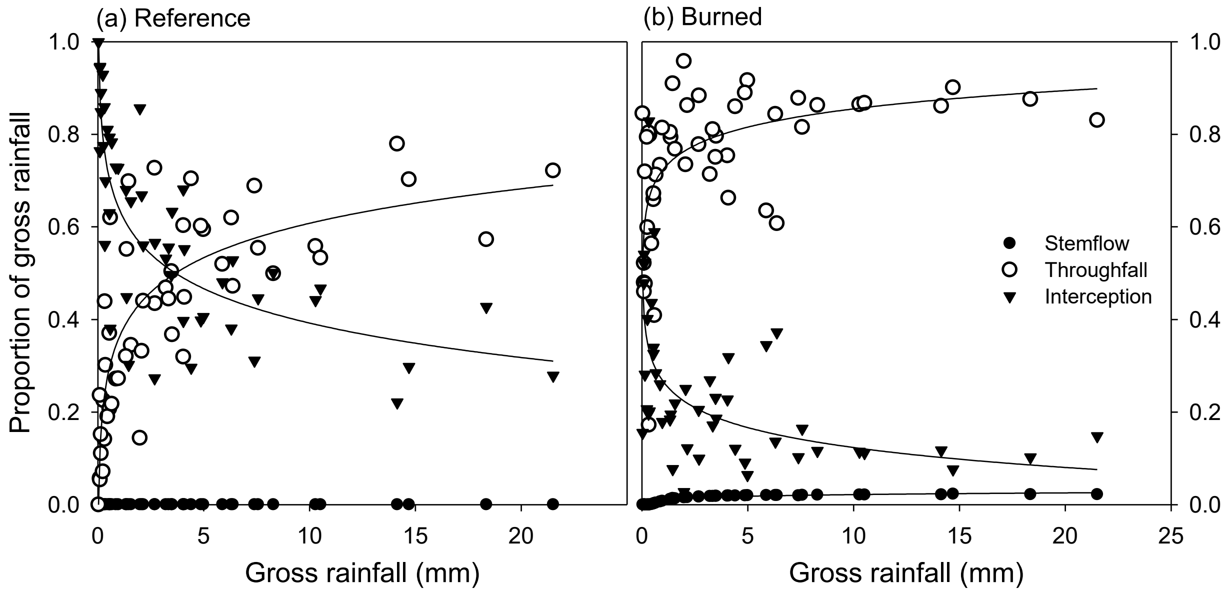

Figure 2.4. *Relationships between throughfall (T_f), stemflow (S_f) and canopy interception (I_C) in the reference stand (left) and burned stand (right) with gross rainfall (R_G) during the three-year measurement period (2006-2008).*

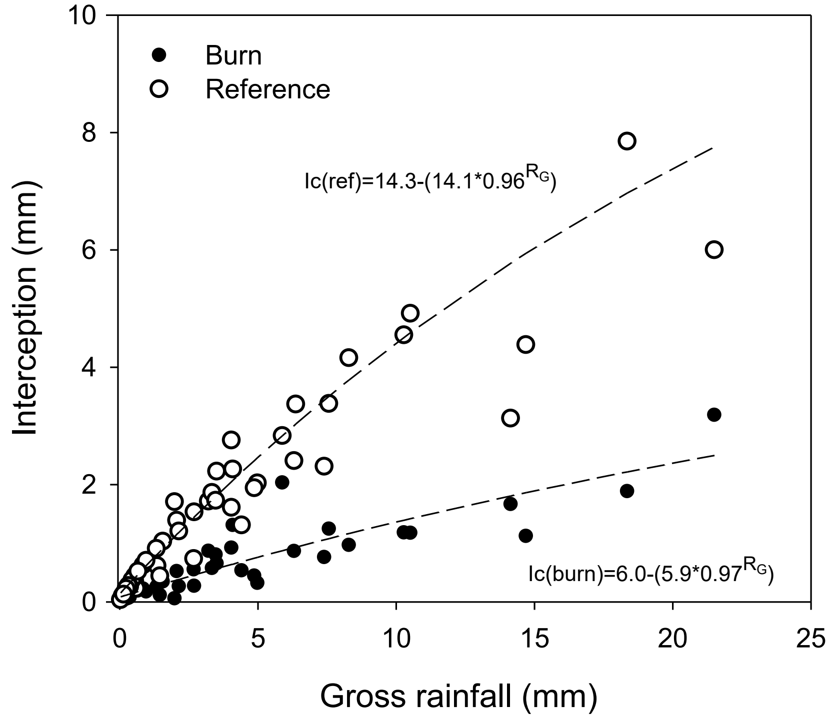

Figure 2.5. *Relationship between gross rainfall (R_G) and canopy interception (I_C) in burned and reference stands during the three-year measurement period (2006-2008).*

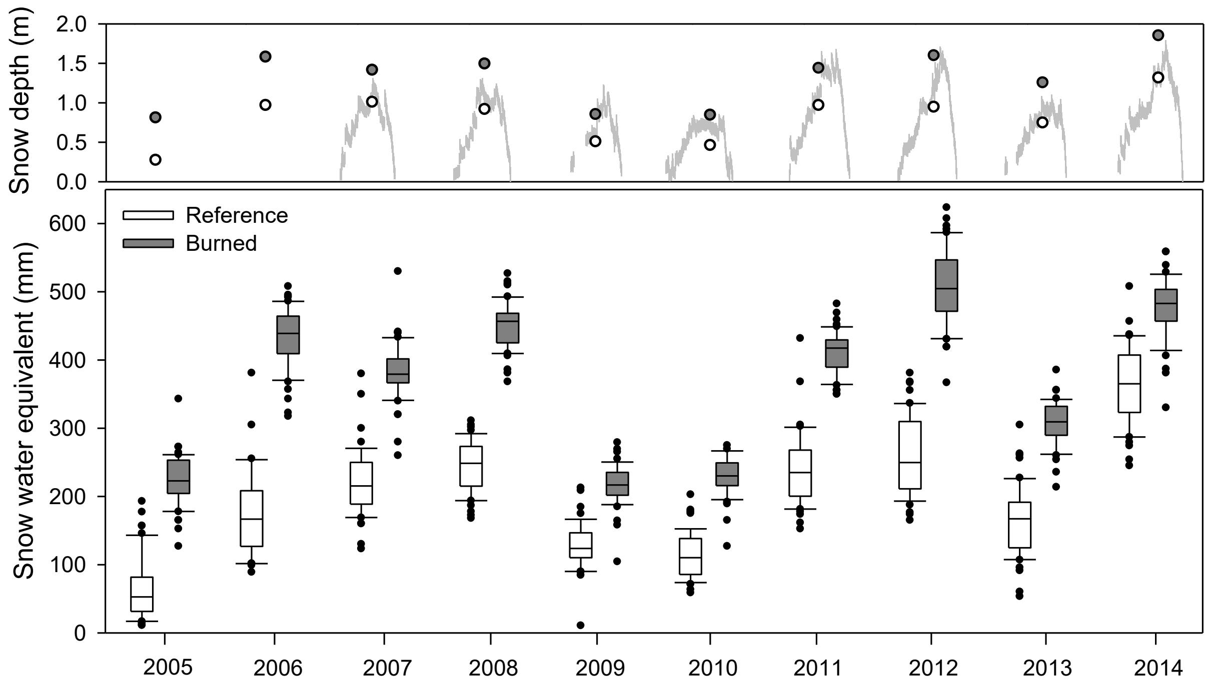

Figure 2.6. *Snow accumulation (S_A) on the snow courses from 2005-2014. Top: Average snow depth at time of measurement indicated by dark grey (burned) and open (reference) circles. Continuous snow depth (recorded in clearing at North York station) indicated by the light grey line. Bottom: Boxplots of annual snow water equivalent near date of peak SWE. Median indicated by the solid line in the boxplots. Box represents 25th and 75th percentiles, whiskers represent 10th and 90th percentiles, and dots are outliers.*

Chapter 3. Investigation of Flow Regime for a Decade Following Wildfire in Rocky Mountain Watersheds, Alberta, Canada.

3.1. Introduction

Wildfire is well recognized as the dominant natural disturbance agent in most Canadian forest regions. However, severe wildfire has become more common over the last 60 years as the frequency of large (>200 ha) fires and annual area burned (AAB) have increased (Hanes et al. 2019; Rogeau et al. 2016; Coogan et al. 2021). Fire size and AAB are projected to further increase 20-64% and 25-93%, respectively, during the 21st century (Wang et al. 2020). Under an extreme climate-warming scenario an average fire season in Canada could burn ~11Mha of forest (Wang et al. 2020), over five times the AAB from 1959-2015 (Hanes et al. 2019). While previous research has shown significant increases in the number of large fires and area burned in the Northern US Rockies (Dennison et al. 2014; Westerling 2016), more fire can likely be expected along the eastern slopes of Alberta's Rocky Mountains. The forested headwaters of this region are vital for providing water for agriculture and ecological instream flow needs across the Prairie Provinces and they provide drinking water to two-thirds of Alberta's ~3.6 million residents (Philipsen et al. 2018; Robinne et al. 2019). Wildfire in these critical source water forest regions can lead to degraded water quality and downstream drinking water treatment challenges because of increased total suspended sediment, turbidity, dissolved organic carbon, nutrients (e.g. nitrogen, phosphorous), metals and other contaminants (Hauer and Spencer 1998; Bladon et al. 2008; Silins et al. 2009; Emelko et al. 2011). Small communities are particularly vulnerable to post-wildfire disruptions in water supply because their treatment plants often do not have the contemporary technologies available to larger urban centers (Robinne et al. 2019). Given the expectation of increased wildfire activity in western Canada, there is a need to understand fire effects on key water resources attributes (quantity, quality, and timing), especially in the mountainous headwaters which constitute a critical water supply source for Alberta.

Wildfire can produce significant changes in hydrologic processes that regulate water supplies, especially in the early post-fire years before the regeneration of vegetation can help stabilize hillslopes (Ebel 2020). While other forest disturbances such as harvest and beetle attack leave relatively intact litter and duff layers on the forest floor, severe wildfire often completely removes this organic material leaving bare mineral soil. Many studies have focused on the short-term hydrologic effects (weeks to <5 years) of wildfire because they can be particularly dramatic and even dangerous in the years following (Wohlgemuth 2016; Cannon et al. 2008). Impacts on hydrologic processes can include significantly reduced forest canopy interception and higher winter snow accumulation (Moore et al. 2008; Williams et al. 2019; Winkler et al. 2011). Soil water repellency (Debano 2000; Doerr et al. 2006), reduced infiltration (Martin and Moody 2001), and soil crusting or surface sealing can lead to significantly more surface runoff than in unburned systems (Cerda and Robichaud 2009). Together, these changes can lead to increased peak flows, runoff, and erosion (Moody and Martin 2001b,c; Benavides-Solorio and MacDonald 2001) after wildfire. However, the majority of research quantifying post-fire change has been conducted on individual hydrologic processes such as infiltration, runoff generation, or erosion at the plot and hillslope scales where broader impacts to watershed scale responses are inferred from these process-focused studies. Watershed-scale observation of these responses are limited to a far fewer number of studies. Moreover, the majority of this work originates from a few fire-prone regions around the world including the Western USA, Australia and the European Mediterranean basin. A review of post-wildfire streamflow response in the Western USA found runoff response of greatest magnitude often occurred in regions with a Mediterranean or semi-arid climate such as Southern California, Arizona, and New Mexico (Hallema et al. 2017). For example, Campbell et al. (1977), studying a ponderosa pine ecosystem in north-central Arizona, found that post-wildfire mean annual water yields in moderately and severely burned watersheds were 300 – 450% of those in an unburned watershed while annual peak flows were orders of magnitude higher in burned watersheds. In the San Dimas Experimental Watershed in southern California, peak flows and flow volume increased by four orders of magnitude in comparison to pre-fire flows during fall rainstorms following a 1960 wildfire (Wohlgemuth 2016). In contrast, Heath et al. (2014) showed no effect of severe fires on water yield from burned eucalypt forests in Sydney's (Australia) water supply watersheds over a 10-year period. Recent research has renewed attention on historical wildfire studies and has begun to focus on longer-term hydrologic recovery in burned watersheds (Niemeyer et al. 2020; Wagenbrenner et al. 2021), but there remains a paucity of information on longer-term wildfire effects on runoff at the watershed scale, especially in the northern Rocky Mountains.

There have been very few studies focused on post-wildfire hydrology in Canada. Further, only a subset of these were undertaken at the watershed scale, and fewer still have been done in the Rocky Mountains (Pomeroy et al. 2012; Mahat and Anderson 2013). A recent review of post-wildfire water research in northern latitudes (i.e. Canada and Alaska) found only 19 studies which investigated changes to runoff and flow regimes over the past 40 years (Robinne et al. 2020). For snow-dominated regions such as the Canadian Rocky Mountains much of the understanding of the hydrologic effects of forest disturbance has come from decades of research focused on forest harvesting. While impacts on streamflow are highly variable following forest disturbance (Bosch and Hewlett 1982; Stednick 1996), it is evident that removal of forest canopy can increase water yield by reducing evapotranspiration. Alberta has a rich history of long-term watershed studies which have provided some indication of possible changes to water yield following disturbance along the east slopes and foothills (Spencer et al. 2016). For example, measurements on 9 logged and 9 control watersheds (7-26 km^2) near Hinton, Alberta showed 27% higher water yield during the gauged season (Apr-Sept) in the logged watersheds and 59% higher yield during the snowmelt freshet (Swanson and Hillman 1977). In the more mountainous, higher elevation Cabin Creek watershed in Southwestern Alberta, a 6% increase in water yield was detected after 50% of the forested area was clearcut in 1974 (Rothwell et al. 2016). However, no impacts to water yield were evident at the larger basin scale (Marmot Creek), possibly indicating some potential resilience to forest disturbance in this region (Harder et al. 2015). While there is a solid foundation of research on hydrologic responses to forest harvest, wildfire has received far less attention, especially at the watershed scale. Thus, potential impacts of wildfire on watershed hydrology in the Canadian Rocky Mountains remains highly uncertain.

The snowmelt freshet and the summertime low flow (baseflow) periods are two of the most important hydrologic periods in the flow regime of Rocky Mountain watersheds. Usually the majority of total annual flow is produced during the snowmelt period (April to June), while mid-late summer low flows can represent a challenge for aquatic life and water managers alike, especially during dry years. Some studies have shown that snow water equivalent (SWE) in wildfire-affected forests can be greater than that in unburned areas and, because of greater energy available for melt, the snow can melt faster (Chapter 2; Burles and Boon 2011; Micheletty et al. 2014). This could result in more water during the freshet, but it may also arrive earlier as suggested by modeling work investigating the effects of fire on mountain runoff (Pomeroy et al. 2012). However, very little information exists describing post-wildfire snowmelt runoff in the northern Rocky Mountains. Likewise, little information exists on both the direction and magnitude of post-wildfire change to summer low flows (Gronsdahl et al. 2019). Studies in other climatic regions show a wide range of potential impacts of fire or other forest disturbances on low flows. In the southwestern United States, streams which had no flow or were intermittent prior to fire were reported to have started running continuously following wildfire in chaparral watersheds (Neary et al. 2005). Kinoshita and Hogue (2015) found large increases to annual low flow volume in two burned watersheds in southern

California while Cingolani et al. (2020) found fire in 12 burned watersheds reduced seasonal low flows by 31-48% compared to 12 similar unburned watersheds in Argentina. In studies examining forest harvest, increases to low flows appear to be common in rain-dominated regions (Moore and Wondzell 2005) while evidence is mixed for snow-dominated environments. For example, Moore and Wondzell (2005) note that there was no significant effect on 30-day low flows at Wagon Wheel Gap (Colorado) resulting from 100% clear-cut logging, while an insignificant 10-15% increase in low flows was measured at Cabin Creek in Alberta after clear-cutting 20% of the watershed area (Van Haveren 1988; Swanson et al. 1986). However, large uncertainties exist when inferring the impacts of wildfire on these key components of the annual flow regime from studies conducted in other climatic regions and focused on other types of forest disturbance. Given the critical importance of the Rocky Mountains to water supplies in Alberta and the Prairie Provinces, this information will be increasingly important for regional water managers.

Here, ten years of streamflow observations from multiple burned and unburned (reference) Rocky Mountain watersheds are used to inform key research questions on potential wildfire effects to the annual flow regime following the 2003 Lost Creek Wildfire in Southwestern Alberta, Canada. Specifically, 1) How did the wildfire affect annual precipitation-runoff relationships and water yield?; 2) Did the wildfire alter streamflow magnitude during: a) the peak snowmelt runoff period, or b) during the late summer low flow period?; 3) How did the fire affect seasonal timing of flows, and lastly; 4) Is there any evidence of recovery from wildfire effects on flow a decade after the fire?

3.2. Methods and Materials

3.2.1. Study Site Characteristics

The study was conducted as part of the Southern Rockies Watershed Project (SRWP) from 2004-2014 in the Front Range Rocky Mountains of the Crowsnest Pass region (SW Alberta) (Silins et al. 2016). Study watersheds extended from 49° 35’ 10” N and 114° 36’ 33” W at their western boundary to 49° 33’ 54” N and 114° 23’ 40” W in the east (Fig. 1). The region is best classified as Dfc on the Köppen-Geiger Climate Classification system, defined as the coldest month averaging below 0 °C and 1–3 months averaging above 10 °C with no significant precipitation difference between seasons (Beck et al. 2018). Mean annual precipitation during the study (2005-2014) was strongly influenced by elevation, ranging from 720 mm (elevation = 1480 m) to 1440 mm (elevation = 1890 m). Mean annual air temperature, measured at an elevation of 1680 m, was 1.6 C° while the mean monthly high and low temperatures were 14.2 C° in July and -9.1 C° in December (Williams et al. 2019). The region is snow dominated with some alpine areas accumulating up to 4 m of snow depth during winter. The snowmelt freshet takes place from April to June; stream recession then occurs, generally reaching its lowest flows in August. Autumn precipitation and the seasonal reduction of evapotranspiration often causes a rise in stream hydrographs in September/October before winter sets in and streams remain in a relatively stable state until March, often with substantial bank ice. Soils in the region can be characterized as poorly developed Eutric Brunisols underlain by Cretaceous shale and sandstone (Bladon et al. 2008). All watersheds were largely forested prior to the fire. Dominant tree species were lodgepole pine (*Pinus contorta* Dougl. ex loud. var. *latifolia* Engelm.) with a minor component of Douglas fir (*Pseudotsuga menziesii*) at lower elevations, and subalpine fir (*Abies lasiocarpa* (Hook.) Nutt.) and Engelmann spruce (*Picea engelmanii)* in higher elevation sub-alpine regions.

3.1.1. The Lost Creek Wildfire and Study Design

The Lost Creek wildfire (July 22 – August 23, 2003) burned as a contiguous crown fire that also consumed large amounts of the forest floor organic layer leaving only mineral soil and rock across extensive areas. Both Landsat dNBR and air photo interpretation were used to calculate burned area, suggesting between 15,369 ha and 18,966 ha were affected (Peddle et al. 2007; ASRD 2006). To the author's knowledge no detailed burn severity assessments were completed. Pre-disturbance hydrometric data are almost never available for watershed-scale wildfire studies because of the random nature of fire on the landscape. Thus, only in rare and fortuitous circumstances are researchers able to implement before-after control-impacted (BACI) watershed study designs, similar to those traditionally used for forest harvesting hydrology studies (e.g. Scott 1993; Helvey 1980). As a result, the same level of control achieved by BACI study designs is generally not possible for wildfire research. The present study employs a replicated post-hoc reference-impact design consisting of five watersheds (3.65 – 10.35 km^2), geographically near one another, and as similar as possible with respect to watershed attributes, particularly elevation and aspect which are the two most dominant controls on snow accumulation and melt (Table 3.1) (Jost et al. 2007; Pomeroy et al. 1998). Two of the watersheds (Star and North York creeks) were instrumented as unburned (reference) controls while three (South York, Lynx, and Drum creeks) were burned to varying extents (52-99% total area) during the Lost Creek wildfire and served as burned "treatments". While significant portions of South York and Lynx Creeks were "unburned" (48 and 29% respectively), these areas consisted of open alpine meadow and rock/talus slopes without vegetation to support the wildfire; thus, the fire consumed close to 100% of the upper montane and subalpine forested area in all three burned watersheds. Watershed attributes for Star, North York, South York and Lynx Creeks, which collectively form the northern end of the Flathead mountain range, are most similar to one another while the mean elevation of Drum Ck. is most similar to that of Star Ck. (the lowest elevation watershed in the Flathead range group, Table 3.1).

3.1.2. Streamflow

Streamflow (Q) was measured using standard velocity-area techniques employing stage-discharge relationships developed at natural control sections in relatively stable stream reaches. New stage-discharge relationships were developed yearly to control for potential errors resulting from changes in the control sections which usually resulted from high flows. New pressure transducers (Waterlog H-350L/H-355 Gas Bubbler System, Design Analysis Associates Inc., Logan, UT; HOBO U-20-001-01 Water Level Logger, Onset Computer Corp., Bourne, MA) were installed in 2005 after widespread malfunction of older instruments deployed in 2004. Thus, this study does not include Q data for the first full post-fire year (2004) to avoid including potentially erroneous or uncertain observations. Stage data were collected at 10-minute intervals and manual measurements of Q (Swoffer Model 2100, Swoffer Instruments Inc., Seattle, WA; Sontek Flowtracker ADV Series, Sontek/YSI Inc., San Diego, CA) were performed approximately every 2 weeks (mid-Apr. – late Oct.). When possible, additional Q measurements were acquired during the snowmelt period to strengthen the stage-discharge relationships at higher flows. Rating curves were developed from measured Q and stage (Rantz et al. 1982):

$$Q = p(G - e)^N \tag{3-1}$$

where Q is streamflow, G is the gauge height (stage) at water surface, e is gauge height at effective zero flow, and p and N are fitted constants. Rating curves were applied to the stage data to produce annual streamflow hydrographs at 10-minute time steps. Quality assurance and control (QA/QC) of annual hydrographs employed several processing steps including error trapping of erroneous stage measurements (i.e., sensor malfunction or over-pressure effects during under-ice winter conditions) along with visual evaluation of correspondence between measured/predicted discharges. Q data for Drum Creek in 2007 were removed from analyses because of a malfunctioning stage sensor for part of that season. Similarly, data were omitted from calculation of annual Q for all streams for an unusually large rain-on-snow event (early January, 2005) because of high uncertainty in automated stage measurements.

3.1.3. Precipitation

The SRWP has maintained an extensive climate station network since 2004, at which time the first equipment was installed, with the network since expanding to eighteen precipitation gauges. Early in the collection period, Belfort Universal gauges were used, but in order to overcome limitations due to their collection capacity, they were replaced by Jarek tipping bucket gauges. Antifreeze overflow systems were installed on the tipping bucket gauges to convert these into universal (rain/snow) gauges for the October through April period to capture snowfall. A statistical interpolation method was used to fill missing precipitation data caused by frozen or otherwise malfunctioning gauges (Ahrens 2006). The Thiessen polygon approach was used to spatially weight precipitation for each watershed with a variable number of gauges available: Star Ck. (9), North York Ck. (6), South York Ck. (4), Lynx Ck. (5) and Drum Ck. (3).

3.1.4. Water Quality

Water quality observations sampled at the same time as manual streamflow measurements for potassium (K) and silica (Si) were used as a proxy indicator to infer the approximate fraction of streamflow originating from surface compared to subsurface runoff pathways (Elsenbeer et al. 1995; Bonnell and Fritsch 1997; Schellekens et al. 2004). Potassium is a key plant macro nutrient which is tightly cycled (released during decomposition of plant litter followed by rapid uptake by plants) in many plant communities whereas silica originates from dissolution of silicate minerals in the soil and surficial geologic materials as water percolates through both surface and deeper soil/till deposits. Thus, the K:Si ratio in streamflow samples can serve as a watershed scale geochemical indicator of the relative fraction of surface:subsurface runoff.

Water quality samples were collected approximately every two weeks when streams were free of ice and snow (April to October) and every five weeks during the overwinter period (November to March) for the duration of the study (2004-2014). Additionally, storm samples were periodically captured when field staff were physically near enough to the sites during significant rainfall events. Using gloved hands, technicians collected depth-integrated samples in acid-washed one-litre bottles in the centroid of flow whenever possible; if high flows posed a safety hazard, samples were collected closer to the stream edge where technicians could safely wade into the water. Potassium and silica concentrations were analyzed at the Biogeochemical Analytical Services Laboratory at the University of Alberta. An inductively coupled plasma-optical emission spectrometer (iCAP 6300; Thermo Fisher Scientific) was used for K^+ analysis and flow injection analysis (Lachat QuikChem

8500 FIA automated ion analyzer) was used to measure Si. Analytical precision for K^+ and Si, respectively, was 2.4% and 3.4% (Spencer et al. 2021). Over the 10-year sampling period, 127 samples were collected from North York and South York Cks., 132 for Lynx, 147 for Drum and 151 for Star Cks. during the snowmelt and low flow periods (April to September).

3.1.5. Data Analysis

Instantaneous streamflow (m^3 s^{-1}) was converted to area-weighted Q (mm) for analysis of water yield at variable time-steps (annual, seasonal, monthly, and weekly). Annual runoff coefficients (C_R) were calculated as the ratio of annual P to Q, and annual half-flow dates (Julian date by which 50% of total annual Q had occurred) were calculated for each watershed. Flow duration curves (FDC) illustrating the distribution of Q across the entire flow regime (Searcy 1959) were calculated from daily Q (mm d^{-1}) for the 10-year record for each stream.

Visual observation of boxplots and the Shapiro-Wilk test confirmed normality of water yield observations at the annual time step. Thus, the Kruskal-Wallis one-way analysis of variance (ANOVA) test was used to assess differences in annual water yield, runoff coefficients (C_R) and half-flow dates between burned and reference watersheds, followed by the Tukey HSD test for pairwise comparisons in the agricolae R package (Mendiburu 2020; R Studio 2021). Additionally, analysis of covariance (ANCOVA) was used to statistically assess differences in water yield between burned and reference watersheds using precipitation as a covariate. ANCOVA accounts for variation in precipitation among burned and reference watersheds where potential differences in water yield are evaluated relative to a common (adjusted) mean precipitation between watershed pairs (Chang 2006). Evidence for watershed-scale hydrologic recovery was investigated by separating water yield data into the first 5 post-wildfire years (2005-2009) and the last 5 post-fire years (2010-2014) to examine if relative differences between burned and reference streamflow changed.

However, water yield data at the sub-annual time step is typically autocorrelated which means errors transfer from one time period to the next, invalidating the assumption of independence (Yue et al. 2002). Thus, water yield data for the monthly, weekly and low flow periods were considered qualitative and only simple comparisons were examined. Fire effects on Q during both the higher seasonal flows associated with snowmelt freshet (April to June) and summertime low flows (July to September) were evaluated from total monthly Q during these periods. Flow duration curves (FDC) were used to graphically compare key differences in the entire flow regime of burned and reference watersheds. Potential post-wildfire recovery of hydrologic processes over time was explored in a similar fashion as water yield. Temporal changes in the distribution of K:Si ratios were evaluated by splitting the data into two post-fire periods, the first 5 years (2005-2009) and the last 5 years (2010-2014). For each watershed, the number of K:Si observations ranged from 59-74 during the first 5 post-fire years and 66-75 for the last 5 years. Additionally, K and Si data were categorized into two conceptual seasonal flow periods (i.e., snowmelt and low flows) based on the timing of water quality samples (i.e. Apr-Jun or Jul-Sept). K:Si ratio data were not normally distributed; thus, the Wilcoxon rank-sum test was used to compare differences between ratios from burned and reference streams.

Given the replicated post-hoc reference-impact watershed study design, a multiple-line of evidence approach was adopted to evaluate fire effects on annual and seasonal flow magnitude and timing based on comparisons of individual burned and unburned reference watersheds. Furthermore, given the breadth of flow parameters (differing time-steps), the conceptual approach used here was to deemphasize interpretation of weak or marginal fire effects in favor of those suggested by stronger wildfire effects or those well-aligned across multiple flow metrics.

3.3. Results

3.3.1. Climate Across Study Period

Across all watersheds, mean water year (Oct. 1 – Sept. 30) precipitation during the 2005-2014 study period was 1121 mm (S.D.=124 mm). Precipitation patterns during the study can broadly be characterized as an initial wet year (2005), followed by a dry period (2006-2010), followed by a wet period (2011-2014) (Table 3.2; Figure 3.2a). While the 2007 water year produced above-average precipitation in most watersheds, unusually high precipitation occurred in November, 2006 and March, 2007 while the summer months were extremely dry. This resulted in the lowest July – September (low flow) water yield across the study period for all watersheds. Annual water yield displayed similar trends as precipitation; 2005 was a high-yielding year, 2006-2010 were relatively low, and 2011-2014 were generally high (Table 3.2; Figure 3.2b). All watersheds experienced their lowest annual water yield between 2006 and 2009. Interestingly, the lowest annual yield occurred in 2009 for the control watersheds (Star Ck. and North York Ck.), but earlier for South York Ck. (2006), Lynx Ck. (2008) and Drum Ck. (2008; however, Q data for 2007 unavailable for Drum Ck.).

Mean water year precipitation in the unburned reference watersheds was 954 mm (Star Ck.; SD=192 mm) and 1252 mm (North York Ck.; SD=218 mm) during the study period (2005-2014; Table 3.2). For the burned watersheds, mean water year precipitation was 799 mm (Drum Ck.; SD=131 mm), 1226 mm (Lynx Ck.; SD=155 mm), and 1348 mm (South York Ck.; SD=143) (Table 3.2). Water year precipitation in North York Ck. (R), South York Ck. (B) and Lynx Ck. (B) was not significantly different ($p>0.50$). Similarly, precipitation in Star Ck. (R) and Drum Ck. (B) was not significantly different ($p=0.48$); however, precipitation in Star Ck. and Drum Ck. was different from the other three watersheds ($p<0.01$). The clear differences in annual precipitation led to the natural grouping of a "high precipitation" (HP) trio of watersheds with one reference (North York Ck.) and two burned (South York and Lynx Cks.), and a pair of "low precipitation" (LP) watersheds, Star Ck. and Drum Ck. (reference and burned, respectively). These differences in annual precipitation likely led to differences in water yield among HP and LP groups unrelated to the wildfire. While the HP group of watersheds was highly comparable because of their similarities in physical characteristics (e.g., elevation range, slope aspect; Table 3.1), the Star and Drum Ck. watersheds (LP group) had some attributes which could potentially lead to confounding results. For example, the greater proportion of "warm" slope aspects in Drum Ck. (Table 3.1) could lead to earlier snowmelt which could also be an expected effect of the wildfire. However, these watersheds were very similar with respect to watershed area, mean elevation, and geology which were some of the initial reasons that led to their *apriori* inclusion in the study. After data collection it also became clear Star and Drum Cks. were highly comparable with respect to precipitation and water yield (Figure 3.2a and 3.2b).

3.3.2. Annual Precipitation-Runoff Relationships and Water Yield

Despite the severity and extent of forest disturbance in the three burned watersheds, wildfire did not produce strong effects on annual precipitation-runoff relationships over the 2005-2014 study period. Mean water year runoff coefficients (C_R) across the study period in burned watersheds (B) were 0.74 (Drum Ck.), 0.88 (Lynx Ck.), and 0.73 (South York Ck.), while C_R for the reference watersheds (R) were 0.61 (Star Ck.) and 0.72 (North York Ck.) (Table 3.2, Figure 3.3a). Differences in mean C_R between burned/reference watersheds were not statistically meaningful in either HP or LP watershed groups. However, despite the lack of statistical significance, mean C_R from burned watersheds were 1-22% higher than those from reference watersheds within the context of the HP and LP groups (Table 3.2).

Mean annual water yield across the study period (2005-2014) was greater in all HP watersheds than in LP watersheds ($p<0.05$). Mean water yield across the study period in the burned HP watersheds was 1083 mm (Lynx Ck.) and 986 mm (South York Ck.) compared to 887 mm in the HP reference watershed (North York Ck., Table 3.2). Using ANCOVA, adjusted mean annual water yield for Lynx and South York creeks was 24% and 6% higher, respectively, than for North York Ck. across the 2005-2014 study period (Figure 3.4a). While the greater water yield in Lynx Ck. was marginally significant ($p<0.05$), the difference between South York and North York creeks was not ($p=0.51$). For the LP watersheds, adjusted means from ANCOVA analysis suggested Drum Ck. (burned) produced about 13% higher (583 mm; SD=143 mm) mean annual water yield than Star Ck. (567 mm; SD=143 mm), but this difference was not significant ($p=0.30$). Trend analysis (not shown) indicated the aforementioned climatic patterns across the study period resulted in significantly increasing annual water yield ($p<0.05$) for the HP watersheds (regardless of wildfire impact), largely driven by the transition from the dry years of 2006-2009 to the wetter years in the latter half of the study.

3.3.3. Streamflow Magnitude During Snowmelt (Apr.-Jun.) and Low Flow (Jul.-Sept.) Periods

3.3.3.1. Snowmelt Water Yield (April to June)

Across the 2005-2014 study period, burned watersheds produced higher water yield than reference watersheds during the snowmelt season (April to June), though differences were more apparent in the HP than LP watershed comparisons (Figure 3.5a,b). In the HP watersheds, April and May water yields were higher in burned compared to reference watersheds, while June water yields were similar between burned and reference (Figure 3.6b,d). Mean April water yield (2005-2014) for the HP reference watershed (North York Ck.) was 28 mm (SD=16 mm) compared to 56 mm (SD=27 mm; 101% greater) and 63 mm (SD=33 mm; 127% greater) in burned HP watersheds (South York and Lynx Cks., respectively). Slightly lower differences in mean water yield were evident between burned and reference watersheds during May when the burned watersheds (South York and Lynx Ck.) produced 43% and 50% greater water yield than North York Ck. (Figure 3.6b,d).

Monthly water yield patterns for the LP group were similar to those of the HP watersheds. The burned LP watershed (Drum Ck.) generally produced much higher April and May mean water yields than the reference (Star Ck.) (Figure 3.6a,c). Across the entire study period (2005-2014), mean water yield in Drum Ck. was 60 mm (SD=34 mm) in April and 157 mm (SD=86 mm) in May, compared to 20 mm and 112 mm in Star Ck. for these same months, respectively. This corresponded to 204% and 40% greater April and May water yield in the burned LP watershed compared to the reference watershed. However, June marked a transition when mean water yield in Drum Ck. (110 mm; SD=53 mm) was 33% (55 mm) less than in Star Ck. (164 mm; SD=62 mm). Thus, despite strong differences in mean water yield during each of the three months, mean yield during the entire snowmelt period (Apr.-Jun.) was very similar between the LP burned/reference watersheds (Figure 3.5b).

3.3.3.2. Low Flow Water Yield (July to September)

Cumulative low flows (total July 1 to September 30 water yield) were generally lower in burned than in reference watersheds for both the HP and LP watershed groups (Figure 3.5c,d). However, monthly differences were not as great as those for the snowmelt period (Figure 3.6a-d). Mean cumulative low flow water yield during the study (2005-2014) for the HP watersheds was 196 mm (SD=66 mm) in North York Ck. (reference) compared to 164 mm (SD=77 mm; 16% less) and 168 mm (SD=54 mm; 14% less) in the burned watersheds (South York and Lynx Cks., respectively). Relationships between annual low flows for North York Ck./South York Ck. and North York Ck./Lynx Ck. across the study period were relatively strong (Figure 3.5c; R^2=0.77 and 0.79). Greater total water yield during the low flow period was observed in North York Ck. than in either of the burned HP watersheds during 8 out of 10 study years. Differences in total water yield during the low flow period between burned and reference HP watersheds were minimal during the drier years of 2009-2010, but much greater during the wetter years of 2013-2014.

A similar pattern of differences between the burned and reference LP watersheds was evident during the low flow period (Figure 3.5d). Mean cumulative low flow was 131 mm (SD=46 mm) in Star Ck. and 113 mm (SD=44 mm) in Drum Ck. across the study (2005-2014), suggesting 14% lower water yield in the burned watershed during the low flow period. Similar to the HP watersheds, the differences in water yield between Star Ck. (reference) and Drum Ck. (burned) were greater during wetter years compared to drier years (Figure 3.5d; R^2=0.51, p=0.02). Interestingly, trend analysis indicated total water yield during the July to September low flow period increased significantly across the 10 years of study in both of the reference watersheds (Star Ck. and North York Ck.; $p<0.05$) but not for any of the burned watersheds ($p>0.13$; not shown). This was particularly evident after the 2006-2009 dry period and was more notable in North York Ck. than in Star Ck.

3.3.4. Streamflow Timing

Metrics describing the timing of streamflow such as half flow dates, flow duration curves (FDC) and weekly water yields all suggested the timing of snowmelt delivery to streams occurred earlier in burned compared to reference watersheds (Figures 3.3b, 3.7, 3.8). The half-flow date generally occurred 7-10 days earlier in the burned watersheds than in either of the reference watersheds (Figure 3.3b). Mean half-flow Julian dates for Star and North York Cks. were 168 (June 16) and 167 (June 15), respectively. In contrast, mean half flow dates for burned watersheds were 158 (June 6), 159 (June 7) and 160 (June 8) in Drum, Lynx, and South York Creeks, respectively. While half-flow dates occurred consistently earlier in burned watersheds, they did not differ strongly between reference and burned watersheds ($p>0.10$).

Flow duration curves (FDC) indicated a clear difference between daily water yield during April and May in burned and reference watersheds (Table 3.3; Figure 3.7). April flows were subdued most of the time in all watersheds, but higher flows generally occurred later in the month during days where air temperature was high, leading to increased snowmelt rates. Daily water yield at the 10, 25 and 50% exceedance frequencies was more than double in the burned HP watersheds (South York Ck., Lynx Ck.) than in the reference (North York Ck.) (Table 3.3). For the same exceedance frequencies, daily water yield in the burned LP watershed (Drum Ck.) was more than three times that of the LP reference (Star Ck.) during April (Table 3.3; Figure 3.7). FDC steepened for all watersheds during May, reflecting more variable flows and higher rates of snowmelt. Daily flows in the HP burned watersheds (South York Ck., Lynx Ck.) were, again, higher than those in the reference (North York Ck.) across all exceedances, but differences were not as large as those during April. Similarly, across the 10, 25 and 50% exceedance levels, the LP burned watershed (Drum Ck.) had daily yields 8-50% higher than those in the reference watershed (Star Ck.) during May.

June FDC revealed the most variable flows across the study period (Table 3.3; Figure 3.7). June also marked a transition period when daily water yield in reference watersheds began to equal or exceed that in the burned watersheds. FDC were very similar across all HP watersheds regardless of burned/reference condition while daily water yields were lower in the LP burned watershed (Drum Ck.) across almost all exceedance levels in comparison to the LP reference (Star Ck.). However, during the lowest exceedance frequencies (<5%), daily water yield in burned watersheds were still generally higher than in reference watersheds. This result must be taken with caution because some of the highest values for all watersheds occurred during an extremely high flow event in 2013 for which peak flows had to be estimated using slope-area equations (Dalrymple and Benson 1968). Thus, there is relatively high uncertainty around the largest June water yields. During July and August, both reference watersheds produced higher daily water yield than the burned watersheds in both LP and HP watershed groups across almost the entire range of exceedance frequencies (Table 3.3; Figure 3.7). However, during September, with the occurrence of higher fall precipitation (along with some snow) and slowing evapotranspiration rates, no clear pattern in daily water yield was evident within watershed groups.

A somewhat stronger pattern of wildfire effects on flow timing was evident in the finer-resolution data on mean weekly water yield which showed the burned HP watersheds produced more water than the reference HP watershed until the week of June 11-17 (week 24) (Figure 3.8). The maximum mean difference (residual) between burned and reference occurred during May 14-20 (week 20) when both South York and Lynx Cks. produced approximately 31 mm more water than North York Ck. Differences in timing of flow between the burned/reference watersheds was slightly different for the LP watershed pair. Drum Ck. produced higher mean weekly water yields than Star Ck. until the week of May 21-27 (week 21), at which point Star Ck. produced higher water yields thereafter through to September. The mean maximum difference between burned/reference watersheds occurred earlier in the LP watersheds, during the week of April 23-29 (week 17), when Drum Ck. produced about 18 mm more water, on average, than Star Ck. The earlier melt timing for the LP watershed pair likely reflects the lower mean elevation and greater early spring air temperatures of the LP compared to the HP watershed groups (Table 3.1).

3.3.5. Evidence of Hydrologic Recovery?

No clear post-disturbance watershed recovery trend was evident for annual water yields across the study period (Figure 3.4b and c). Analysis of covariance indicated water yield during 2005-2009 (2-6 years after the fire) in burned HP watersheds was modestly elevated by 2.3% and 8.9%, respectively, in South York and Lynx Cks. compared to North York Ck. (reference), but this was not significant ($p>0.5$). During the last 5 years of study (2010-2014, 7-11 yr. after the fire), differences were actually larger than for the earlier period: 12.3% and 31.8% higher in South York Ck. ($p=0.15$) and Lynx Ck. ($p=0.02$), respectively, compared to North York Ck. Similarly, annual water yield in Drum Ck. (LP burned watershed) was 18% higher during the earlier period (2005-2009) but approximately 3% lower during the later period (2010-2014) than Star Ck. (LP reference watershed). However, these differences were not significant ($p>0.3$).

Consistent with annual water yield, no clear trend in hydrologic recovery of monthly water yield was evident across the 2005-2014 study period (Figure 3.6a-d). For example, the percentage difference between the burned and reference HP watersheds during snowmelt (Apr.-Jun.) was greater during the last five years of the study period. The burned watersheds produced 105-187% greater April water yield and 44-61% greater May water yield than North York Ck. during the last five years; these differences were larger than during 2005-2009, the first five years of study (April=67-98%, May=40-41%) (Figure 3.6b,d). Water yields during June (peak monthly water yield for the HP watersheds) were similar across burned and reference conditions regardless of post-wildfire period, with the exception of yields in Lynx Ck. (burned) which were 23% higher than those in North York Ck. (reference) during the last five years (Figure 3.6d). Similarly, no trend was evident in the LP watersheds; during April, Drum Ck. produced 213% (2005-2009) and 189% (2010-2014) more water than Star Ck. (Figure 3.6a,c). For May, these values were 14% and 54% (it is worth noting the absence of streamflow data for Drum Ck. in 2007 likely skewed the early period results). Thus, while the five-year pre- and post-wildfire periods were still relatively short in relation to timeframes that may be required for hydrologic recovery in forested systems, no noticeable signs of recovery were apparent during years 2-11 following wildfire in this environment.

In contrast to water yields, trends in potassium:silica (K:Si) ratios suggested some recovery to hydrologic processes (runoff pathways) may have taken place over the course of the study (Figure 3.9a-f). In general, K:Si ratios for burned streams were highest in the early post-fire period (2005-2009) and decreased over time, while ratios for the reference watersheds showed no trend during the study period. However, the wildfire appeared to affect K:Si ratios in the HP burned watersheds (South York Ck., Lynx Ck.) differently than the LP burned watershed (Drum Ck.). During the early (2005-2009) post-wildfire period, median K:Si ratios for South York Ck. (0.283) and Lynx Ck. (0.286) were significantly higher than those for North York Ck. (0.207) across snowmelt and lowflow periods combined ($p<0.05$) (Figure 3.9a). During the later five-year period (2010-2014), median K:Si ratios for South York Ck. (0.249) and Lynx Ck. (0.273) were still significantly greater than in North York Ck. (0.225) for combined data (Figure 3.9d). However, this appeared to be driven by differences during low flow periods, especially for South York Ck.; both South York Ck. (0.270) and Lynx Ck. (0.283) had significantly higher K:Si ratios than North York Ck. (0.224) during low flow periods (Figure 3.9f). During the snowmelt period, K:Si ratios in South York Ck. were not significantly different ($p>0.05$) from those of North York Ck. (Figure 3.9e).

Interestingly, in the LP watersheds (Star and Drum Cks.), the only significant differences in K:Si ratios occurred during the last five years (2010-2014) for both the overall combined and the snowmelt periods (Figure 3.9d,e). The median K:Si ratios for Drum Ck. (burned) during these periods was, respectively, 0.219 and 0.216 and 0.236 and 0.240 for Star Ck. It is noteworthy that the K:Si ratio for Drum Ck. was lower than that of Star Ck. during the last five years; this could indicate that the pre-wildfire (background) K:Si ratio for Drum Ck. may have been lower than that for Star Ck.

3.4. Discussion

3.4.1. Annual Water Yield: Muted Effects of Wildfire

Annual water yield and runoff coefficients (C_R) generally showed more runoff in burned than reference watersheds but most comparisons did not show differences large enough to be statistically significant (Figure 3.3a and Figure 3.4a-c). While ten years of study is a longer period than most post-wildfire studies, power to detect differences may have been too low given the high year-to-year variability in water yield. Further, it is possible some hydrologic recovery occurred in burned watersheds during the study period which could have reduced differences between watersheds. However, this is unlikely for processes expected to take many years to fully recover such as canopy and litter interception, and solar radiation inputs. South York and Lynx Cks. (HP burned watersheds) produced 6-24% higher mean annual water yield than North York Ck. (HP reference) from ANCOVA analysis (Figure 3.4a). Further, South York and Lynx Cks. had mean C_R of 0.73 and 0.88, respectively, compared to 0.72 for North York Ck. (Table 3.2; Figure 3.3a). Notably, Lynx Ck. C_R was very near or greater than 1 during three years, which is unusually high and potentially a first-order indication of precipitation undercatch (Wortmann et al. 2018). One reason for this might be the possibility that the Lynx Ck. high-elevation precipitation gauge was not situated where the greatest alpine precipitation occurred in that watershed. In comparison to the high elevation gauges in South York and North York Cks., the Lynx Ck. High gauge is at least 160 m lower in elevation and ~450 m further away from the western ridgetop. Thus, precipitation may be higher in the upper part of the Lynx Ck. basin than our data reveal which would have the effect of elevating C_R slightly. However, mean annual water yield was consistently higher in Lynx Ck. than for any other watershed, suggesting this watershed was highly efficient at generating streamflow. For LP watersheds, ANCOVA suggested mean annual water yield was slightly higher (13%) in Drum Ck. (LP burned) than in Star Ck. (LP reference) across the study period. Further, mean C_R for Drum Ck. (0.74) were higher than those for Star Ck. (0.61), potentially suggesting more efficient routing of runoff to streamflow in Drum Ck. (Table 3.2). Elevated water yield would not be surprising for Drum Ck. given that almost 100% of its area was disturbed by the wildfire, the most of any burned watershed (Table 3.1).

In earlier work, Mahat et al. (2016) compared water yield during the first five years (2005-2010) for some of the same watersheds used in this study (excluding Drum Ck). The authors reported mean annual water yield 1.2 to 2.0 times higher in burned watersheds (South York and Lynx Cks.) when compared to the reference watersheds (Star and North York Cks.). However, Mahat et al. (2016) acknowledged that, when Star Ck. (LP reference watershed) was excluded from the analysis, "fractional increases in water yield from the burned watersheds were found to be less and varied between 1.1 and 1.2 (10% to 20%)." This result is far more in line with those from the present study and highlights the importance of selecting appropriate reference watersheds for comparison. Further, this study is notable because it demonstrates how variable climatic drivers (e.g., precipitation) can be even when watersheds are geographically near one another.

While annual water yields and C_R showed some evidence of elevation in burned watersheds, differences were relatively small given the severity of the wildfire disturbance. Further, plot-scale work showed up to 78% greater mean snow accumulation and ~50% greater mean year-round net precipitation in burned compared to reference forest stands, leading to the expectation of larger runoff responses in burned watersheds (Burles and Boon 2011; Williams et al. 2019). However, the magnitude of the fire effect on annual water yield observed in this study is consistent with results from other work conducted relatively nearby. Pomeroy et al (2012) used the Cold Regions Hydrological Model to simulate wildfire and streamflow in the Marmot Creek basin, a similar mountain environment approximately 160 km to the north of the present study. The researchers found that when 60% of the basin area was burned (100% of forested area) and burned trunks were retained, annual streamflow increased by up to 8%. During a field study following the 2003 McLure wildfire in interior British Columbia (430 km NW of present study), Eaton et al. (2010) and Owens et al. (2013) found only weak evidence for increased annual water yield in a burned watershed (Fishtrap Creek). The authors suggest desynchronization of snowmelt in burned versus unburned areas of the watershed, and dry climatic conditions combined with quick vegetation recovery following the fire could have been key factors muting annual streamflow response. Watersheds used for the B.C. study are >10 times larger than those examined in the present study, and they are much lower in both elevation (Fishtrap elevation range = 320-1620 m) and annual precipitation (<500 mm/year). Another study focused on forest harvesting disturbance situated in interior B.C. showed only a 5% increase in annual water yield after 47% of a watershed was harvested (Winkler et al. 2017). These relatively nearby western Canadian studies, despite differences in watershed scale, precipitation (especially snow accumulation), type of forest disturbance and other controls, seem to indicate relatively muted streamflow response can be expected in mountainous watersheds at similar northern latitudes despite severe forest disturbance.

3.4.2. Snowmelt (Apr. to Jun.) Magnitude and Timing

This study strongly suggested earlier onset of snowmelt occurred in the burned watersheds, delivering much more melt water in April and May, in particular, compared to reference watersheds (Figures 3.3b and 3.5-3.8). Mean monthly differences were largest in April for both LP and HP watershed comparisons (100-200% higher in burned than comparable reference), but still large for May (40-50% higher in burned than comparable reference) (Figure 3.6). June water yields were very similar between burned and reference HP watersheds, while those of the burned LP watershed (Drum Ck.) were generally lower than its unburned counterpart (Star Ck.). These results are broadly similar to modeling work reporting a 45% increase in snowmelt volume after simulation of wildfire in a nearby Rocky Mountain watershed (Pomeroy et al. 2012). Additionally, the half-flow date indicated earlier arrival of water yield by 7-10 days (Figure 3.3b) which is similar to results from Fishtrap Creek (B.C.) where the occurrence of peak flows and start of the snowmelt freshet were approximately two weeks earlier in the burned watershed than in the unburned control (Eaton et al. 2010; Owens et al. 2013).

Several additional studies have provided process-scale evidence demonstrating how wildfire can cause earlier, more intense snowmelt in burned areas. The dominant explanatory factor is likely much higher shortwave radiation because of the reduced canopy coverage in burned forests. Working in the present study area, Burles and Boon (2011) found 30% more energy available for snowmelt in a burned forest plot in comparison to an undisturbed forest plot. Moreover, two winters of observation confirmed melt rates were 2.2 times higher and the date of complete snowpack removal was 7 and 13 days earlier in the burned plot. Similarly, researchers working in the Oregon Cascades observed 60% greater shortwave radiation reaching the snowpack surface and snowpack disappearance 23 days earlier in burned forest than in unburned forest (Gleason et al. 2013). During the ablation period, Gleason et al. (2013) also found more than double the concentration of debris (e.g. charred woody debris, soot, dust) in snowpack surface samples from the burned forest. The authors suggest this likely lowered albedo, contributing an additional radiative effect. This research from fire-affected forest stands is broadly consistent with studies from forest harvesting literature which shows snowmelt rates can be 30% to >100% higher in clearcuts than in undisturbed forests (Moore and Wondzell 2005). Winkler et al. (2017) showed April and May water yields increased 29% and 19%, respectively, after logging in a watershed in interior British Columbia. The authors attribute this shift in snowmelt timing to synchronization of melt in the upper portions of south-facing cutblocks with that from lower elevations. The synchronization of snowmelt from north-facing or high elevation parts of the burned watersheds with that from lower elevations could be another key factor contributing to flows of greater magnitude early in the melt period (Gluns 2001; Moore and Wondzell 2005; Winkler et al. 2005; Smith et al. 2008).

3.4.3. Low Flow Period (Jul. to Sept.)

Low flow analyses revealed 15-18% lower July to September water yield in burned compared to reference watersheds of similar precipitation (i.e. HP and LP watersheds) (Figures 3.5c-d). Thus, while more snow likely accumulated in burned watersheds, it appears to have melted at faster rates, resulting in more runoff early in the season and slightly depressed streamflows later, during the low flow period. Forest hydrology literature reveals mixed results from investigations of low flows following forest disturbance. In a recent review, Goeking and Tarboton (2020) examined 25 studies which investigated low flows after a range of disturbance types in North American coniferous forests and found that 14 showed increased low flow magnitude, 9 found no change and 9 found decreases. In an analysis of 82 Western U.S. watersheds affected by wildfire, Saxe et al. (2018) found elevated low flows for 1-2 years post-fire; this response was most strongly related to area burned. Kinoshita and Hogue (2015) found that annual low flow volume in two burned watersheds in southern California increased by 118% (City Creek) and 1090% (Devil Canyon) when compared with pre-fire data. While these studies, as well as several from harvested watersheds, have shown increased low flows following disturbance, others have shown decreases. For example, in their nearby research (British Columbia), Winkler et al. (2017) observed 20% and 17% decreases (not statistically significant) in July and August streamflow after 47% of a watershed was harvested; this is broadly consistent with differences observed in the present study between burned and reference watersheds. In Argentina, Cingolani et al. (2020) found low flow reductions of 31-48% when comparing 12 small burned to 12 unburned watersheds. Cingolani et al. (2020) allude to the "infiltration-evapotranspiration trade-off hypothesis" (Bruijnzeel 1989, 2004), which suggests reduced infiltration following forest disturbance leads to reductions in groundwater recharge, and the potential for reduced dry-season low-flows. While fire effects on infiltration is a key factor, the direction and magnitude of post-wildfire low flow change also depends on the tradeoff between reductions in interception and transpiration (favouring low flow increases) and increases to post-disturbance radiation and evaporative effects (favouring low flow decreases). The influence these processes exert on groundwater recharge is likely very important because groundwater provides most of the contributions to summer low flows in the present study watersheds.

Very little is known about the longer-term recovery of post-wildfire low flows. Recent studies from forest harvesting research have suggested 10 years may not be long enough to characterize disturbance effects on low flows. In a study from interior British Columbia, Gronsdahl et al. (2019) found that summertime low flows were unaffected by forest harvesting for almost two decades, at which time reduced low flows were observed in the disturbed watershed, suggesting increased water use by the young regenerating forests. Similarly, other long-term work in the Pacific Northwest has shown that watersheds with young Douglas-fir plantations (34-43 years old) had 50% lower mean streamflow during July to September (within 15 years of planting) than mature forested watersheds (Perry and Jones 2017). These results suggest future summer low flows (2020 or later) in our burned watersheds could be influenced by transpiration rates of regenerating conifers, among other factors.

3.4.4. Hydrologic Recovery

A paradox emerged between insights from water yield results and potassium-silica (K:Si) ratios over the study period. Specifically, water yield showed no evidence of hydrologic recovery in burned watersheds while K:Si ratios did suggest some recovery of surface:subsurface flow path partitioning during the 10-year period (Figures 3.4b-c, 3.6a-d, 3.9). The lack of water yield recovery in burned watersheds is perhaps not surprising given the slow growth rates of the higher-elevation coniferous forests in the study area. It may take decades for processes such as canopy interception, evapotranspiration and incoming radiation to recover sufficiently to detect their influence on seasonal or annual water yield. While most studies have focused on the early (<5 years) hydrologic effects of wildfire, some work is beginning to examine longer-term impacts. For example, while annual discharge was strongly elevated (+150% to 202%) in three burned watersheds during the first 7 year period (1971-1977) after wildfire in Washington, results from post-fire years 35-41 (2005-2011) suggested management actions aided hydrologic recovery — discharge in two watersheds, which were salvage-logged and aerially seeded, appeared to have completely recovered (i.e. returned to pre-fire levels) while a watershed which was burned and left to recover without human intervention continued to show elevated discharge even after decades of recovery (Niemeyer et al. 2020).

While water yield can be viewed as a measurement of the outcome of many hydrologic processes regulating watershed-scale streamflow, K:Si ratios more specifically focus on a particular set of hydrologic processes. Potassium originates in both living and dead terrestrial materials and is generally associated with near-surface hydrologic pathways whereas silica is associated with geological substrate and the slow movement of water through the subsurface (Elsenbeer *et al.* 1995). Thus, the ratio of the two (K:Si) describes the relative contribution to streamflow of fast (surface) versus slow (subsurface) pathways. This study showed generally elevated K:Si ratios for the burned watersheds and a decrease in the ratio during the 10-year study period, though response differed between burned HP and LP watersheds (Figure 3.9). Further, HP and LP reference watersheds (North York and Star Cks.) did not have significantly different K:Si ratios during any combination of post-wildfire time period or flow condition (all/snowmelt/baseflow), demonstrating consistency among undisturbed watersheds. The decreasing K:Si ratios in burned watersheds would be consistent with greater plant uptake of K^+ as vegetation regenerated in the disturbed watersheds (Tripler et al. 2006; Jung et al. 2009) though accurate quantification of surface/subsurface shifts in flow were not possible within the context of this study. Other research suggests the measurement of ions in additional independent stream water sources (e.g. groundwater and precipitation) would be required to perform end-member mixing analyses (Jung et al. 2009) which might allow more robust characterization of differences in hydrologic flow pathways (Bonnell and Fritsch 1997). However, this was outside the scope of this study.

3.4.5. Uncertainty Within LP and HP Watershed Groups

Inherent differences in physical characteristics between burned and reference watersheds would be expected to lead to some differences in runoff behaviour, independent from the influence of wildfire. Physical characteristics serving as key controls on runoff timing and magnitude in snow dominated watersheds include watershed size, aspect distribution, slope gradient, elevation gradient, percent alpine area, vegetation (density, canopy coverage, etc.), and geology (Green and Alila 2012; Jost et al. 2007; Pfister et al. 2017). Several studies have shown that elevation is the dominant control over snow accumulation and that alpine areas capture a large proportion of SWE in mountainous watersheds because of the combination of very low interception and high precipitation (Jost et al. 2007; Grunewald et al. 2010; Dixon et al. 2014; Spencer et al. 2019). For example, alpine snow courses at the Marmot Creek watershed study displayed greater than four times the SWE measured at lower elevation snow courses from 2005-2013 (Harder et al. 2015). Similarly, earlier snowmelt would be expected for watersheds with proportionally more slope aspects receiving high solar radiation (e.g. south and west-facing). Despite broad similarities in physical characteristics between the five study watersheds, they differed somewhat with respect to precipitation and watershed physiography. Annual precipitation in three (North York, South York, and Lynx Cks) was clearly higher than that in the other two watersheds (Star and Drum Cks). This still allowed reasonable comparisons because one unburned reference watershed could be included in the high precipitation

(HP) and one in the low precipitation (LP) groups (North York and Star Creeks, respectively). However, uncertainty in the interpretation of results likely differs within the groups.

Based on the physical characteristics of the watersheds in this study, differences in elevation gradient, slope aspect and percent alpine area are the most likely to have caused potential confounding effects on streamflow (timing) within the HP and LP groups (Table 3.1). However, watersheds in the HP group likely represent a near-ideal comparison for a replicated watershed study design owing to their strong physical similarities and very close proximity. Solely based on aspect, earlier snowmelt might be expected in the HP burned watersheds (Lynx and South York Cks.) in comparison to the reference watershed (North York Ck.) because their aspect distributions include slightly more south-facing and less north-facing slopes than North York Ck. (Table 3.1). The potential confounding effect because of differences in aspect would be expected to influence water yield in the same direction as wildfire (i.e. earlier snowmelt). However, the effect of elevation would be expected to exert the opposite influence. While the elevation of the North York Ck. hydrometric station is approximately 1550 m, the elevations of the burned HP hydrometric stations are 1650-1700 m (Lynx and South York Cks.) (Table 3.1). Thus, earlier melt would be expected in the reference watershed based only on the influence of elevation, an effect which could compensate for the potential confounding effect of aspect. While North York Ck. has a slightly larger alpine area than South York and Lynx Cks., the latter two watersheds lost most of their forest canopy cover to the wildfire suggesting remaining canopy interception should not contribute to large differences in snow accumulation at higher elevations in these three watersheds. These key influences combined with the very similar annual precipitation among the HP group suggest lower uncertainty in water yield results between burned and reference watersheds.

A similar comparison of physical characteristics for the LP watersheds (Star and Drum Cks.) suggests there could be higher uncertainty within this group than for the HP group. In addition to Star and Drum Ck. being further apart (potentially leading to slight differences in weather patterns), differences in maximum elevation, alpine area and slope aspect are larger than for the HP group, potentially confounding the interpretation of water yield results. Perhaps the most important difference is the lower maximum elevation and absence of a true alpine zone in Drum Ck. relative to Star Ck. (Table 3.1; maximum elevation ~500 m lower). These features could lead to comparatively less snow accumulation in Drum Ck. Additionally, the Drum Creek watershed featured more slope aspects which would be expected to produce snowmelt earlier (i.e. more “warm” aspects; Table 3.1) thereby potentially influencing melt in the same direction as the wildfire. However, despite these physical differences, precipitation and resulting water yield were very comparable between watersheds in the LP group (Figure 3.2) which provides strong rationale supporting comparisons between these watersheds. While the removal of the LP group was considered in order to focus on the most comparable watersheds and simplify analyses, this comparison was included for three main reasons. First, inclusion of this group respects the original, *apriori* study design which was conceived without prior knowledge of the meteorological conditions in the watersheds. Second, at a high level, Star and Drum Cks. are far more similar than different with respect to many characteristics including watershed area, mean elevation, annual precipitation, water yield, and geology, making for a very reasonable comparison. Lastly, the LP group is an interesting comparison in its own right and represents an important opportunity to shed additional light on wildfire effects across northern Rocky Mountain watersheds with variable precipitation and runoff. This opportunity would be lost without the inclusion of the LP watershed group here. Still, greater caution is likely warranted with respect to results for the LP group than for the HP group.

3.5. Key Findings

This study generated a number of insights on the potential changes to the magnitude and timing of water yield in Canadian Rocky Mountain watersheds after wildfire. While the study design precluded the use of some formal statistical techniques, some consistent trends were revealed across the burned watersheds during the ten-year study period. Annual water yield was higher in burned than in reference watersheds by 6-24% in the HP watersheds (South York and Lynx Cks.) although this was only marginally significant for the North York Ck./Lynx Ck. comparison (Figure 3.4a). Similarly, annual yield in the burned LP watershed (Drum Ck.) was 13% higher than in the LP reference (Star Ck.) despite its lower elevation, lack of alpine zone and moderately lower annual precipitation compared to Star Ck. (Figure 3.4a; Tables 3.1 and 3.2). Much higher April and May water yields were evident across all burned watersheds in comparison to reference watersheds with similar precipitation (Figures 3.6 and 3.7). Further, half flow dates (earlier in burned watersheds), flow duration curves and weekly water yield results strongly suggested advanced snowmelt and a shift in timing of burned hydrographs to earlier in the year (Figures 3.3b, 3.7, 3.8). Many of these findings are highly consistent with past studies on the effects of forest disturbance on snowmelt processes and streamflow. One of the most surprising findings here was lower summertime low flows in the burned watersheds (Figures 3.5c-d and 3.6). This is not the first study to observe this, but it contrasts with many hydrologic studies from the forest disturbance literature showing higher low flows in disturbed watersheds.

Higher precipitation during the latter half of the study period resulted in significant increasing trends in some water yield metrics, but no clear post-disturbance recovery trends were evident for water yield in burned watersheds. Hydrologic recovery can be expected to occur with vegetation regrowth and reestablishment of soil hydraulic properties. At the present study site, and depending on elevation, some vegetative ground cover can regenerate within 1-2 years, but 15-20 years are required for trees to reach two metres in height owing to slow growth rates at higher elevations. Thus, while this ten-year investigation is longer than many post-wildfire studies, hydrologic recovery may not be evident (or occurring) over this time period. In contrast to water yield results, potassium-silica (K:Si) ratios revealed some recovery of surface:subsurface flow path partitioning from the early (2005-2009) to the later (2010-2014) periods especially in the HP burned watersheds (South York and Lynx Cks.). Determining whether these results indicate a return to pre-fire hydrologic pathways in the burned watersheds likely requires further research.

3.6. Tables

Table 3.1. *Watershed characteristics. "Alpine Area" includes exposed bedrock, talus, open meadow and shrubland. Aspect information pertains, conceptually, to low (N; North), neutral (E+W; East + West), and high (S; South) solar energy inputs. Low precipitation (LP) and high precipitation (HP) watershed groups indicated in Watershed column.*

Watershed	Condition	Watershed Area (ha)	Burned Area (ha / % of watershed)	Alpine Area (ha; %)	Mean Elevation (Range) (m)	Mean Watershed/Stream Slope (degrees)	Aspect (% area by class N / E+W / S)
LP group							
Star Ck.	reference	1035	0 (0.0)	448 (43)	1496 (1496-2632)	24 / 6	41 / 54 / 5
Drum Ck.	burned	719	712 (99)	0 (0.0)	1466 (1466-2162)	26 / 8	20 / 66 / 13
HP group							
North York Ck.	reference	865	2 (0.2)	370 (43)	1555 (1555-2657)	25 / 8	38 / 47 / 14
South York Ck.	burned	365	191 (52)	115 (32)	1704 (1704-2639)	22 / 7	37 / 43 / 20
Lynx Ck.	burned	781	553 (71)	192 (25)	1643 (1643-2641)	23 / 8	33 / 39 / 28

Table 3.2. *Water year (Oct 1 – Sept 30) precipitation (P), water yield (Q) and runoff coefficient (C_R) for the study watersheds. Drum streamflow data were not available for 2007 because of stage sensor malfunction. Runoff ratios equal to or >1 likely contain relatively large errors and are highlighted in red. Low precipitation (LP) and high precipitation (HP) watershed groups indicated above stream names.*

	LP group						*HP group*								
	Star Ck. (R)			Drum Ck. (B)			North York Ck. (R)			South York Ck. (B)			Lynx Ck. (B)		
Water Yr.	P (mm)	Q (mm)	C_R	P (mm)	Q (mm)	C_R	P (mm)	Q (mm)	C_R	P (mm)	Q (mm)	C_R	P (mm)	Q (mm)	C_R
2005	1215	706	0.58	1072	693	0.65	1385	1097	0.79	1388	1113	0.80	1425	1097	0.77
2006	754	597	0.79	596	553	0.93	946	880	0.93	1266	751	0.59	1077	954	0.89
2007	1031	459	0.45	799	N/A	N/A	1407	719	0.51	1430	828	0.58	1253	876	0.70
2008	809	379	0.47	775	423	0.55	1080	681	0.63	1281	810	0.63	1174	611	0.52
2009	740	342	0.46	630	393	0.62	948	554	0.58	1063	809	0.76	957	801	0.84
2010	933	468	0.50	894	527	0.59	1302	787	0.60	1298	987	0.76	1177	1025	0.87
2011	735	736	1.00	815	631	0.77	1160	1026	0.88	1428	1113	0.78	1138	1505	1.32
2012	1028	647	0.63	781	541	0.69	1387	1008	0.73	1299	1252	0.96	1318	1365	1.04
2013	1248	632	0.51	814	625	0.77	1625	1008	0.62	1605	1132	0.71	1466	1335	0.91
2014	1050	699	0.67	813	864	1.06	1278	1110	0.87	1423	1064	0.75	1279	1261	0.99
mean	954	567	0.61	799	583	0.74	1252	887	0.72	1348	986	0.73	1226	1083	0.88
median	981	615	0.54	806	553	0.69	1290	944	0.68	1343	1026	0.75	1215	1061	0.88
st. dev.	192	143	0.18	131	143	0.17	218	193	0.15	143	174	0.11	155	282	0.21

Table 3.3. *Daily flow exceedance values (mm) at the 10%, 25%, and 50% thresholds during April-September for the study watersheds across the study period. Values come from flow duration curves produced for 2005-2014 study period (Figure 3.7). Low precipitation (LP) and high precipitation (HP) watershed groups indicated in Stream column.*

	April			*May*			*June*			*July*			*August*			*September*		
Stream	*10*	*25*	*50*	*10*	*25*	*50*	*10*	*25*	*50*	*10*	*25*	*50*	*10*	*25*	*50*	*10*	*25*	*50*
LP group																		
Star Ck. (R)	1.0	0.7	0.5	7.4	5.1	2.4	9.4	7.1	5.0	4.2	2.8	1.9	1.7	1.4	1.1	2.1	1.1	0.8
Drum Ck. (B)	3.5	2.3	1.5	8.9	5.5	3.6	5.9	3.7	2.5	2.3	1.8	1.4	1.5	1.3	1.0	2.5	1.5	0.8
HP group																		
North York Ck. (R)	2.0	1.1	0.6	13.0	8.6	5.2	14.5	11.5	8.4	6.6	4.7	3.1	2.4	1.9	1.5	2.5	1.5	1.1
South York Ck. (B)	4.4	1.9	1.1	16.9	12.1	7.2	14.6	11.5	8.5	5.9	3.6	2.3	2.3	1.6	1.1	3.0	1.5	1.1
Lynx Ck. (B)	4.2	2.3	1.5	15.9	11.8	7.9	16.2	11.6	8.4	5.8	3.9	2.5	1.9	1.6	1.2	2.3	1.4	1.0

3.7. Figures

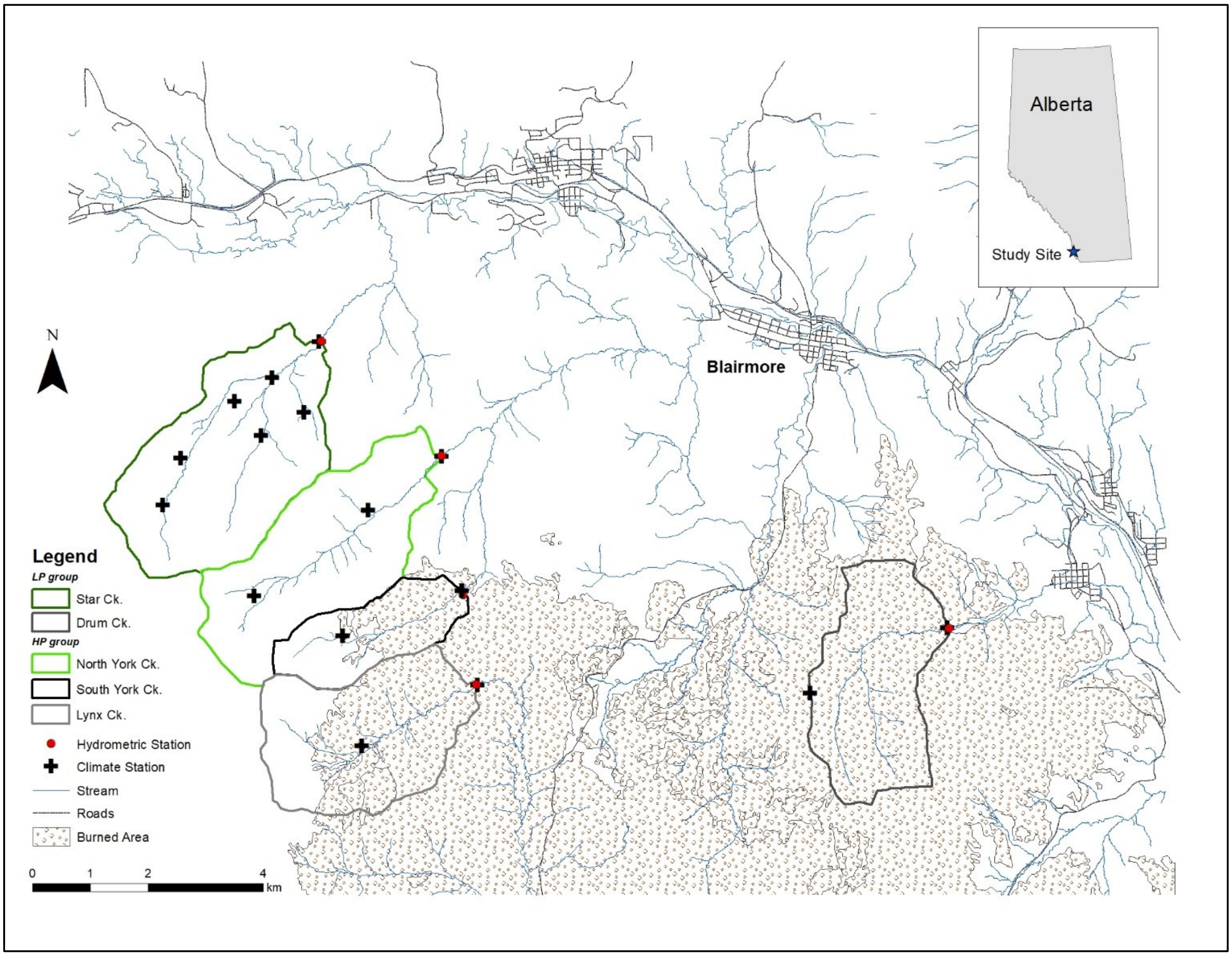

Figure 3.1. *Map of study watersheds situated near the northern extent of the 2003 Lost Creek wildfire. Star Ck. (reference) and Drum Ck. (burned) represent the low precipitation (LP) group. North York Ck. (reference), South York Ck. (burned) and Lynx Ck. (burned) represent the high precipitation (HP) group.*

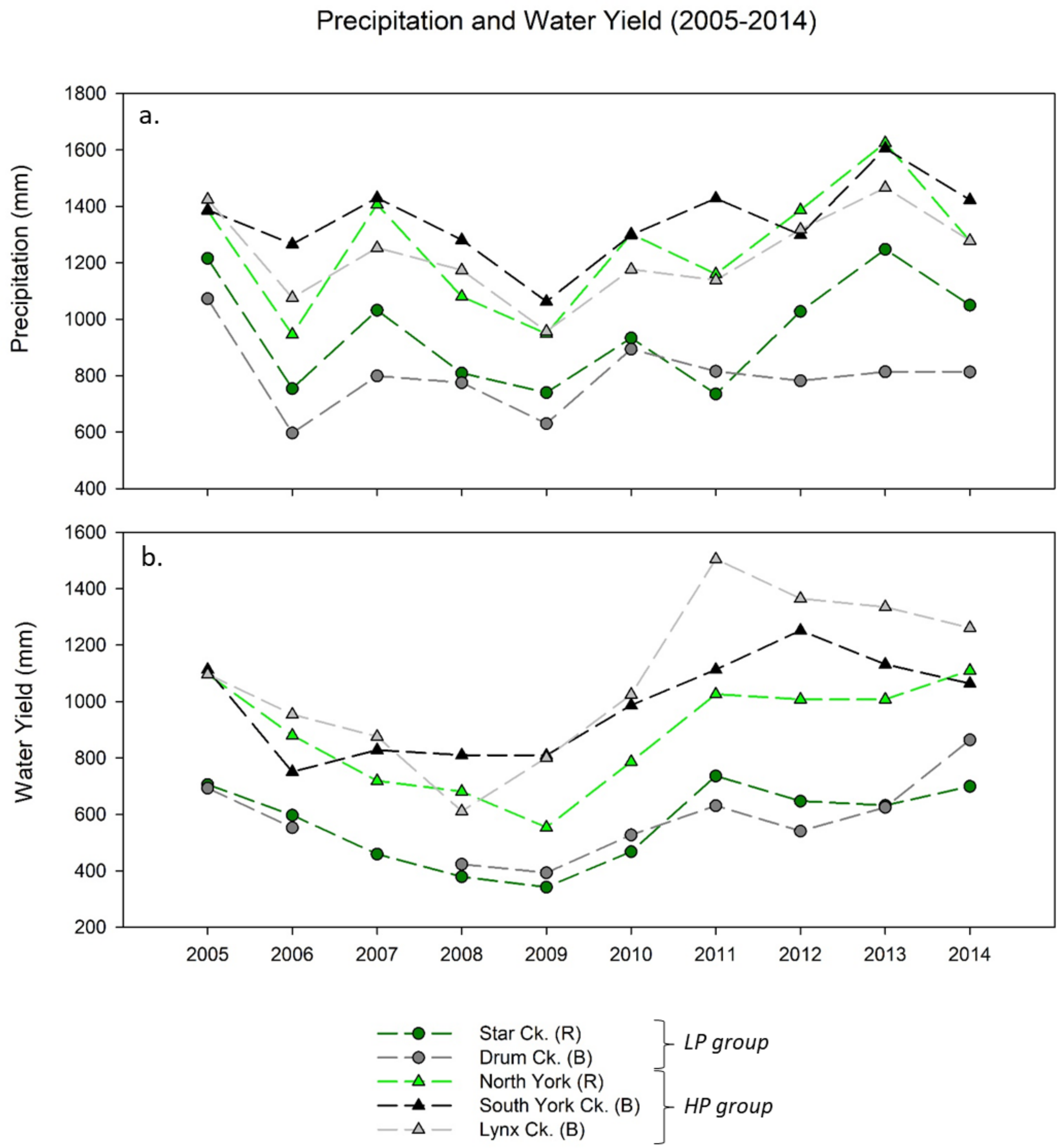

Figure 3.2. *Water year precipitation (a) and water yield (b) for each of the study watersheds. In the legend, "R" indicates unburned reference watersheds and "B" indicates burned watersheds. Triangles are used for "high precipitation" (HP) watershed group and circles for "low precipitation" (LP) watershed group in figures.*

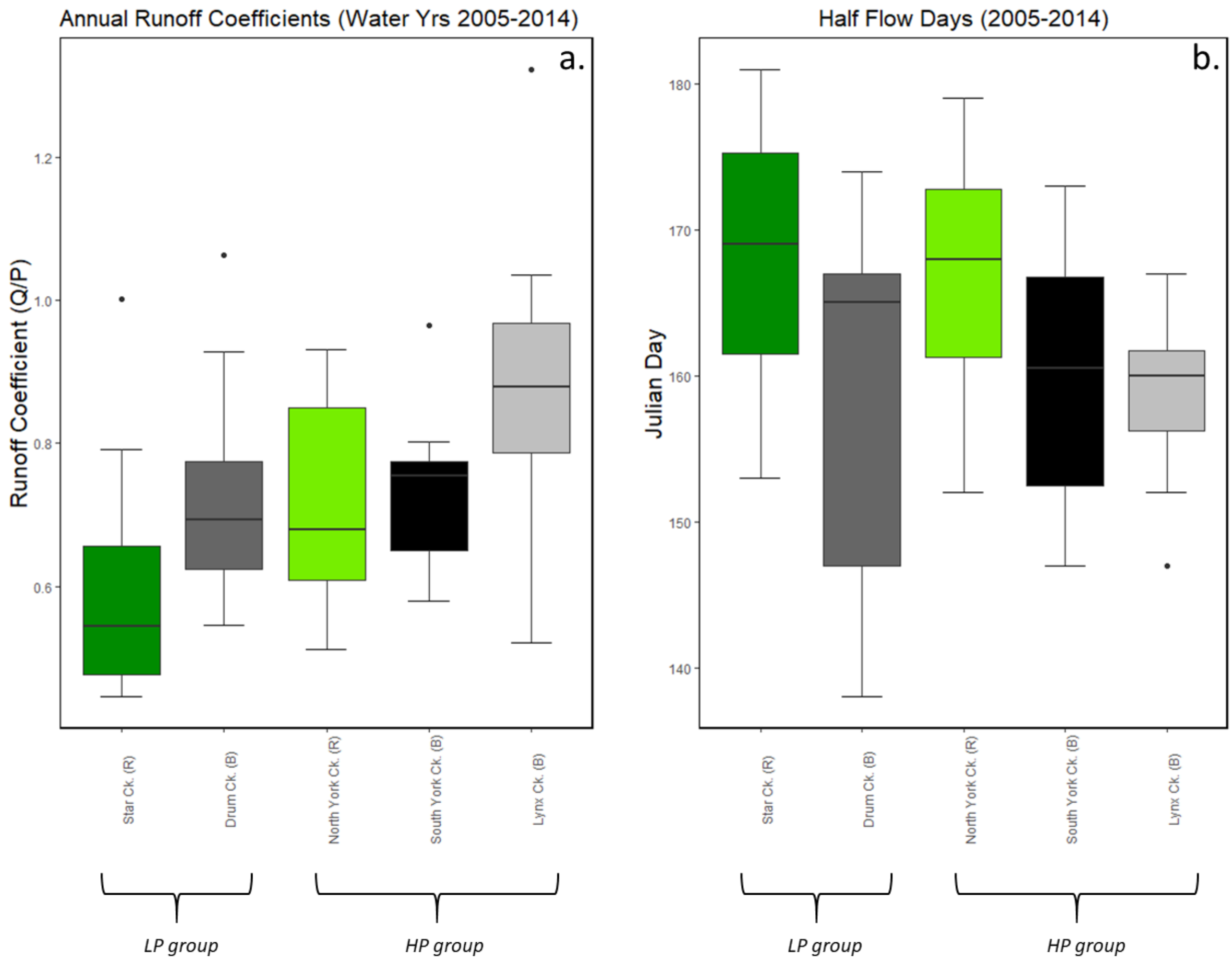

Figure 3.3. *Left panel (a): Water year (Oct. 1 – Sept. 30) runoff coefficients (C_r) for reference (R) and burned (B) watersheds across the study period (2005-2014). Right panel (b): Half flow dates for each stream across the study period. The half flow date is defined as the Julian day upon which half of the calendar-year streamflow has passed the gauging station. Low precipitation (LP) and high precipitation (HP) watershed groups indicated below each boxplot. Median indicated by horizontal line inside each box. Upper and lower hinges indicate 25th and 75th percentiles. Upper and lower whiskers extend to the highest (or lowest) value that is within 1.5 * IQR of the hinge. Outliers indicated by black points.*

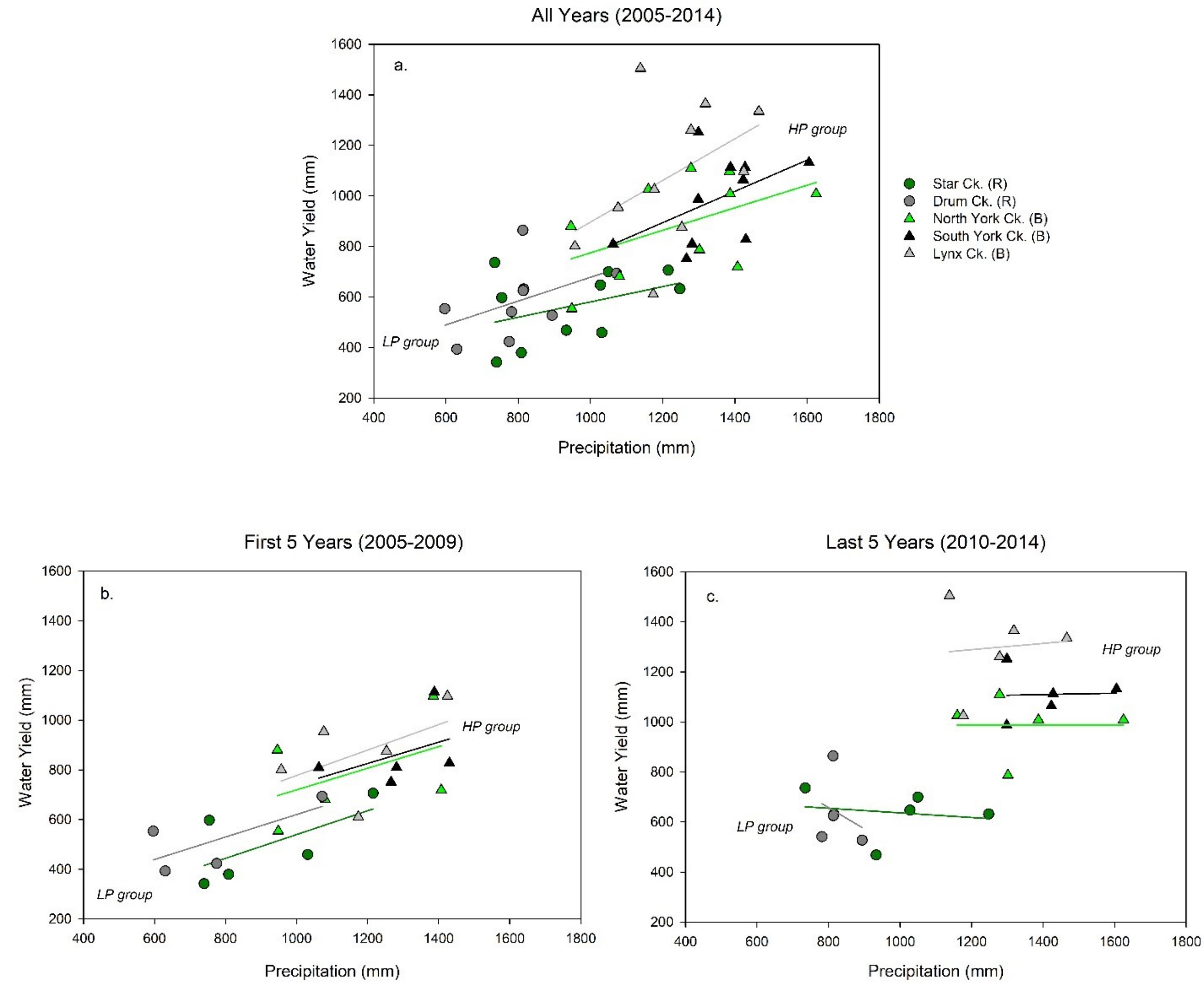

Figure 3.4. *Relationship between water year (Oct. 1 – Sept. 30) precipitation and water yield for all watersheds across a) all study years (2005-2014); b) the first 5 years of study (2005-2009); c) the last 5 years of study (2010-2014). Circles indicate low precipitation (LP) watershed group and triangles indicate high precipitation (HP) group.*

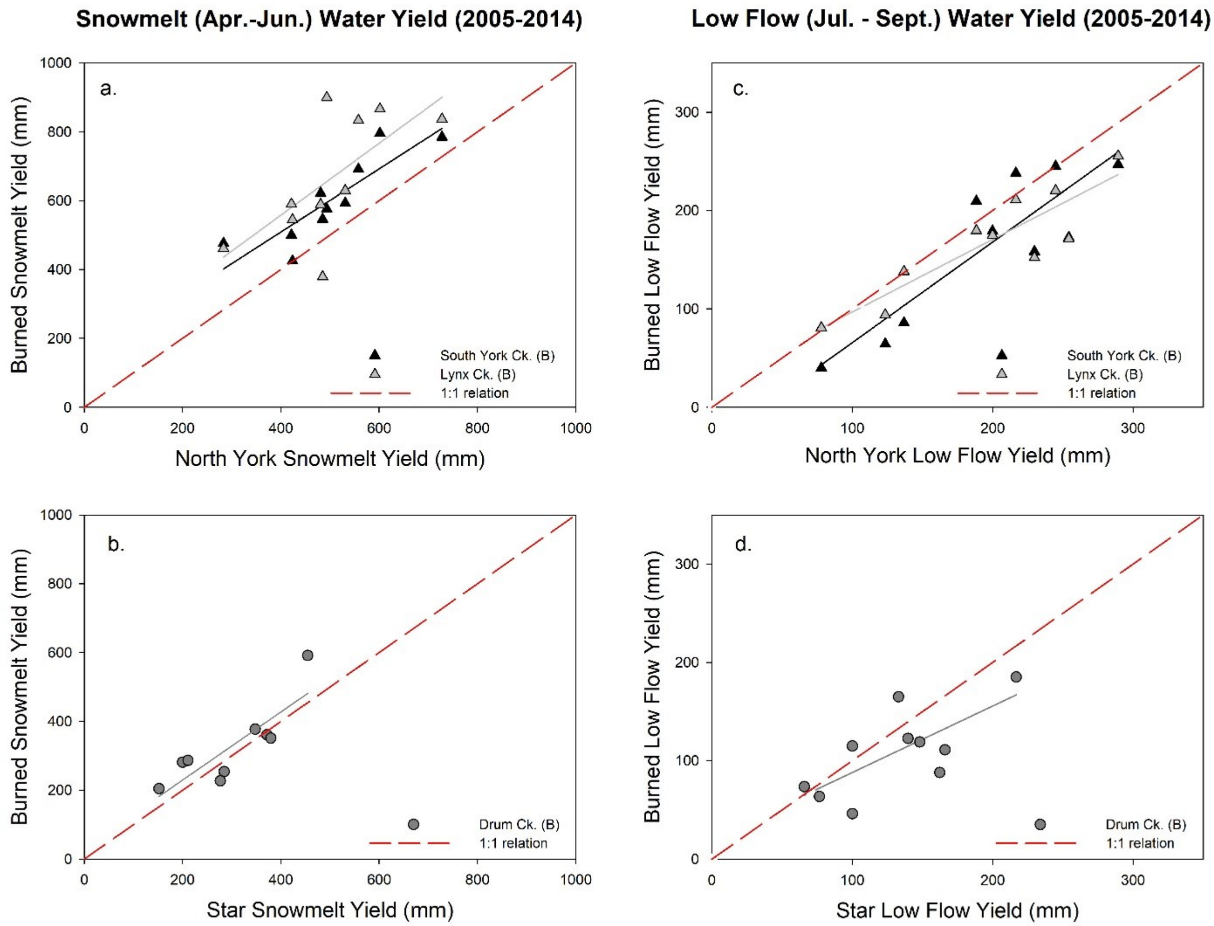

Figure 3.5. *Water yield from burned watersheds in comparison with that from unburned reference watersheds for the snowmelt (April to June) and low flow (July to September) periods across the study (2005-2014). Left-hand plots show relationships during the snowmelt period for: a) high precipitation (HP) watersheds using North York Ck. as reference and; b) low precipitation (LP) watersheds using Star Ck. as reference. Right-hand panels show relationships during the low flow period for: c) HP watersheds and d) LP watersheds using same references as snowmelt period. Red dashed line is the 1:1 relation for comparison.*

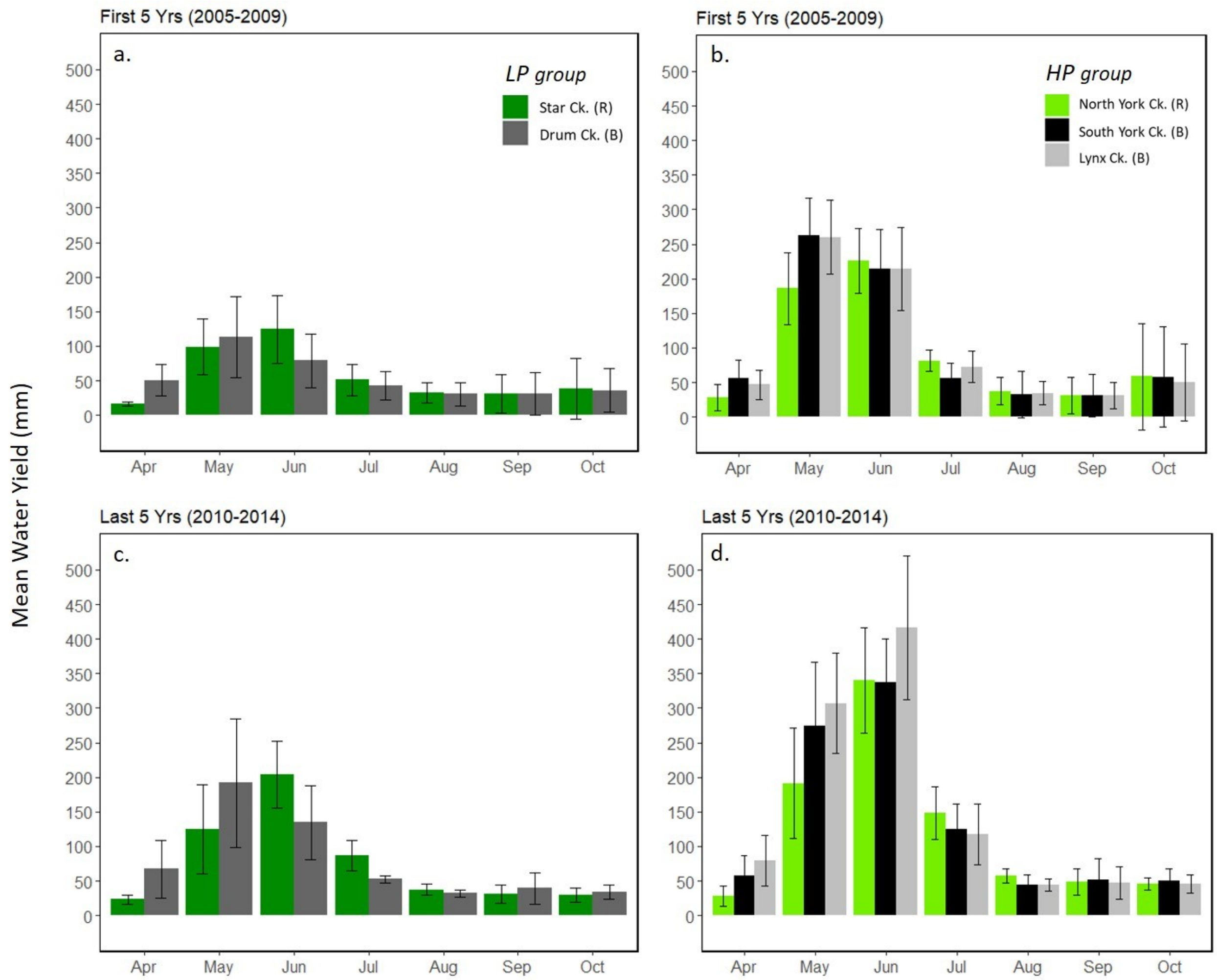

Figure 3.6. *Mean monthly water yield during ice-free season (Apr. – Oct.) in the five study watersheds: a) low precipitation (LP) watershed group during first 5 years (2005-2009); b) high precipitation (HP) watershed group during first 5 years (2005-2009); c) low precipitation (LP) watershed group during last 5 years (2010-2014); d) high precipitation (HP) watershed group during last 5 years (2010-2014). In legend, (R) and (B) symbolize reference and burned watersheds, respectively. Error bars indicate standard deviation.*

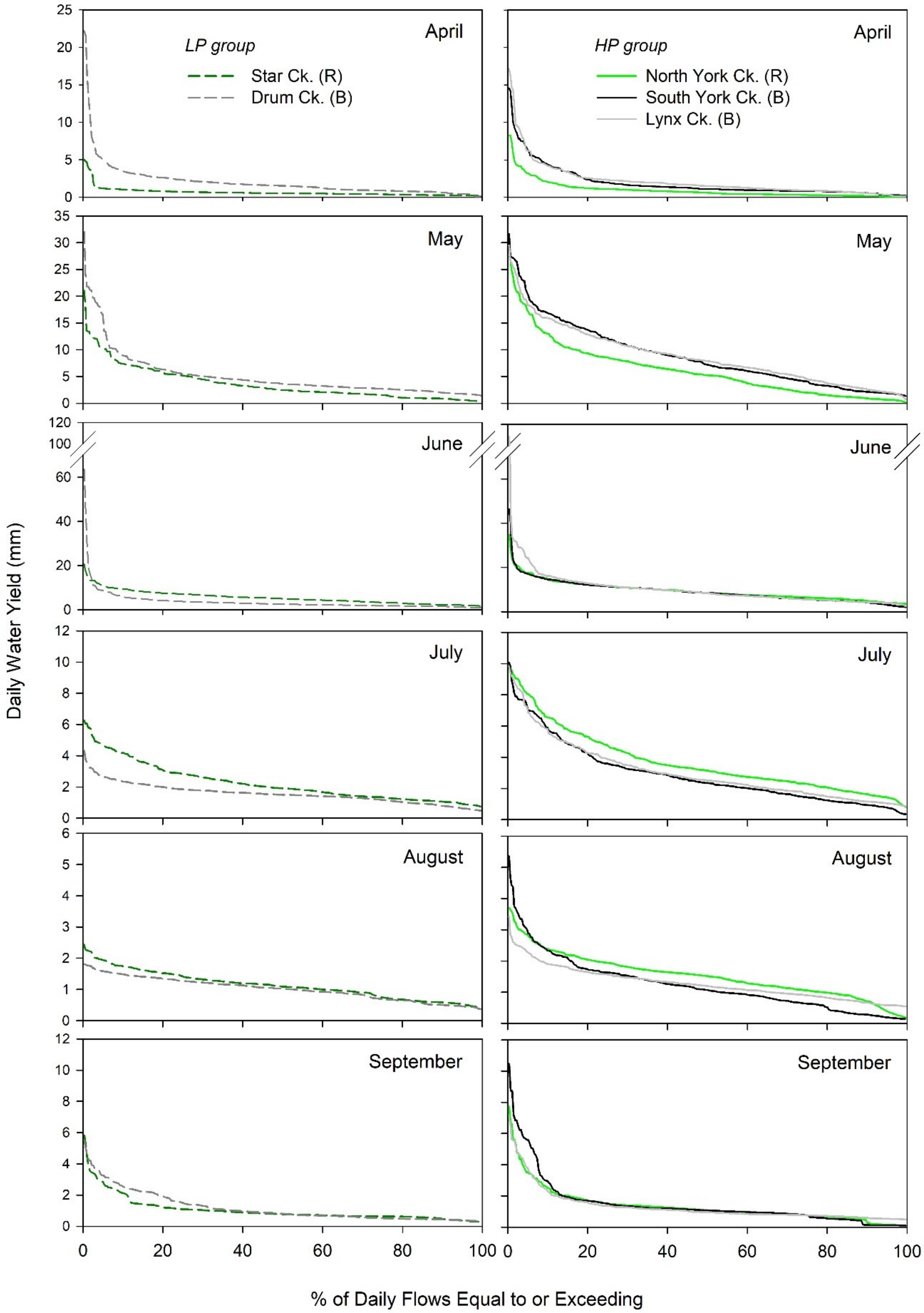

Figure 3.7. *Flow duration curves for daily water yield (Apr. to Sept) for reference and burned watersheds across the study period (2005-2014). Low precipitation (LP) group on left, high precipitation (HP) group on right.*

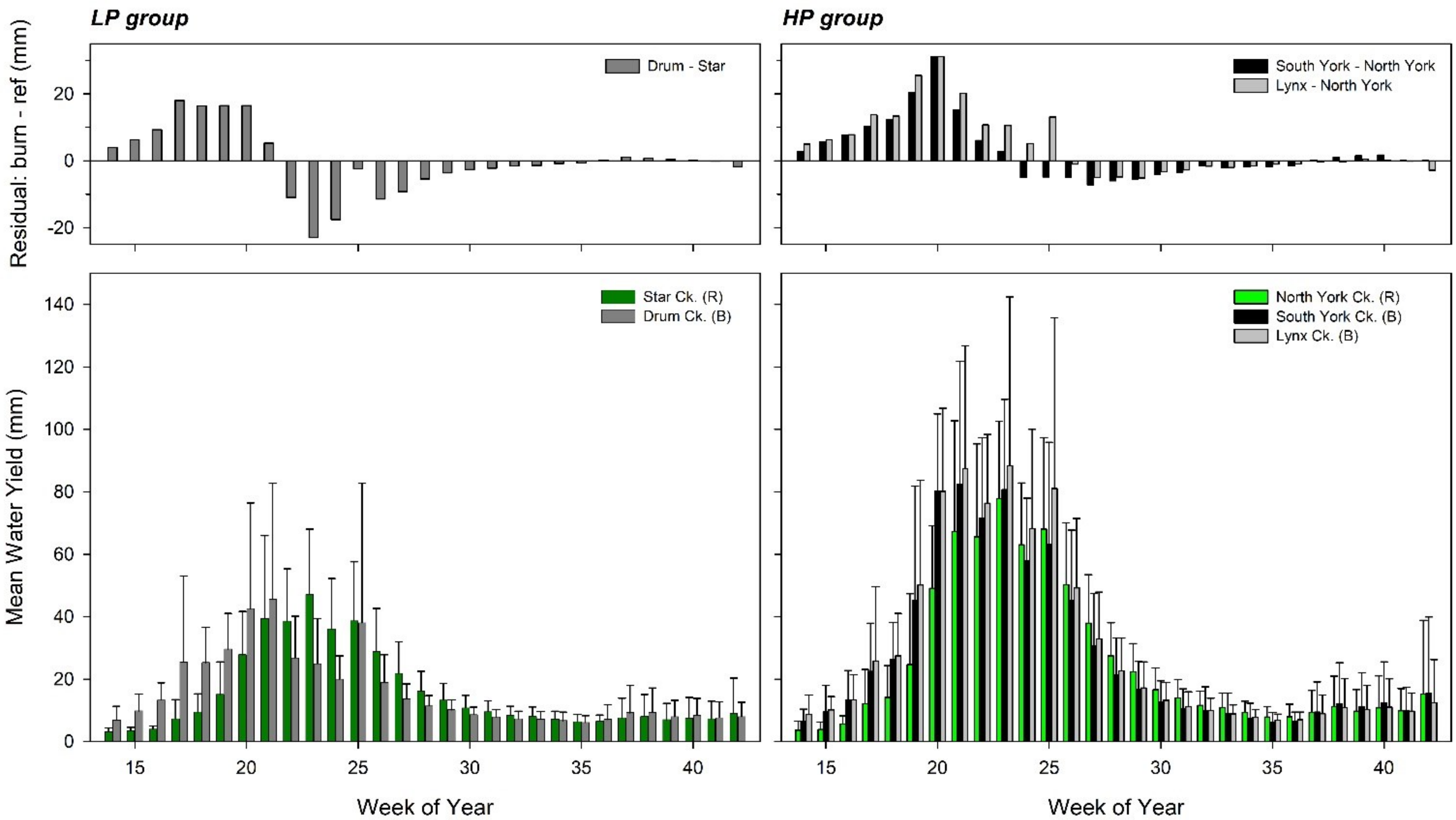

Figure 3.8. *Bottom graphs: Mean weekly water yield over the ten years of study (2005-2014) during the ice-free part of the year, generally encompassing week 14 (Apr. 2-8) through week 42 (Oct. 16-22). Top graphs: Residual differences in mean weekly water yield between burned and reference catchments of similar annual precipitation (values >0 indicate more yield in burned relative to reference watershed). Low precipitation (LP) watershed group on the left, high precipitation (HP) group on the right. Error bars indicate standard deviation.*

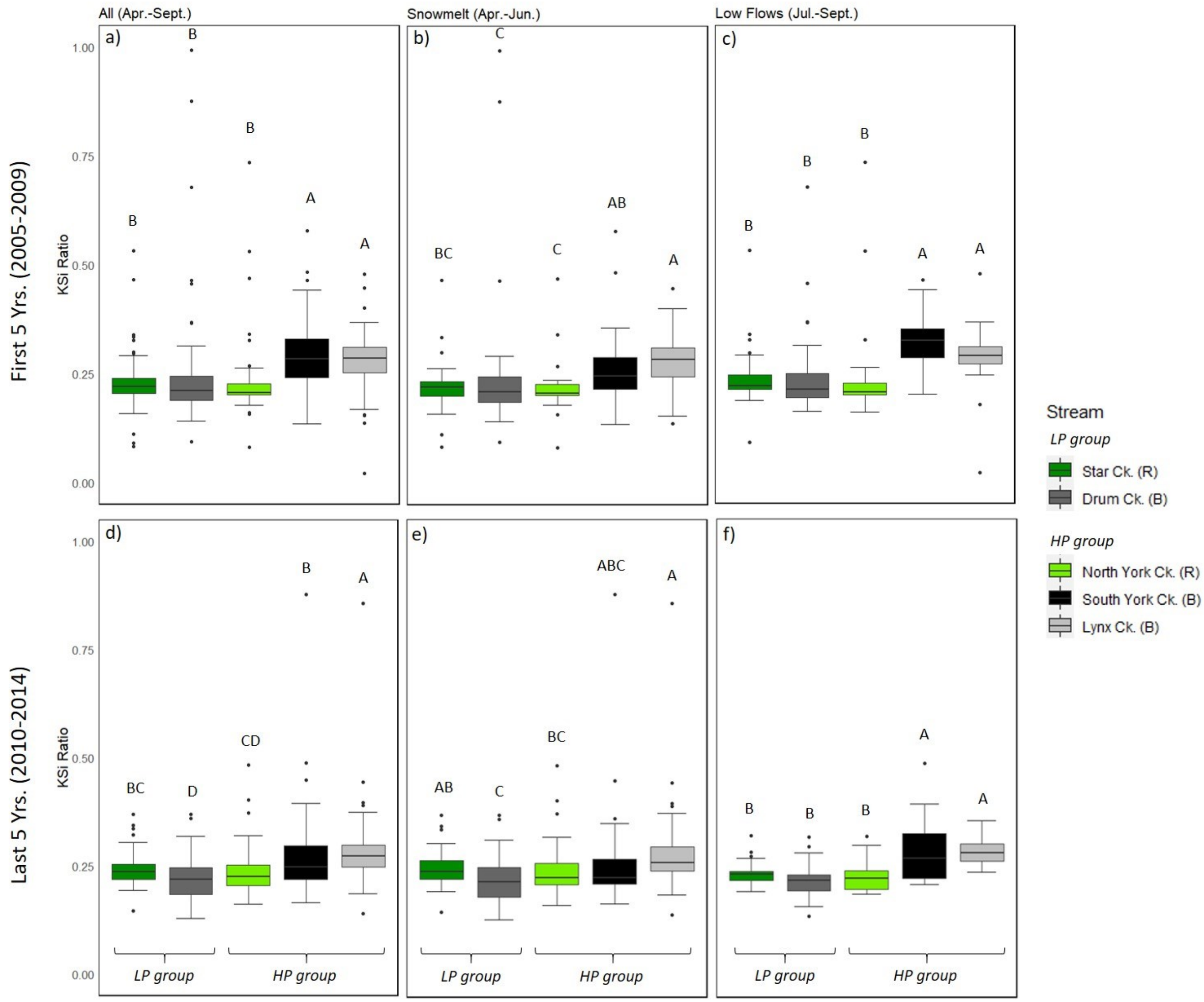

Figure 3.9. *Potassium:Silica (KSi) ratios for each stream during the first 5 years (2005-2009; top panels a-c) and last 5 years (2010-2014; bottom panels d-f) of data collection following the wildfire (2003). Median indicated by horizontal line inside each box. Upper and lower hinges indicate 25th and 75th percentiles. Upper and lower whiskers extend to the highest (or lowest) value that is within 1.5 * IQR of the hinge. Outliers indicated by black points. In legend, reference streams indicated with (R) and burned with (B). "LP group" indicates low-precipitation watersheds and "HP group" indicates high-precipitation watersheds. Uppercase letters (A-D) above boxplots indicate statistical significance – streams with identical letters (within same panel) are not significantly different from one another. Columns (left, middle, right, respectively) depict 1) all data for snowmelt and low flow period combined; 2) snowmelt (Apr. to Jun.); 3) low flow period (Jul. to Sept.).*

Chapter 4. Rainfall – storm runoff relationships after wildfire over a 10-year period in Rocky Mountain watersheds, Alberta, Canada

4.1. Introduction

Increasing frequency of large, severe wildfires is a growing concern in North America. In the Western U.S. the frequency of large wildfires, wildfire duration, and fire season length have all increased in recent decades and these changes have coincided with increased drought severity (Westerling et al 2006; Dennison et al 2014). The trends are similar in Canada; during the 1959-2015 period, annual area burned (mainly in Western Canada) and number of large fires have increased significantly. Large fires (>200 ha) are responsible for >90% of the area burned nationally; the size of the largest fires is trending upwards as well (Hanes et al 2019). Canada's two western-most provinces have experienced particularly severe wildfires in recent years. The 2017 fire season in British Columbia was the worst on record, burning 1,210,000 ha of land, but was quickly exceeded by area burned during the 2018 fire season (Coogan et al 2019). In Alberta, the 2016 Horse River wildfire was one of the costliest natural disasters in Canadian history, destroying several homes in the city of Fort McMurray and causing water quality impacts detectable even at large basin scales (Emmerton et al. 2020). Given the increasing prevalence of wildfire, governments and water managers are increasingly concerned about potential hydrologic and water quality impacts from these events.

Wildfire can affect a number of hydrological processes, potentially accelerating the routing of rainfall to streams. This can increase storm runoff and potentially result in damaging post-fire flow events in some regions. Consumption of the forest canopy by severe wildfires greatly reduces the interception of precipitation allowing more rain and snow to reach the forest floor (Moore et al 2008; Williams et al 2019). Evapotranspiration can be greatly reduced (Niemeyer et al. 2020) and result in increased soil moisture which, in turn, can promote greater runoff. Depending on the severity and intensity of the fire, much of the understory vegetation and organic layers can be burned, leaving an ash-covered mineral soil surface (Pereira et al 2015; Ebel et al. 2012). Combustion of litter and organic layers reduces surface roughness and physiochemical changes to the soil surface have been shown to cause soil water repellency, reducing infiltration of precipitation (Debano 2000; Doerr et al. 2006). Further, soil sealing in areas lacking ground cover (Larsen et al. 2009) and reduced infiltration due to the clogging of soil pores (Woods and Balfour 2010) can lead to additional routing of precipitation to surface runoff. In some regions, these impacts can lead to sediment-laden floods, widespread soil erosion and debris flows (Robichaud et al. 2000; Cannon et al. 2008; Ryan et al. 2011; Kean et al. 2011) that have resulted in significant downstream damage or even loss of life in some instances. Other areas experience less dramatic hydrogeomorphic response, but many studies suggest greater runoff via near-surface hydrologic pathways is likely in most post-wildfire landscapes. However, because much of this research has focused on the period immediately following wildfires (the first year or two), the longer-term effects of wildfire on peak flows generated from large precipitation events remains unclear. This is especially important in the Canadian Rocky Mountains where previous research has suggested potential catchment-scale resilience to disturbance (Harder et al. 2015; Spencer et al. 2019). However, to our knowledge, no studies have examined fire effects on peak flows or larger runoff events in this region.

While a relatively large body of post-wildfire literature has focused on fast hydrologic pathways at the plot or hillslope scale, far fewer studies have investigated rainfall-runoff response at the watershed scale. Past research conducted in other regions has suggested changes to peak flows and storm runoff can be quite large. For example, Scott (1993) observed 290% and 1110% increases in peak discharge during the first year following wildfire in South African pine and eucalypt catchments, respectively. After wildfire in the Entiat Experimental Forest in northwest Washington, Helvey (1980) reported at least a doubling of flow at each increment along flow duration curves produced from the affected streams. For the same watersheds, Seibert et al. (2010) showed that observed peak flows in burned watersheds were 120% higher than those modeled (simulated) for undisturbed (reference) conditions. More recently, Moreno et al. (2020) observed an increase of two orders of magnitude for event runoff in the Camp Creek watershed after the 2012 Waldo Canyon fire in Colorado, USA.

Rainfall intensity during shorter duration storms (i.e., 30 minutes or less) has been shown to correlate with peak discharge after wildfire sometimes producing thresholds, above which, runoff magnitude increases at a much faster rate. For example, maximum 30-minute rainfall intensity (I30) thresholds of 5-10 mm h^{-1} have been identified for burned watersheds in the western and southwestern USA (Moody and Martin 2001; Moody 2012). Moody (2012) noted that peak discharge spanned six orders of magnitude while the I30 spanned only one highlighting the sensitivity of the runoff response to this intensity measure. However, it is unclear if such precipitation intensity thresholds exist in regions of the Canadian Rocky Mountains where the distribution of large, high intensity convective storms may be less common or where highly fractured sedimentary bedrock may promote more muted flow responses (Spencer et al. 2019).

Furthermore, while increases in post-wildfire streamflow have been observed more often, some studies have shown little to no change in flows after wildfire (Tomkins et al. 2008; Owens et al. 2013; Surfleet et al. 2014). Some work has suggested peak flow and annual water yield responses to wildfire are greatest in Mediterranean and semi-arid climates while those in "highland" regions such as the Rocky Mountains and Pacific Northwest may be less severe (Hallema et al. 2017). However, post-wildfire studies in the Canadian Rockies are rare and there remains great uncertainty surrounding the magnitude and longevity of impacts to the rainfall-runoff process in burned watersheds.

Here, we investigate rainfall-runoff relationships during the snow-free season (late June to late September) during the 2nd to 11th years (2005-2014) after a severe wildfire in the Canadian Rocky Mountains. The focus on the snow-free season was used to necessarily limit the additional complexity caused by melting snowpacks to better isolate or constrain precipitation-runoff responses to those caused by rainfall events. Given the expectation of higher magnitude and faster runoff responses after rain storms, key questions investigated in this chapter were 1) How did wildfire affect the magnitude of storm runoff in burned watersheds over the 10-year study period?; 2) Was there evidence of post-fire watershed recovery as signalled by differences in early runoff response (<2 years after fire) compared with runoff response in later years?; 3) Were there differences in the timing of storm runoff between burned and unburned reference watersheds?; 4) Which rainfall-related variables appeared to be most important in the prediction of storm runoff?

4.2. Methods and Materials

4.2.1. Study Site

A detailed description of the study region and precipitation/streamflow data collection is outlined in Chapter 3. Briefly, five study watersheds (3.65 to 10.35 km^2) were established following the 2003 Lost Creek wildfire in the Crowsnest Pass region (SW Alberta) (Figure 3.1). No pre-fire data existed for the any of the study streams precluding a before-after control-impact (BACI) study design. Therefore, a replicated post-hoc reference-impacted study design was employed where precipitation and streamflow was monitored in both burned and unburned (reference) watersheds from 2005-2014.

Star and North York Creeks were established as unburned reference watersheds enabling comparisons with three burned watersheds (South York, Lynx and Drum Cks.). All five watersheds were generally similar in their physical attributes (area, aspect, slope, etc.) and were located in a similar geologic and hydroclimatic setting. However, results from Chapter 3 showed meaningful differences in annual precipitation and water yield between two groups of higher- and lower-elevation watersheds each containing at least one reference and burned watershed. Thus, comparison of rainfall-runoff relationships between reference and burned was similarly separated between watersheds of high elevation / precipitation (HP) and low elevation / precipitation (LP) watershed groupings. North York, South York and Lynx Cks. comprised the HP group (mean annual P = 1230-1350 mm) while the LP watershed group included the Star and Drum Ck. watershed pair (mean annual P = 800-950 mm).

4.2.2. Precipitation

Jarek tipping bucket precipitation gauges (Geo Scientific Ltd., Vancouver, BC) were used to collect precipitation data at 10-minute time intervals from a network of 16 climate/precipitation stations across the five watersheds (Figure 4.1, Chapter 3). Minimally, each watershed had one high and one low-elevation precipitation gauge. Data were collected using Campbell Scientific CR10X or CR1000 data loggers (Campbell Scientific, Logan, UT) or at stand-alone precipitation stations with Hobo Pendant loggers (Onset Computer Corp., Bourne, MA). The Thiessen polygon approach was used to calculate spatially weighted mean precipitation for each watershed using data from the network of climate stations.

4.2.3. Streamflow

Standard velocity-area techniques were used for manual measurements of streamflow (Q) (Swoffer Model 2100, Swoffer Instruments Inc., Seattle, WA; Sontek Flowtracker ADV Series, Sontek/YSI Inc., San Diego, CA). Q was typically measured every two weeks from April through October with additional measurements during the high-runoff snowmelt period. These measurements were combined with automated stage data from natural control sections to produce annual rating curves for each stream from which streamflow hydrographs were computed (USGS 1982). New rating curves were developed each year (2005-2014) and after extreme high flow events to account for potential changes to stream channel shape. Waterlog gas bubbler systems (YSI International, Yellow Springs, OH) and Hobo U20 pressure transducers (Onset Computer Corp., Bourne, MA) were used to collect stage data at 10-minute time intervals. Instantaneous Q (m^3/s) was converted to mm to standardize for watershed area and allow comparability between watersheds. A malfunctioning stage sensor at Lynx Ck. was not able to cleanly record several events; thus, they were removed from the data set. Additionally, the entire 2007 streamflow record at Drum Ck. was removed because of a damaged stage sensor. However, the snow-free period in 2007 produced almost no measureable rainfall-runoff events.

4.2.4. Rainfall and Runoff Variables

The initial intention was to examine precipitation-runoff relationships from discrete precipitation events across the open-water period from the spring snowmelt freshet through the late summer/fall baseflow period. However, mixed precipitation during spring and the high complexity of disentangling event rainfall from snowmelt contributions presented formidable challenges for such analyses. While approaches to estimate the potential partial snowmelt contributions to total combined rain and snowmelt "events" was explored in earlier analyses (e.g., temperature-index snowmelt modeling), these introduced high uncertainty into the broad objectives for a rigorous, observation-based analysis of post-fire precipitation-runoff relationships. Thus, the analysis here reflects the seasonal period without meaningful presence of snowpacks in study watersheds to exclude the effects of melting snow on rainfall-runoff events. Snow depth sensors (SR50) (Campbell Scientific, Logan, UT) were used to identify the date on which the high elevation snowpack disappeared each spring and started to accumulate each fall. The snow-free period varied slightly from year to year, beginning as early as June 17 and ending as late as October 17.

Runoff characteristics during significant rainfall events were examined using a combination of five independent (predictor) variables, and five dependent (response) variables describing the resulting runoff responses from storm events observed over the 10-year (2005-2014) post-fire period (Table 4.1). Preliminary analyses showed that the ten-minute time-step was needed to adequately characterize the range of rainfall-runoff (storm) responses for each study watershed. While a very large number of smaller precipitation events occurred during the study period, many of these produced little to no detectable runoff response. The minimum-magnitude "rainfall-runoff event" considered in this analysis was defined as a combination of both a) a contiguous, discrete rainfall event exceeding 5 mm *and* b) one that resulted in a measurable streamflow response. Event hydrographs were manually analyzed individually to verify the flow response. This resulted in a total population of 366 discrete rainfall-runoff events from all watersheds combined, with 49-94 observations identified across each watershed from 2005-2014 (Table 4.2).

To enable calculation of event quickflow (Q_e), baseflow separation was performed using the method of Hewlett and Hibbert (1967) (Figure 4.1). After examining several other techniques, this approach was chosen for three main reasons: 1) It has been widely used, allowing a certain degree of comparability with previous studies; 2) The determination of the endpoint for runoff events is objective because the baseflow separation line intersects with the runoff hydrograph; 3) Its relative simplicity compared to other methods. After baseflow separation, quickflow (Q_e), event rise (Q_Δ) and runoff coefficients (C_r) were calculated for each rainfall-runoff event. Q_e is the summation of area-weighted streamflow between the line of constant-slope and total event streamflow (Table 4.1; Figure 4.1). In contrast, Q_Δ is simply the absolute difference between pre-event and peak streamflow. As such, Q_Δ ignores the temporal component of the storm and is purely a measure of the maximum change in runoff magnitude initiated by the rainfall. C_r is the ratio of Q_e to total event precipitation (P_{tot}) and is a frequently-used metric to express the efficiency of the conversion of rainfall into runoff (e.g. Blume et al. 2007). In addition to the Q variables, two timing metrics, basin lag (T_{lag}) and rise time (T_r), were computed for each event to assess possible shifts in the timing of the delivery of rain water to streamflow (Table 4.1).

4.2.5. Data Analysis

Effects of wildfire on runoff from rainfall events was explored by comparing precipitation-runoff relationships (P_{tot} with Q_e and Q_Δ) between burned and unburned reference watersheds within catchment groups of similar annual precipitation (i.e. the HP and LP watershed groups defined in Chapter 3). Rainfall and runoff variables were normalized using log10 transformation to enable analysis of covariance (ANCOVA) to test for differences in runoff between reference and burned watersheds. The non-parametric Mann Whitney U test was used to compare C_r, basin lag (T_{lag}), and rise time (T_r) among the same pairs of burned/unburned watersheds. To determine if there was any evidence of post-fire recovery of rainfall-runoff relationships in the years following the fire, a selection of matched events from similar hydrologic periods (2005 and 2011/2012) were examined for the HP watershed group (North York, South York and Lynx Cks.). Additionally, rainfall-runoff responses caused by a single relatively large-magnitude event (August, 2005) were compared across the three HP watersheds (the event was deemed too dissimilar within the LP group for comparison). Finally, the influence of rainfall intensity ($I30_{max}$) was examined as a key predictor of event runoff response (event rise (Q_Δ).

4.2.6. Multiple Linear Regression

Additionally, a multiple linear regression approach was used to investigate the influence of several predictors, together, on the following streamflow response variables: runoff coefficient (C_r), quickflow (Q_e), and event rise (Q_Δ) (Julian and Helsel 2021). Storm precipitation (P_{tot}), maximum 30-minute rainfall intensity ($I30_{max}$), average hourly rainfall intensity ($I60_{avg}$), storm duration (P_{dur}) and pre-event streamflow (Q_{pre}) were used as predictor variables. Q_{pre} was used as a proxy for antecedent wetness. Additionally, a dummy variable (FIRE) was used to indicate watershed condition, taking on a value of 0 for a reference condition and 1 for burned condition. The variance inflation factor (VIF) and Pearson's R were used to check predictor variables for high correlation (Helsel and Hirsch 2002). Partial plots were used to determine if any predictor variables needed transformation; this decision was based on whether the transformation(s) produced significant reductions in model AIC (Akaike Information Criteria). Using this method, it was determined cube root transformation of P_{tot} and natural log transformation of Q_{pre} produced the "best" model values. It should be noted these transformations are different from those depicted in Figures 4.2 and 4.3 because of this methodology. The above approach resulted in the following regression model,

$$\text{Ln(dependent variable)} = \beta_0 + \beta_1 \text{cub}P_{tot} + \beta_2 I30_{max} + \beta_3 \ln Q_{pre} + \beta_4 \text{FIRE} + \varepsilon \tag{4-1}$$

Where β_0 is the intercept, β_1 to β_4 are the coefficients for the predictor variables and ε is the remaining error unaccounted for.

4.3. Results

4.3.1. Rainfall

During the study period, the LP watershed pair of Star and Drum Cks. experienced fewer qualifying rainfall events than the HP watersheds (Table 4.2). This was expected given their lower annual precipitation which led to a lower frequency of rainfall events greater than 5 mm in magnitude. Occasional failure of stage sensors also resulted in the removal of some event data, which reduced n for Lynx, Star and Drum Cks. However, the median event size (range = 10.2 – 11.9 mm) and $I30_{max}$ (7.6 – 8.4 mm h^{-1}) was very similar across all watersheds. The duration of precipitation (P_{dur}) was notably lower for Star Ck. than in all other watersheds (Table 4.2).

4.3.2. Quickflow, Event Rise and Runoff Coefficients (2005-2014)

Variation in annual precipitation among watersheds was reflected in the regression relationships between total event precipitation (P_{tot}), and the dependent variables quickflow (Q_e) and event rise

(Q_Δ) (Figures 4.2 and 4.3). The three HP watersheds (North York, South York and Lynx Cks.) generally had higher Q_e and Q_Δ across the range of precipitation event sizes during the study period (2005-2014) than the two LP watersheds (Star and Drum Cks.). The adjusted mean from analysis of covariance (ANCOVA) suggested Q_e response in the LP burned watershed (Drum Ck.) was approximately double that of the LP reference watershed, Star Ck. ($p<0.01$, Figure 4.2). In contrast, adjusted mean quickflow for South York and Lynx Cks. (burned HP watersheds) was only 9% and 21% higher, respectively, than Q_e for North York Ck. (reference HP watershed) (Figure 4.2). However, these differences were not statistically significant ($p>0.15$).

Similar patterns emerged for the relationships between total event precipitation (P_{tot}) and event rise (Q_Δ), however ANCOVA analysis showed some subtle wildfire effects (Figure 4.3). Relative differences in adjusted mean Q_Δ between reference and burned watersheds were somewhat greater than those shown for Q_e. Adjusted mean Q_Δ in Drum Ck. (burned LP watershed) was 46% higher than that in Star Ck. (reference LP watershed) ($p<0.01$). While Q_Δ in Lynx Ck. was 8% greater than that of North York Ck., this difference was not significant ($p=0.36$). However, a larger 23% difference in event rise was evident ($p=0.02$) between South York (burned) and North York (reference) Cks. It is notable that regression slopes for all five watersheds shown in the Q_e and Q_Δ analyses are similar, with the possible exception of Drum Ck. (Figures 4.2 and 4.3). This suggests stormflows generally responded similarly to increasing storm precipitation across this group of five watersheds.

Event-based runoff coefficients (C_r) were generally very low in all watersheds during the 2005-2014 study period (Figure 4.4a). Median C_r ranged from 0.002 (0.2%) in Star Ck. to 0.007 (0.7%) in South York Ck., while approximately 90% of events across all watersheds had $C_r < 0.05$ (5%). For the HP watersheds the median C_r was significantly higher (50%) in South York Ck. (burned) than in North York Ck. (reference; $p=0.039$), but not for Lynx Ck. (burned; 36% greater, $p=0.18$) using the non-parametric Mann-Whitney U Rank Sum test. Median C_r in Drum Ck. (burned LP watershed) was also significantly higher (123%) than that of Star Ck., the reference LP watershed ($p<0.01$; Table 4.2; Figure 4.4a).

4.3.3. Runoff Response Early After Wildfire

A selection of matched rainfall-runoff events from as early as possible after the wildfire (2005) and from later years (2011-2012) were compared in order to explore if there were clear signs of hydrologic recovery 8-9 years after the fire. This would be evidenced by greater Q_e early after the fire, in the second post-fire year (Figure 4.5). However, there was no clear difference in Q_e between the reference and two burned watersheds in the HP watershed group during 2005 (each regression line crosses the others). Further, Q_e during the later years (dashed regression lines) was generally higher in all watersheds regardless of fire effects (Figure 4.5). While Q_e in Lynx Ck. (burned) during this period was greatest across the range of event precipitation, no meaningful differences in Q_e=F(P_{tot}) were evident for any of the watershed pairs in the HP watershed group.

Similarly, there was no clear evidence suggesting a strong wildfire effect on streamflow generation from the large rainfall-runoff event which occurred August 11 (20:40) to August 12 (8:40), 2005 (Figure 4.6 and Table 4.3). While limited by small differences in rainfall amount and intensity between watersheds, this event was one of the largest and most comparable during this early post-fire year. P_{tot} was very similar across the HP watersheds (24.1 mm to 27.2 mm) while it was slightly less (21.2 mm) in Star Ck. (LP reference watershed) and much less in Drum Ck. (10.2 mm). Therefore, the LP watershed group was excluded from this analysis. Among the HP watersheds, Q_e and C_r were highest in South York Ck. (burned) followed by North York Ck. (reference), while runoff response in Lynx Ck. (burned) was lowest. Similarly, Q_Δ was highest in South York Ck. (0.0106 mm) and lower in North York and Lynx Cks. (both 0.0074 mm) (Table 4.3).

4.3.4. Rainfall Intensity (I30)

Relationships between storm event rise (Q_Δ) and 30-minute maximum rainfall intensity (I30) were highly variable and generally weak across all five study watersheds (Figure 4.7). Furthermore, no clear effect of wildfire on these relationships was apparent. In each watershed, a strong majority of storm events had $I30_{max}$ less than 15 mm h^{-1} while corresponding Q_Δ was less than 0.02 mm for the HP watersheds and 0.01 mm for the LP watersheds (Figure 4.7). Coarse analysis of Q_Δ values greater than 0.02 mm showed that 82 to 90% of these events in HP watersheds occurred during periods of higher antecedent moisture (either before July 15 or after September 15) while rainfall intensity ($I30_{max}$) was often relatively low. Similarly, 70% and 90% of Q_Δ events greater than 0.01 mm in Drum Ck. (burned LP watershed) and Star Ck. (reference LP watershed), respectively, occurred during these same periods of higher antecedent moisture and were also poorly correlated with $I30_{max}$.

Similarly, the majority of events with $I30_{max}$ > 15 mm h^{-1} also produced relatively low response in Q_Δ (<0.02 mm for HP and <0.01 mm for LP watersheds), with around 75% of events occurring during the driest seasonal period between July 15 and September 15. Overall, these results suggest rainfall intensity, by itself, is not an adequate predictor of storm event runoff response in this region (Figure 4.7).

4.3.5. Basin Lag and Rise Time

Median basin lag in the HP watersheds was 100, 120 and 100 minutes, respectively, for North York (reference), Lynx (burned) and South York Creeks (burned) (Table 4.2; Figure 4.4b). Median basin lag time of the HP reference watershed did not differ from that of either Lynx Ck. ($p=0.12$) or South York Ck. ($p=0.93$) using the Mann Whitney test. However, basin lag was significantly different between the LP watersheds ($p<0.01$); median basin lag in Drum Ck. (burned) and Star Ck. (reference) was 120 and 70 minutes, respectively. Further, the upper hinges of the boxplots (below which 75% of the data exist) were greater in burned watersheds of both the LP and HP groups than in reference watersheds, ranging from 170 (South York Ck.) to 212 minutes (Lynx Ck.). The upper hinges for the North York and Star Cks. boxplots were 140 and 120 minutes, respectively.

Similarly, for the HP watersheds, median rise time was not significantly different between North York (130 mins.) and Lynx Creeks (150 mins.; $p=0.18$), nor between North York and South York Creeks (160 mins.; $p=0.44$) (Table 4.2; Figure 4.4c). In contrast, and similar to findings for basin lag, rise time was significantly longer in Drum Ck. when compared to Star Ck. ($p<0.01$); median rise time in Drum (burned) was 200 minutes and, in Star Ck. (reference), 120 minutes. Similar to basin lag, the upper hinges on the rise time boxplots were generally higher for the burned watersheds (both LP and HP), ranging from 280 to 360 minutes, while the same values from the reference watersheds were 180 (Star Ck.) and 250 (North York Ck.) minutes.

4.3.6. Factors Explaining Post-Wildfire Stormflow Response

Multiple regression analysis was used to illuminate which independent variables were most important in the prediction of runoff response. Precipitation event duration (P_{dur}) and average 60-minute rainfall intensity ($I60_{avg}$) were found to be highly correlated with P_{tot} and $I30_{max}$, respectively (Pearson's correlation coefficients = 0.88 and 0.59). Further, a negative coefficient for $I60_{avg}$ resulted when it remained during late stages of model selection which can be an additional indicator of high correlation between similar predictors (Helsel and Hirsch 2002). As such, these two variables were excluded from model selection.

The final regression models explaining the suite of stormflow responses (lnC_r, lnQ_e and lnQ_Δ) and companion ANOVA tables are shown in Tables 4.4 and 4.5. Adjusted R^2 for the three models were

0.66 (lnC_r), 0.83 (lnQ_e), and 0.82 (lnQ_Δ) (Table 4.4). Three predictors, $cubP_{tot}$, lnQ_{pre}, and FIRE (dummy variable), were strongly significant for all models ($p<0.01$). In contrast, significance of the $I30_{max}$ varied from moderate ($p=0.04$) for the lnC_r model to high ($p<0.01$) for the lnQ_Δ model. ANOVA suggested total event precipitation (lnP_{tot}) accounted for the most variance, by far, in each of the three models followed by the proxy indicator of antecedent wetness (lnQ_{pre}) (Table 4.5). The dummy variable (FIRE) representing burned or reference watershed conditions accounted for a relatively small amount of variance in comparison but was still significant. Rainfall intensity ($I30_{max}$) did not account for enough variance to be significant ($p=0.13$) in the prediction of C_r. However, it was moderately significant ($p=0.023$) in the quickflow (lnQ_e) model and highly significant ($p<0.01$) in the event rise (lnQ_Δ) model (Table 4.5).

Overall, these analyses (Table 4.5) are highly consistent with results on wildfire effects to individual stormflow metrics, where wildfire explained only 2-4% of the total variation across all three stormflow responses over the 10-year period (2005-2014).

4.4. Discussion

4.4.1. Near-surface versus Deeper Hydrologic Pathways

This study sought to determine if severe wildfire in Canadian Rocky Mountain watersheds caused changes to stream runoff magnitude or timing during rainstorms, and to illuminate which factors appeared to be most important in the generation of post-wildfire runoff. Greater storm runoff would be expected to materialize via several different processes. First, and likely the most frequently cited, is because of soil water repellency and decreased infiltration caused by physiochemical and structural changes to fire-affected soils. These phenomena can lead to higher probability of infiltration-excess overland flow by reducing the proportion of storm rainfall that enters the soil and deeper geologic layers, instead routing it along near-surface pathways toward streams. Second, owing to greatly reduced transpiration, subsurface soil moisture could be higher across burned landscapes (especially in the vadose zone and near riparian areas), priming burned watersheds for quicker runoff events of greater magnitude than would otherwise be the case in an unburned watershed. Indeed, several studies have indicated the importance of soil and groundwater in the production of stream runoff (Sklash and Farvolden 1979; Bazemore et al. 1994; Penna et al. 2011).

While no field measurements were collected on soil water repellency (SWR) or infiltration metrics, there are several reasons why it is unlikely SWR substantially influenced event runoff in the burned watersheds. First, most studies have found that SWR recovers within 1-2 years following wildfire (Robichaud 2000; MacDonald and Huffman 2004; Ebel and Martin 2017). Because our work began in the 2nd post-fire year, data were not collected for what was likely the most important year from a SWR perspective. Further, very few rainfall-runoff events of significance occurred during 2006-2008 (3rd to 5th post-wildfire years) which would have allowed for substantial SWR and vegetation recovery. Thus, the wetter year of 2005 would have been the most likely to exhibit SWR. However, two analyses shown here do not suggest elevated runoff responses in 2005 (Figures 4.5 and 4.6; Table 4.3). Other factors that are known to be important in the breakdown of hydrophobicity are wetting, drying and freeze-thaw cycles (Doerr et al. 2000; Rakhmatulina and Thompson 2020). These processes may be important within the context of the present study because, even at lower elevations, snow cover can be present for 7 months (Oct – Apr). Two winters elapsed before the first rainfall-runoff measurements were available; the effect this may have had on the magnitude and longevity of SWR is unknown.

4.4.2. Runoff Magnitude During Rain Storms and Comparison with Previous Studies

Rainfall-runoff analyses (Q_e, Q_Δ, C_r) revealed mixed results, generally suggesting muted effects of the wildfire in burned HP watersheds (South York and Lynx Cks.), but larger effects in the burned LP watershed (Drum Ck.). While none of the three runoff metrics indicated a significant difference between Lynx and North York Cks. (burned and reference HP watersheds, respectively), Q_Δ and C_r were significantly higher in South York Ck. (burned) when compared to North York Ck. Other studies using similar metrics have shown much higher runoff response following wildfire. For example, Moreno et al. (2020), working after the Waldo Canyon Fire in Colorado, found that event-average runoff coefficients (Q^*/P_{Tot} or "effective runoff") increased by two orders of magnitude when comparing similar pre- and post-fire events. Additionally, maximum flows and event peak flows both increased by an order of magnitude (Moreno et al. 2020). These more dramatic post-wildfire responses are consistent with previous research in Colorado (Moody and Martin 2001; Kunze and Stednick 2006) where reduced infiltration capacity, SWR and burn severity have been shown to lead to greater runoff response (Moody et al. 2008; Moody and Ebel 2012; Hallema et al. 2017).

Working in burned and reference watersheds in South Africa, Scott and Van Wyk (1990) found quickflow volumes had risen by 2.2 mm (201%) while the mean response ratio increased to 7.5% from a pre-fire mean of 2.3% (+242%) during the first year after wildfire. The authors attributed the higher post-fire flows to SWR (Scott and Van Wyk 1990). However, there are some important differences between the present study and the South African one. First, Scott and Van Wyk (1990) used 20 mm as the lower cutoff for rainfall event size, and still managed to acquire data for 35 storms during the two-year calibration period, plus another 18 in the first post-fire year. This reveals a much higher frequency of large (>20 mm) storms than for our study. In contrast, there were only 14 events during the snow-free season with rainfall totals >20 mm in North York Ck. during our entire study period (2005-2014). This difference can likely be explained partly by the much longer period of pure rainfall-runoff events in the South African study area without mixed precipitation or snow. Outside of the narrow summer window that is the focus of the present study, precipitation more often falls as mixed rain/snow in Canada's southern Rockies which may act to mute or negate runoff responses. Second, rainfall in the South African catchments appears to be more intense than in our region; the mean 60 minute maximum rainfall intensity ($I60_{max}$) measured during their calibration period was 9.9 and 10.3 mm h^{-1} for the control and treatment catchments, respectively (Scott and Van Wyk 1990). Calculated for comparison here, the mean $I60_{max}$ for North York was approximately 6 mm h^{-1}.

To the author's knowledge, no Canadian studies exist on post-wildfire rainfall-runoff response during storm events. However, some work has shown relatively little impact on annual peak flows. During earlier work in the present study watersheds, Mahat et al. (2016) investigated annual peak flows and found the differences between North York, South York and Lynx Cks. were "not noteworthy, indicating that wildfire had an insignificant impact on peak flow." Similar to findings from the present study, Star Ck. displayed comparatively lower peak flows than the other watersheds, owing to its lower precipitation (Mahat et al. 2016). Geographically, the nearest similar study to ours occurred about 450 kms to the northwest at Fishtrap and Jamieson Creeks in British Columbia (Owens et al 2013). While these authors did not specifically examine rainfall-runoff events, they observed no change in the annual maximum daily mean flow in the post fire period (2004-2010). Owens et al. 2013 attributed this muted response to low winter precipitation totals (low snowpacks) and relatively low intensity summer rainfall events in the immediate post-fire period (2003-04), as well as quick recovery of understory vegetation. In comparison to the BC research area, the present study region receives approximately twice the annual precipitation and the study watersheds are more than 10 times smaller than Fishtrap (135 km^2) and Jamieson (230 km^2). Nonetheless, available western Canadian studies set in mountainous watersheds suggest relatively subdued peak flows after wildfire. Geology and groundwater storage capabilities may play important roles in dampening post-disturbance runoff responses, concepts Spencer et al. (2019) highlighted for Star Ck., specifically.

4.4.3. Diminished Importance of Rainfall Intensity ($I30_{max}$) During Dry Season

While rainfall intensity has been identified in past studies as an important predictor of threshold behavior in post-wildfire landscapes (Moody and Martin 2001; Moody 2012; Wilson et al. 2018) the $I30_{max}$, alone, was a relatively weak predictor of runoff response (Q_{Δ}) in our study (Figure 4.7). However, multiple regression analysis suggested it was still important in combination with other variables (Table 4.3). Reasons the importance of intensity may have been limited include: some recovery of infiltration and limited recovery of interception in burned watersheds, generally low rainfall intensities in relation to other regions, and dry antecedent conditions during the study window. First, vegetation recovery during the 10-year study period may have been an important factor. Previous work has shown a much stronger connection between rainfall intensity and runoff response while also exhibiting evidence of hydrologic recovery. Moody and Martin (2001) studied the influence of rainfall intensity on post-wildfire runoff response in three burned watersheds in South Dakota, New Mexico and Colorado (USA), and found threshold behaviour which indicated $I30_{max}$ above approximately 10 mm h^{-1} accelerated the magnitude of peak flow increases. The rainfall-runoff events were generally captured between the first and fourth post-fire years and the authors observed some evidence that intensity-runoff thresholds were higher in the latter two years, perhaps signaling some recovery of infiltration and interception (understory vegetation) properties (Moody and Martin 2001). Given that data for the present study were collected between years 2 and 11 following the fire, some recovery to infiltration and interception would be expected to reduce the magnitude of runoff response. Further, the vast majority of rainfall events in the present study region were relatively small in magnitude — greater than 67% were less than 20 mm for all watersheds. Moreover, the dry summers of 2006-2008 produced few events large enough to elicit a runoff response (zero in 2007); similar to the Fishtrap Ck. study (Owens et al. 2013) this would have allowed for some recovery before the onset of the wetter period during the last 4-5 study years.

Another reason for the diminished role of rainfall intensity might have been generally lower $I30_{max}$ in our study region in comparison to others. Moody and Martin (2001) observed 1-year return intervals for $I30_{max}$ of 20-32 mm h^{-1} (Moody and Martin 2001). These were far greater than the 1-year return intervals for watersheds in the present study, which were all less than 13 mm h^{-1}. Further, work by Moody and Martin (2009) suggests rainfall intensities for the present study may be relatively low in comparison to other regions of North America; our region is comparable to the Sub-Pacific regime cited in this study which has 2-year rainfall intensities ($I30_{max}$) ranging from 10-20 mm h^{-1} while every other region (Pacific, Plains, Arizona) receives higher intensity rainfall (in some cases the "extreme" end of the range is >58 to 100 mm h^{-1}) (Moody and Martin 2009). For comparison, the mean 2-year $I30_{max}$ for the SRWP study region across all watersheds was 17.4 mm h^{-1}, though this is based only on the 10-year record. These studies suggest generally greater rainfall intensities may have made the $I30_{max}$ a more important predictor of runoff response in the Western USA than in the present study region. It is also important to note that the calculation of the $I30_{max}$, itself, may distort comparisons between studies. For example, if an $I30_{max}$ calculation is based on an average of values from multiple precipitation gauges, this may have the effect of diminishing the apparent intensity because higher intensities observed at one gauge would be offset by lower intensities observed at other gauges. In contrast, if a study uses a single precipitation gauge for an $I30_{max}$ calculation, higher intensity values are more likely. Ongoing studies have continued to address the question of which intensity indicator is most meaningful as a predictor of runoff variables. For example, Dunkerley (2020) recently proposed the use of the EDf5 which is defined as the wettest 5% of a given storm event.

4.4.4. Antecedent Watershed Conditions

At the temporal scale of the storm event (i.e. minutes to hours), near-surface processes early after wildfire have been a primary focus for hydrologists (e.g. Ebel et al. 2012), rather than deeper hydrologic reservoirs which may be influenced by strong reductions in transpiration which can raise water tables or increase soil moisture over time. It is usually the latter mechanism which can lead to higher peak flows following forest harvesting (e.g. Winkler et al. 2021). Consistent with this, pre-event streamflow (Q_{pre}), our proxy for antecedent watershed wetness, was significant in multiple regression analyses ($p<0.01$) and appeared to influence the magnitude of Q_{Δ} in our examination of rainfall intensity (Table 4.3; Figure 4.7). While no studies have focused on antecedent wetness in wildfire-affected watersheds in the Canadian Rockies, Fang and Pomeroy (2016) examined antecedent moisture in relation to a significant flood event that caused severe damage in Calgary, Alberta (June 21, 2013). Using the measured meteorological conditions at Marmot Creek which led to this flood event, they found that if those identical conditions had occurred earlier (May 10), the flood peak could have been 13% higher (peak = 2.91 $m^3\ s^{-1}$) than the actual flood peak (2.57 $m^3\ s^{-1}$), but 14% lower if those conditions had occurred on July 26 (peak=2.2 $m^3\ s^{-1}$). These findings are instructive because they highlight the dominance of the snowmelt period in these high-elevation mountain watersheds and its subsequent effect on antecedent wetness and the magnitude of rainfall-runoff events. Runoff responses of greater magnitude can be expected when rainfall events occur nearer in time to peak snowmelt (Marks et al. 1998; Schnorbus and Alila 2004); in contrast, responses will be more subdued for events occurring during the drier summer period. Further, it appears advancement of the timing of snowmelt in burned watersheds may have led to drier sub-surface conditions during the low-flow (snow-free) period (Chapter 3) which, in turn, likely helped to reduce runoff magnitude during storms. Thus, while many forest harvesting studies have reinforced the expectation of increased antecedent wetness in wildfire-affected watersheds because of reduced transpiration, these effects are possibly offset by earlier disappearance of the spring snowpack, and greater evaporative losses owing to increased radiative inputs (Burles and Boon 2011; Gleason et al. 2013).

4.4.5. Timing Metrics

While T_{lag} and T_r were not significantly different between burned and reference HP watersheds, both of these metrics were significantly higher in the burned LP watershed (Drum Ck.) when compared to the reference LP watershed (Star Ck.) (Figures 4.4b and 4.4c). Further, boxplots generally seemed to indicate higher medians and quantiles for burned watersheds, especially for T_r (Figure 4.4c). These results run counter to expectations because the hydrologic processes wildfire impacts (i.e. interception, infiltration, soil water repellency) should generally lead to quicker routing of rainfall to streams, especially in high-relief mountainous areas. Few studies have examined post-wildfire lag times. However, Cydzik and Hogue (2009), modelling outcomes for six storms in the City Creek watershed, found significant reductions in post-fire lag time (136 mins pre-fire to 96 mins post-fire) in the San Bernadino Mountains, California. Lag times had not recovered after 3 seasons. Studies on the effects of forest harvesting have also shown reduced lag times after disturbance, such as Wright et al. (1990) who found a 1.5-hour average decrease in lag time after road building and logging in a 424 ha watershed in the Pacific Northwest. The physical processes which may have led to longer lag times in burned watersheds in the present study are not clear. It is possible that soils were drier in the burned watersheds and, if infiltration processes were fully recovered or unimpacted by wildfire, more soil moisture storage may have been available, leading to delayed runoff responses in comparison to the reference watersheds. It is also possible unique basin characteristics played larger roles than wildfire impacts in the timing of runoff responses. For example, the lower lag times in Star Ck. (compared to Drum Ck.) may relate to scale, basin shape or drainage density. In general, basin lag tends to be longer in larger watersheds (Melone et al. 2002). The especially muted runoff response in Star Ck. could be caused not only by its unburned (fully forested) state, but perhaps varying temporal responses from the three sub-basins. The passage of event runoff is likely not in temporal alignment among the three sub-basins which may have the effect of dampening runoff responses in Star Ck.

Nonetheless, this study suggests there are likely other factors at play in the timing of rainfall-runoff responses apart from wildfire effects.

4.5. Conclusions

Generally, runoff responses to rain storms in wildfire-affected Rocky Mountain watersheds were not large for streams in this study, especially when compared with those observed in the southwestern USA. Responses in the burned LP watershed (Drum Ck.) were significantly greater than those in the reference LP watershed (Star Ck.), but most of the comparisons for the HP watersheds were marginal or not significant. Further, there did not appear to be greater runoff response in the 2nd year after fire, the most likely to still exhibit SWR if this condition was present. Furthermore, the timing metrics, T_{lag} and T_r, indicated consistently longer basin lag and rise time for stormflows in burned watersheds which is clearly opposite of expectations based on conventional understanding of fire effects on runoff generation. Lastly, multiple regression analysis indicated several predictors were significant in combination. From most important to least important, these were: total event precipitation (P_{tot}), antecedent wetness or pre-event Q (Q_{pre}), the FIRE variable (indicating burned or unburned) and maximum 30-minute rainfall intensity ($I30_{max}$). The minimal influence of rainfall intensity on storm runoff response was somewhat surprising, but similar results have been shown in previous work (Hewlett and Bosch 1984). It is particularly notable that wildfire explained only 2-4% of the total variation in stormflows across 2 reference and 3 burned watersheds over a 10-year period. Overall, multiple lines of evidence from this study suggest that in comparison to studies conducted in other fire affected regions, the effects of wildfire on generation of elevated storm runoff is weak or minimal at best.

4.6. Tables

Table 4.1. *Predictor (P) and response (R) variables for precipitation and runoff calculated for each storm event.*

Variable	Units	Predictor/Response	Definition
P_{tot}	mm	P	Total event precipitation.
$I30_{max}$	mm-h	P	Maximum 30-minute rainfall intensity.
$I60_{avg}$	mm-h	P	Average 60-minute rainfall intensity.
P_{dur}	min	P	Duration of precipitation event.
Q_{pre}	mm	P	Minimum streamflow just prior to rise of runoff hydrograph.
Q_e	mm	R	Event quickflow, calculated after baseflow separation.
Q_{Δ}	mm	R	Change in streamflow from pre-event to peak flow (i.e. peak Q - pre-event Q).
C_r	unitless	R	Ratio of quickflow to total event precipitation. Expresses amount of P routed to Q.
T_{lag}	min	R	Time from half of event P to half of event quickflow.
T_r	min	R	Time from start of rising limb to event peak flow.

Table 4.2. *Median (range) of rainfall and runoff variables across all five watersheds (2005-2014). The variables are: total event precipitation (P_{tot}), maximum 30-minute rainfall intensity ($I30_{max}$), precipitation event duration (P_{dur}), event quickflow (Q_e), event rise (Q_Δ), runoff coefficient (C_r), basin lag (T_{lag}), and rise time (T_r).*

Median and (Range) for Rainfall and Runoff Variables

Stream	Condition	Events	P_{tot} (mm)	$I30_{max}$ (mm h^{-1})	P_{dur} (mins)	Q_e (mm)	Q_Δ (mm)	C_r	T_{lag} (mins)	T_r (mins)
LP group										
Star Ck.	reference	59	10.5 (5.1 - 115.5)	7.9 (2.0 - 27)	210 (60 - 2900)	0.020 (0.001 - 1.733)	0.0027 (0.0007 - 0.0357)	0.0021 (0.0001 - 0.0621)	70 (20 - 770)	120 (40 - 1030)
Drum Ck.	burned	49	11.9 (5.4 - 87.1)	7.9 (2.6 - 49.3)	320 (40 - 2560)	0.063 (0.003 - 7.172)	0.0044 (0.0012 - 0.0506)	0.0048 (0.003 - 0.0824)	120 (10 - 950)	200 (60 - 980)
HP group										
North York Ck.	reference	94	10.2 (5 - 88.8)	7.6 (2.5 - 38.6)	300 (50 - 3580)	0.050 (0.003 - 12.554)	0.0043 (0.0010 - 0.0555)	0.0048 (0.0004 - 0.1939)	100 (-30 - 1910)	130 (60 - 2440)
South York Ck.	burned	86	11.9 (5 - 77.5)	7.9 (1.9 - 34.8)	320 (30 - 3040)	0.069 (0.003 - 16.205)	0.0061 (0.0008 - 0.1299)	0.0071 (0.0005 - 0.2474)	100 (40 - 1410)	160 (50 - 2310)
Lynx Ck.	burned	78	10.6 (5 - 73.3)	8.4 (2.4 - 30)	315 (40 - 3450)	0.067 (0.002 - 7.558)	0.0056 (0.0008 - 0.0761)	0.0065 (0.0003 - 0.2235)	120 (30 - 1260)	150 (40 - 2660)

Table 4.3. *Rainfall-runoff variables for a >20 mm event in August, 2005 for the high precipitation (HP) watersheds.*

Stream	**P_{tot} (mm)**	**$I30_{max}$ (mm h^{-1})**	**Q_e (mm)**	**Q_Δ (mm)**	**C_r**	**T_{lag} (mins)**	**T_r (mins)**
North York Ck. (R)	25.1	21.7	0.221	0.0074	0.0088	220	450
South York Ck. (B)	24.1	12.3	0.258	0.0106	0.0107	230	460
Lynx Ck. (B)	27.2	20.4	0.17	0.0074	0.0063	270	460

Table 4.4. *Results of multiple regression model predicting the transformed runoff response variables. Predictors are total event precipitation (P_{tot}), 30-minute maximum rainfall intensity ($I30_{max}$), pre-event streamflow (Q_{pre}), and a dummy variable (FIRE) indicating burned or reference watershed. Significance codes: *** (p=0 – 0.001), ** (p=0.001 – 0.01), * (p=0.01 – 0.05).*

Response Variable	Intercept β_0	cub(P_{tot}) β_1	$I30_{max}$ β_2	ln(Q_{pre}) β_3	FIRE β_4	Adj. R^2
ln(C_r)	-4.359	1.181 ***	0.015 *	0.957 ***	0.555 ***	0.66
ln(Q_e)	-4.502	2.285 ***	0.020 **	0.958 ***	0.546 ***	0.83
ln(ΔQ)	-5.819	1.121 ***	0.031 ***	0.607 ***	0.357 ***	0.82

Table 4.5. *ANOVA tables for each of the runoff variables used in multiple regression analysis. Top: runoff coefficient (C_r); middle: quickflow (Q_e); bottom: event rise (Q_Δ).*

$\ln(C_r)$

x-variable	D.F.	S.S.	M.S.	F statistic	P
$cub(P_{tot})$	1	248.1	248.1	417.8	<0.01
$I30_{max}$	1	1.4	1.4	2.3	0.130
$\ln(Q_{pre})$	1	154.0	154.0	259.4	<0.01
FIRE	1	27.1	27.1	45.7	<0.01
Residuals	361	214.4	0.6		

$\ln(Q_e)$

x-variable	D.F.	S.S.	M.S.	F statistic	P
$cub(P_{tot})$	1	827.2	827.2	1435.6	<0.01
$I30_{max}$	1	3.0	3.0	5.2	0.023
$\ln(Q_{pre})$	1	154.6	154.6	268.3	<0.01
FIRE	1	26.3	26.3	45.6	<0.01
Residuals	361	208.0	0.6		

$\ln(\Delta Q)$

x-variable	D.F.	S.S.	M.S.	F statistic	P
$cub(P_{tot})$	1	225.0	225.0	1202.9	<0.01
$I30_{max}$	1	9.2	9.2	49.3	<0.01
$\ln(Q_{pre})$	1	62.0	62.0	331.4	<0.01
FIRE	1	11.2	11.2	60.0	<0.01
Residuals	361	67.5	0.2		

4.7. Figures

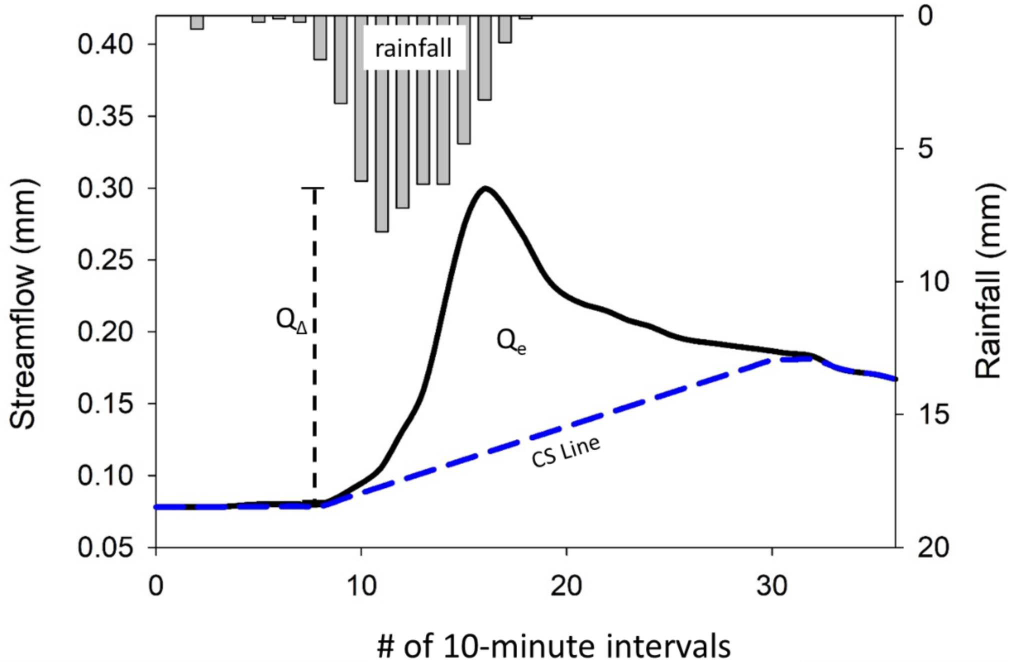

Figure 4.1. *Schematic depiction of hydrograph separation for a rainfall-runoff event showing the main streamflow variables; Q_Δ (event rise) and Q_e (quickflow). The constant slope (CS) line was derived using the baseflow separation method of Hewlett and Hibbert (1967).*

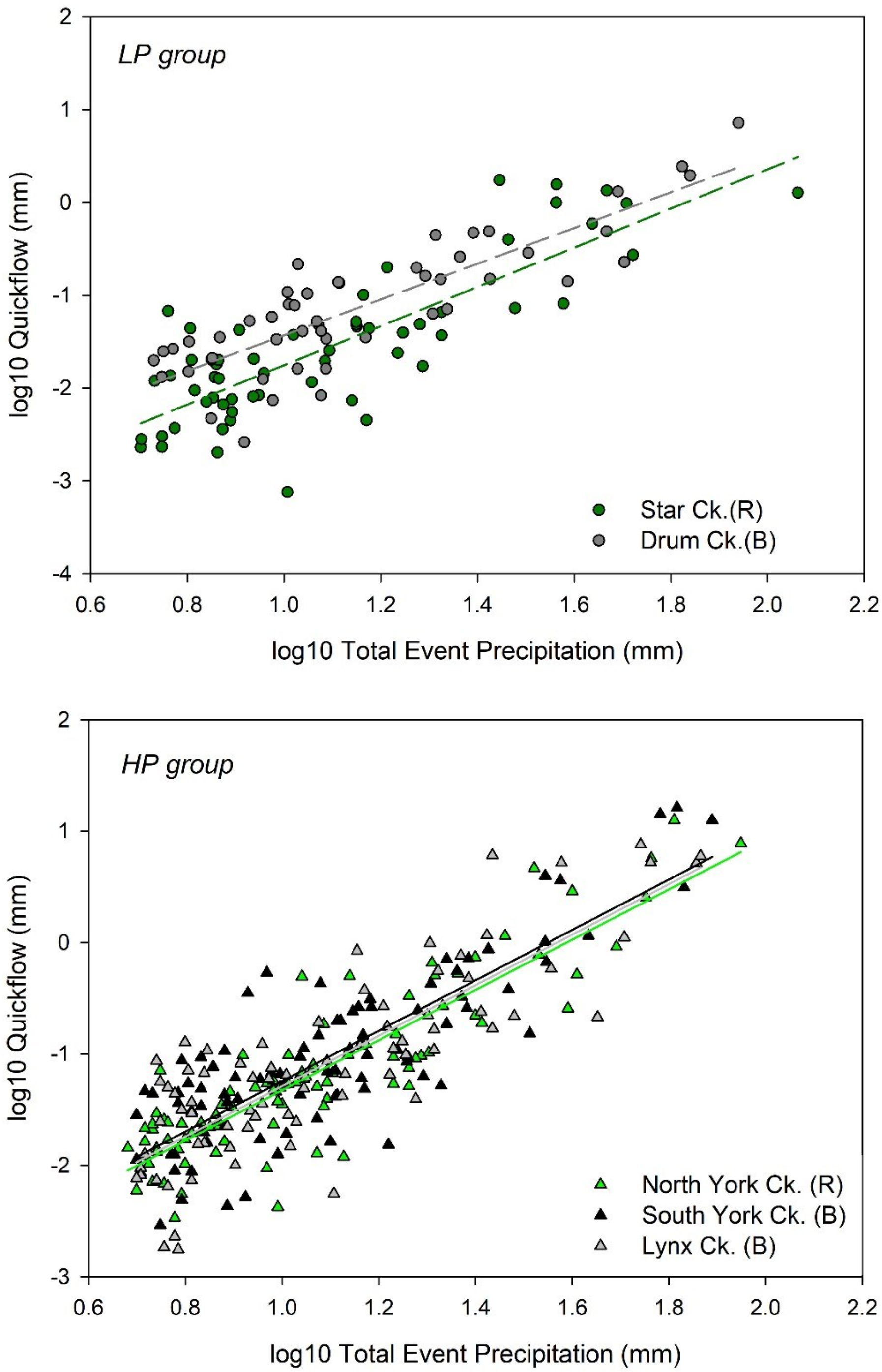

Figure 4.2. *Regression relationship between log10 total event precipitation (P_{tot}) and log10 quickflow (Q_e) during summer rain storms across complete study period (2005-2014). Top plot shows low precipitation (LP) group and bottom plot shows high precipitation (HP) watershed group. Reference and burned watersheds indicated by (R) and (B) in legend, respectively.*

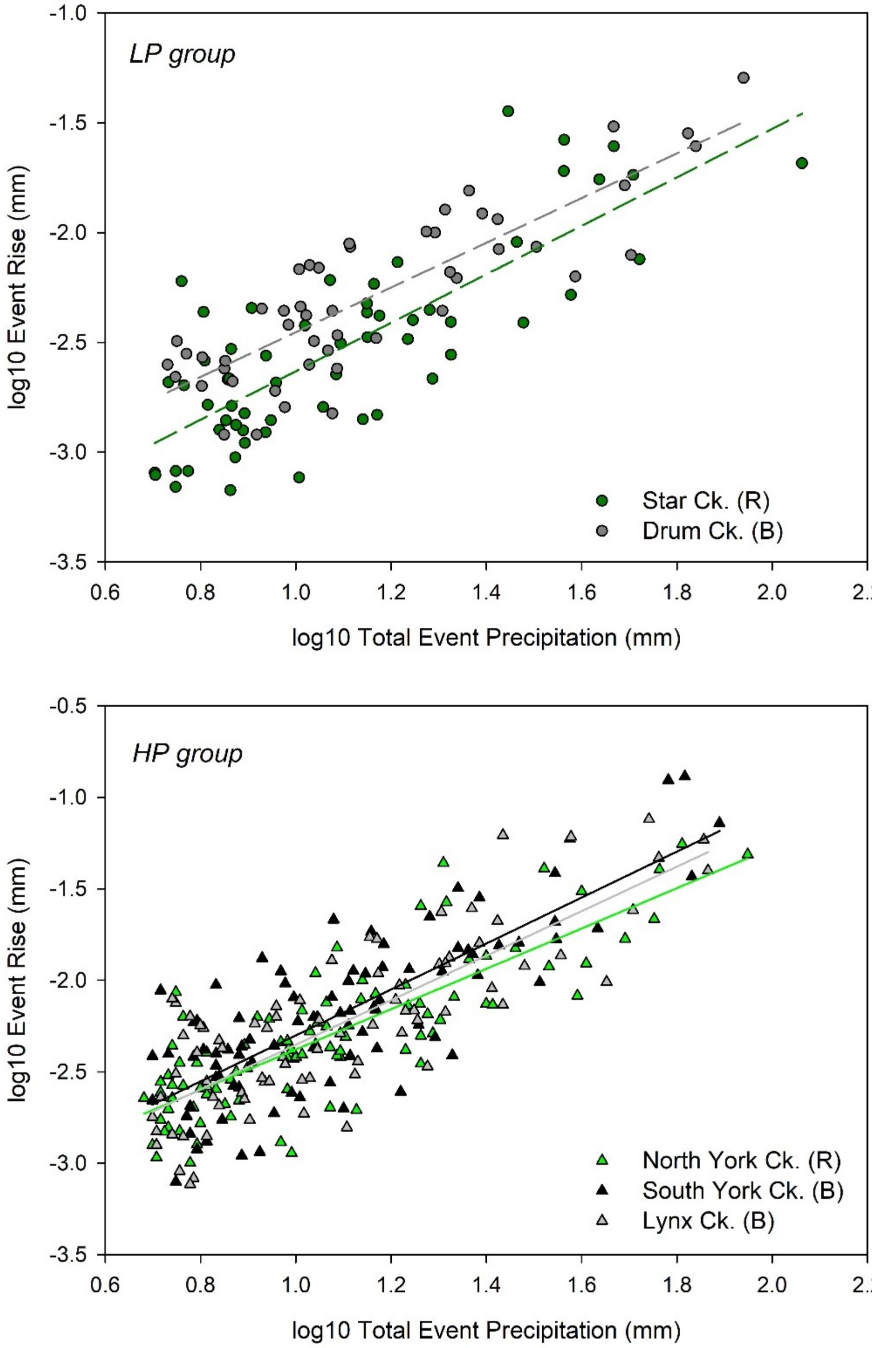

Figure 4.3. *Regression relationship between log10 total event precipitation (P_{tot}) and log10 event rise (Q_{Δ}) during summer rain storms across complete study period (2005-2014). Top plot shows low precipitation (LP) group and bottom plot shows high precipitation (HP) watershed group. Reference and burned watersheds indicated by (R) and (B) in legend, respectively.*

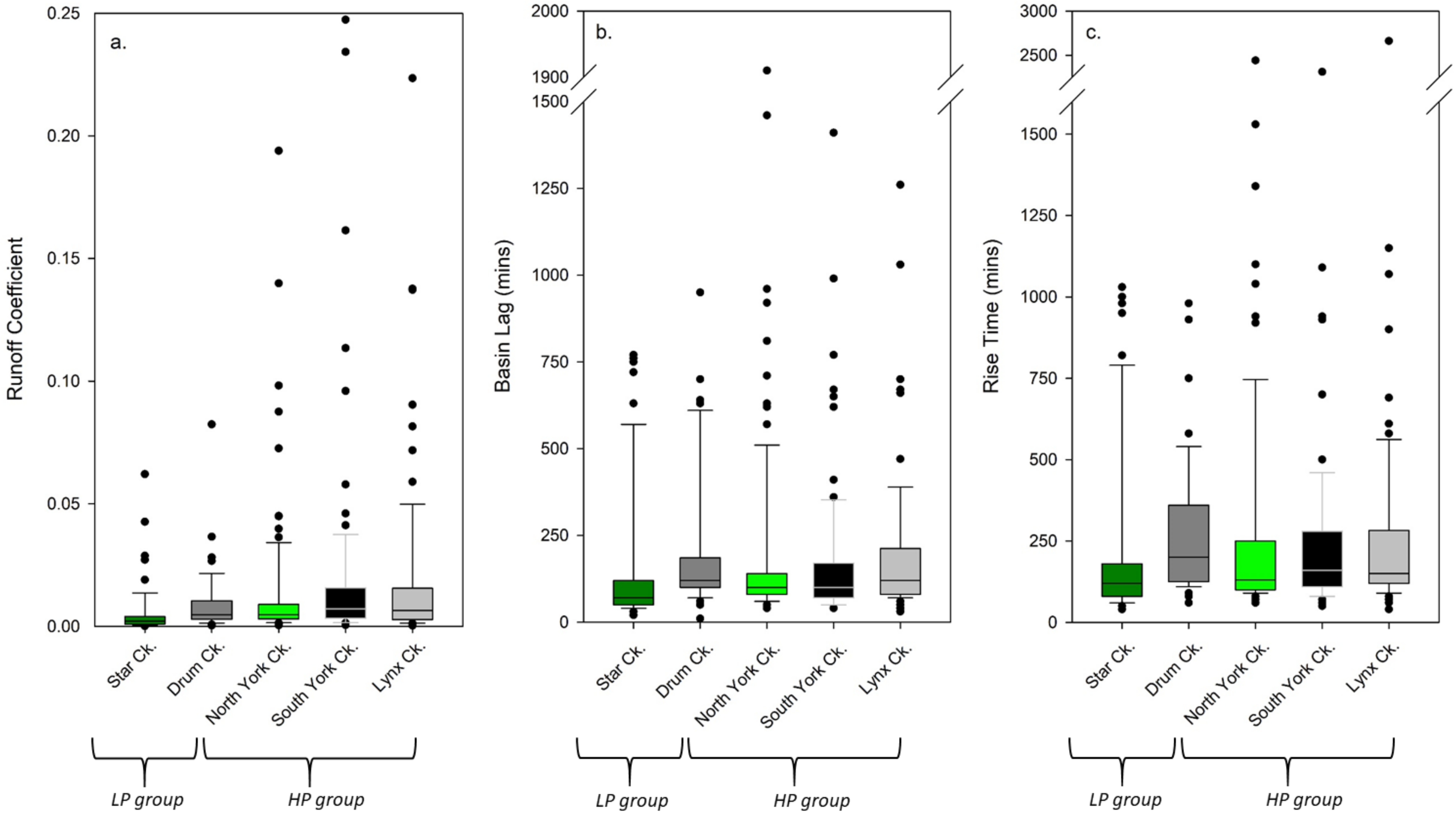

Figure 4.4. *Boxplots for each watershed across the study period (2005-2014) showing a) the runoff coefficient (C_r), b) basin lag (T_{lag}), and c) rise time (T_r). Low (LP) and high (HP) precipitation groups indicated below panels. The boundary of the box closest to zero indicates the 25th percentile, a line within the box marks the median, and the boundary of the box farthest from zero indicates the 75th percentile. Whiskers (error bars) above and below the box indicate the 90th and 10th percentiles.*

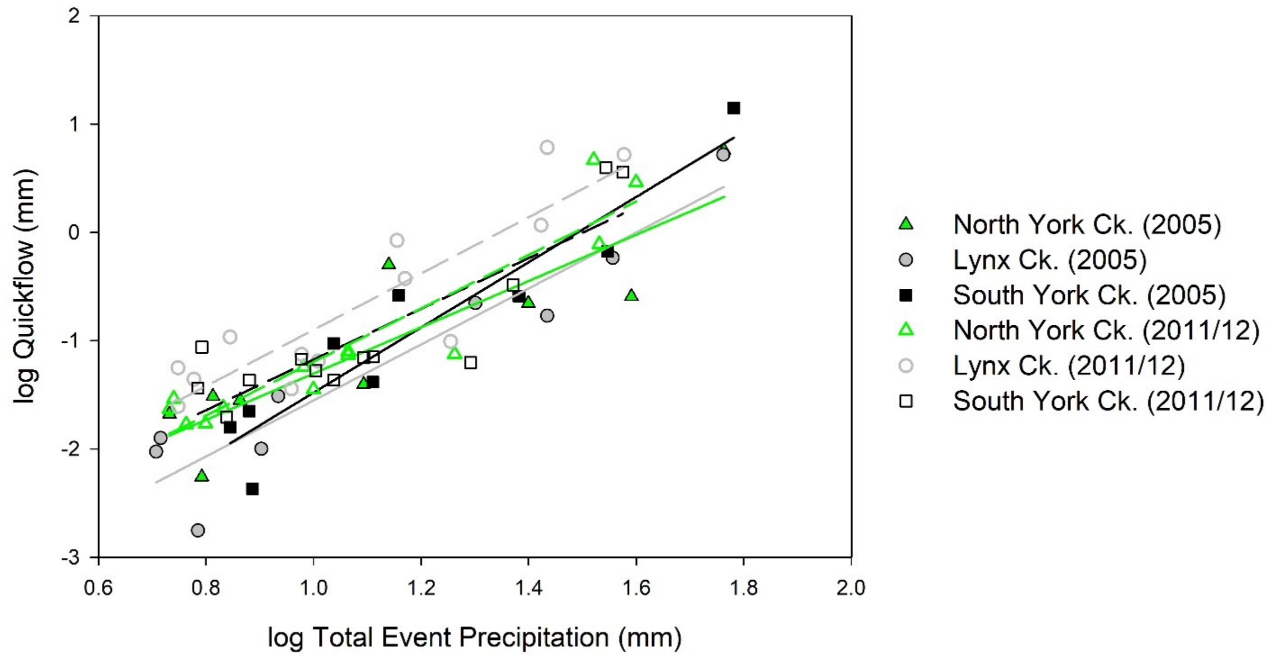

Figure 4.5. *A comparison of matched post-wildfire rainfall-runoff events during an early period (2005) and later period (2011-2012) for the high precipitation (HP) watersheds: North York Ck. (reference), Lynx Ck. (burned), and South York Ck. (burned). Solid regression lines are for 2005 and dashed lines are for 2011-2012.*

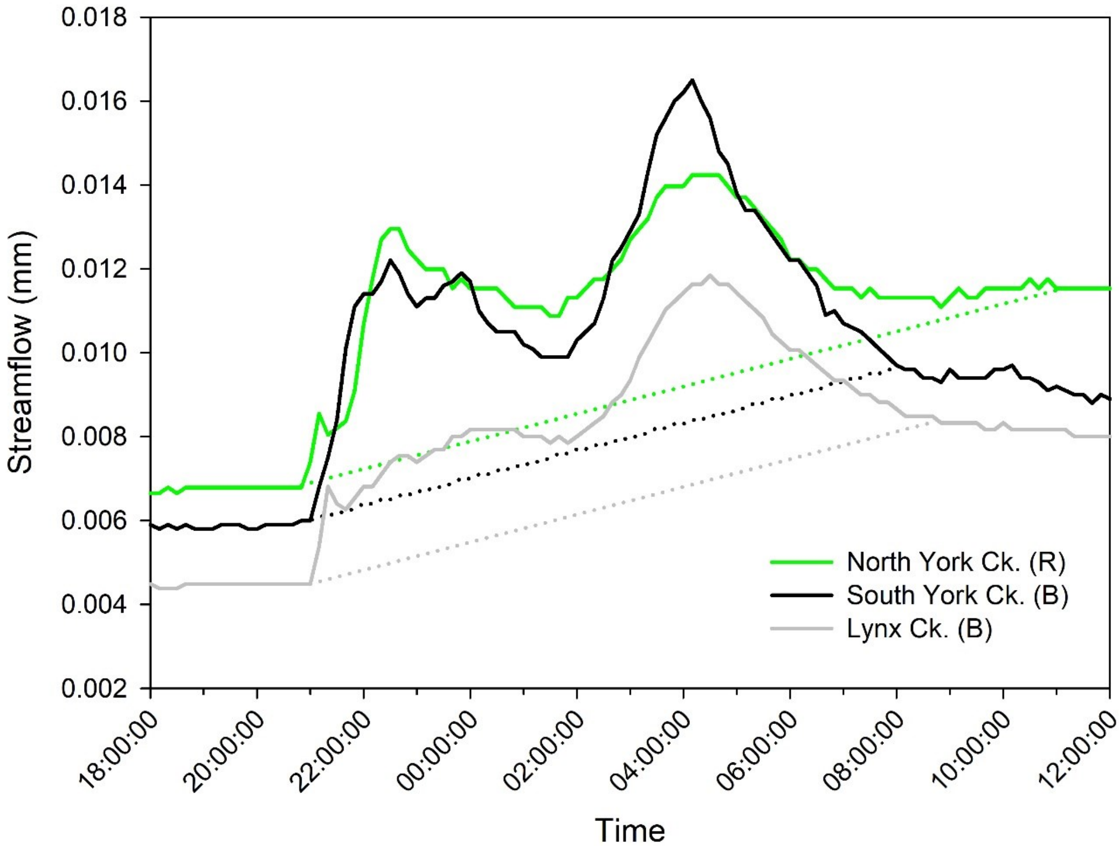

Figure 4.6. *Runoff responses for a >20 mm rainfall event which occurred August 11-12, 2005 (2nd year after wildfire) in the high precipitation (HP) study watersheds. Rainfall and runoff variables are detailed in Table 4.3 for this storm. Sloping dotted lines represent the constant-slope baseflow separation line (Hewlett and Hibbert 1967).*

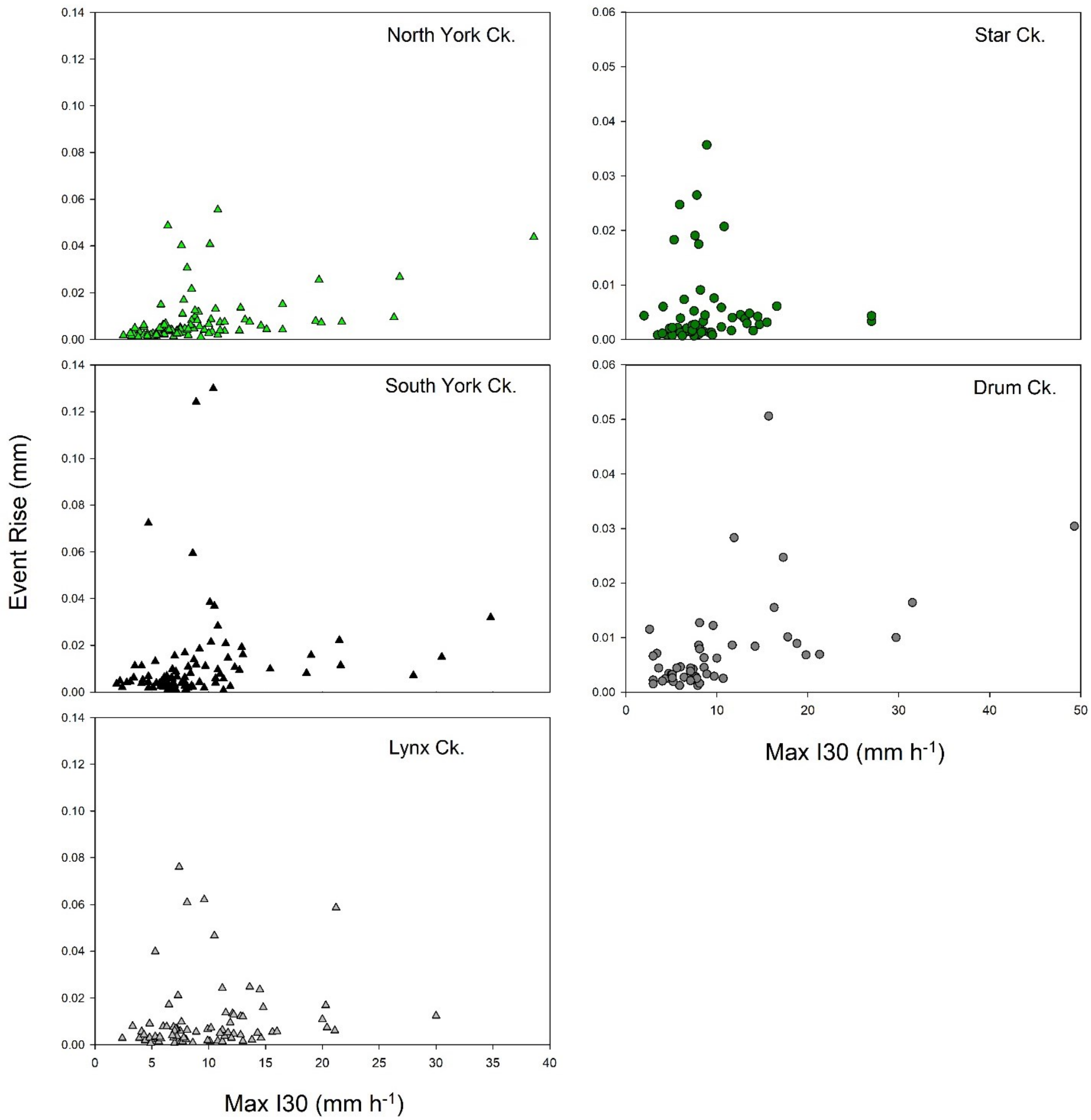

Figure 4.7. *Relationship between rainfall intensity (I30max) and runoff event rise (Q_Δ). The three HP watersheds are shown in the left panels and the two LP watersheds are shown in the right panels.*

Chapter 5. Synthesis

This thesis focused on three broad aspects of post-wildfire hydrology in the Canadian Rocky Mountains following the 2003 Lost Creek wildfire: 1) Differences in net precipitation between burned and unburned subalpine forest stands; 2) Potential changes to the flow regime at the watershed scale during the 2nd to 11th post-wildfire years (2005-2014); 3) Effect of wildfire on summertime rainfall-runoff (storm) events during the same time frame. This chapter summarizes key findings, their potential implications and recommendations for future research.

5.1. Summary of Key Findings

In Chapter 2, throughfall and stemflow were measured in burned and unburned subalpine forest stands during three summers (2006-2008) to derive relationships between gross event rainfall and canopy interception. These relationships were then applied to the ten-year data set (2005-2014) of rainfall events to estimate differences in net rainfall between burned and unburned stands. Additionally, snow depth and density measurements during each of the ten years near the date of peak snow water equivalent provided an estimate of wildfire effects on snow accumulation. The study showed that net rainfall and snow accumulation (SWE) across the study period were 122 mm (36%) and 152 mm (78%) higher, respectively, in burned subalpine forest stands than in unburned reference stands. This represented 274 mm (51%) additional net precipitation in the burned stands, a substantial increase in potential hydrologic forcing caused by wildfire.

Chapter 3 focused on potential differences in water yield in burned and unburned reference watersheds during 2005-2014. Investigations were done at various time scales (annual, monthly, weekly) and changes to the snowmelt (Apr-June) and low flow periods (Jul-Sept) were examined. Evidence for shifts in seasonal timing of streamflow and potential recovery trends were also investigated. Measured differences in annual precipitation between watersheds required grouping them by “high” (North York, South York, and Lynx Cks.) and “low” (Star and Drum Cks.) precipitation categorizations. Annual water yield in burned watersheds was 6-24% higher than that in unburned reference watersheds, but only the Lynx and North York Ck. comparison was statistically significant. Perhaps the largest and most important result from this chapter is evidence for a shift in the annual hydrograph to earlier in the season. Half flows arrived in burned watersheds approximately 7-10 days earlier than in reference watersheds and April and May water yields were 100-200% and 40-50% higher, respectively, in burned watersheds. Results also suggested approximately 15% lower water yield in burned watersheds during the low flow period. While there was some evidence of process-scale hydrologic recovery from potassium:silica ratios, there was no indication of recovery of water yields in burned watersheds.

Chapter 4 investigated the magnitude and timing of runoff responses from rainstorm events in burned and reference watersheds during the snow-free season each year (generally late June to late September). For the high precipitation (HP) trio of watersheds, runoff indicators (quickflow, event rise, runoff coefficients) for most burned/reference comparisons were not significantly different. In contrast, storm runoff (all indicators) in the low precipitation (LP) burned watershed (Drum Ck.) was significantly greater than the LP reference watershed (Star Ck.). Additionally, a multiple regression analysis suggested total event precipitation was, by far, the most important predictor of storm runoff, while pre-event streamflow (i.e., antecedent wetness) was the next most important. A dummy variable representing watershed condition (burned or unburned) was also significant, but did not account for much variability in the model. Finally, rainfall intensity was only marginally significant, accounting for almost no variance in the regression model. Thus, while there was some evidence that wildfire may have led to runoff responses of greater magnitude, especially in the LP burned watershed, responses were very muted in comparison to studies from more southern latitudes (e.g. Moreno et al. 2020). Information on lag times was the opposite of what would be expected (i.e., longer lag times in burned watersheds), likely suggesting physical watershed differences influenced stormflow timing more than the wildfire.

5.2. Implications

The Chapter 2 study on net precipitation in burned and unburned forest stands is likely the first attempt to address wildfire effects on both net rainfall and snow accumulation in a single study. Moreover, the research spanned a 10-year period which is unusually long compared to existing studies. Extensive literature focused on rainfall interception suggests canopy interception can be high in coniferous forests (Carlyle-Moses and Gash 2011). However, little prior research existed for subalpine forest types, generally, and burned forests in particular. Thus, the study outlined in Chapter 2 helps fill several key knowledge gaps. Additionally, the research on stemflow was the first, to my knowledge, reported in the literature for burned trees. The results of this work suggest the volume of water delivered to the ground near burned trees and to decaying root channels beneath them is significant in burned forests and far exceeds stemflow for live subalpine trees. Combined with potentially higher nutrient concentrations, the fate of stemflow takes on greater importance (Spencer and van Meerveld 2016). The measured increase in snow accumulation was relatively large (+78% snow water equivalent) which we expected to have implications for the snowmelt runoff period. Reported differences from previous work on post-wildfire snow accumulation were not as large as those measured for the present study, especially in more southerly locations. This seems to reaffirm the contention of Maxwell et al. (2019) that post-wildfire increases in snow accumulation may be larger in more northern latitudes.

The change in annual water yield in burned watersheds was not large given the magnitude of the difference in post-wildfire net precipitation at the stand scale. This result is consistent with those from both burned and harvested watershed studies in other western Canadian mountainous regions (Pomeroy et al. 2012; Winkler et al. 2017; Owens et al. 2013). However, the significantly greater snow accumulation in burned forest stands studied here, combined with greater incoming radiation (Burles and Boon 2011) suggested the potential for changes to the magnitude and timing of snowmelt which was subsequently confirmed by the studies in Chapter 3. While no serious flooding was observed in study watersheds owing solely to high spring snowmelt rates, infrastructure managers downstream of burned watersheds in similar environments may consider plans to address these types of high flow events because of increased potential for their occurrence. In particular, the additive effect of rain-on-snow during the high-flow melt period could pose a flooding hazard (Marks et al. 1998). During some high flow events observed in the study region, dead trees and other woody debris caused jams at bridges, raising the potential for flooding and infrastructure damage. Additionally, given evidence already showing earlier spring snowmelt in some mountainous regions of the western US, wildfire could contribute to even earlier melt in burned watersheds which has implications for late summer streamflows (Cayan et al. 2001). If managers are concerned with preserving snowpack later into spring after wildfire, silvicultural strategies designed to reduce incoming solar radiation could be considered in strategic parts of burned watersheds to accelerate forest regeneration. In the stand used for snow accumulation measurements, the taller regenerating lodgepole pine are currently only ~5 m in height almost 20 years after wildfire, suggesting substantial time is required to restore shading processes in this forest.

Several studies from other regions have shown significant storm runoff response to rainfall in the first year or two after wildfire (e.g. Scott and Van Wyk 1990; Moody and Martin 2001; Moreno et al. 2020). However, findings from this study suggest much smaller storm runoff responses might occur in some northern Rocky Mountain catchments; while storm runoff was generally elevated in burned watersheds, the differences relative to the unburned reference watersheds were relatively small. Moreover, to our knowledge, no major debris flows were documented in the burned study watersheds. However, it is important to note that meteorological conditions (e.g., long duration or high-intensity rainfall) in the first 2-3 post-wildfire years can be an important determinant of stormflow and debris flow behaviour (Cannon et al. 2008; Jordan 2015). Relatively widespread debris flow activity was documented following the severe 2003 wildfire season in British Columbia especially where "gentle-over-steep" topography (i.e., plateaus over steep gullies or channels) coincided with high burn severity (Jordan 2015). Generally low rainfall intensities may have also played a role in subdued stormflow activity in our study watersheds especially in comparison to some regions of the US or the Mediterranean basin where, in the latter case, days with 300 mm of rainfall are "not unusual" (Moody and Martin 2009; Cerda and Doerr 2005). Multiple regression analysis also indicated antecedent wetness was an important determinant of storm runoff magnitude. This was evident during the snow-free period in this study as generally dry conditions seemed to provide some hydrologic buffering for storm rainfall later in the active flow season. The generally low-magnitude runoff responses are especially notable given the large increase in net rainfall observed in Chapter 2.

5.3. Limitations

The primary limitation for Chapter 2 was a lack of spatial replication for rainfall interception and snow accumulation work which was largely driven by resource constraints (e.g. money, equipment, labour). As such, net precipitation insights reflect the characteristics of those particular study stands, including aspect and forest canopy structure/coverage. Studies for Chapters 3 and 4 were necessarily limited by a lack of pre-disturbance data which is a common constraint for watershed-scale wildfire hydrology studies because researchers have no control over the location of the wildfires. However, this study had replication of both reference and burned watersheds and a relatively long post-fire period (11 years) of precipitation and streamflow observation, both of which are rare and contributed substantial additional insights into catchment-scale flow after wildfire in relation to previous studies.

5.4. Recommendations for Future Research

Studies detailed in Chapter 2 improved our understanding of rainfall interception and snow accumulation in burned subalpine forests. This study is one of the first to indicate the magnitude of possible wildfire-induced changes to these processes. However, there remains a paucity of research on net rainfall and interception measurements in burned forests. Further, a comparison of functions to predict canopy interception from the present study and from nearby work in British Columbia indicate relatively large differences in estimates of interception and/or net rainfall (Moore et al. 2008). This work could benefit from further replication because it focused on only four total forest plots for the rainfall and snow accumulation work. Investigations in additional stand types and on other slope aspects would help contextualize this work and may explain why relative changes in water yield in burned watersheds were relatively small given the >50% increase in stand-level net precipitation. Further, these results imply some of the largest increases in snow accumulation in burned forests in the literature; further verification of this result would be prudent. As of this writing, the Lost Creek fire occurred almost 19 years ago and, while forest regeneration is relatively sparse in some areas, regenerating lodgepole pine trees are approximately 5-6 m in height. Additional research is recommended in these stands as they regenerate to determine how net precipitation and interception change over time. This would help both forest and water managers better understand and predict forest and hydrologic recovery after severe wildfires in northern North American mountainous regions.

Research reported on in Chapter 3 significantly improved our understanding of wildfire effects on the longer-term flow regime in Canadian Rocky Mountain environments. Highly valuable additional research could include characterization of the post-wildfire flow regime after two decades or more of forest recovery. As wildfire-hydrology science matures, some studies are beginning to examine older burned watersheds with a fresh eye (e.g. Niemeyer et al. 2020). Studies such as this will be vital to verify decades-old results, often acquired without the benefit of a BACI-designed experiment. Specific questions of interest related to those outlined in Chapter 3 could focus further on the magnitude of (and shift in) the spring snowmelt and the magnitude of low flows. It is unclear if the large differences in water yield during snowmelt will still be present as these burned watersheds regenerate. Recent advances in post-harvesting hydrology studies have shown that low flows could only begin to decrease two decades after disturbance (Gronsdahl et al. 2019) but more studies are needed in more regions. These questions will continue to have implications for downstream water supply, forest management, and the integrity of aquatic ecosystems.

Similarly, research in Chapter 4 has provided new scientific insights on wildfire effects on the magnitude and timing of storm runoff at the watershed scale in the Canadian Rocky Mountains. However, hydrograph separation using graphical techniques is a coarse approach to quantifying the quickflow component of storm runoff. While it allows comparison between watersheds, it does not accurately parse various contributing sources of streamflow during storms. Further studies making use of isotopic tracers (i.e., end-member mixing analysis) in Canadian Rocky Mountain settings would help to better define potential fire disturbance effects on partitioning of quickflow and baseflow components. A common approach to this technique would be to collect water samples from the streams and from the main sources contributing to streamflow (e.g., precipitation, shallow groundwater, etc.) to develop a baseline dataset, then collect these samples at a high resolution during a series of rainfall-runoff events. End-member mixing analysis could potentially allow the researcher to more accurately quantify quickflow and baseflow volumes. Moreover, with the addition of snowmelt lysimeters, this approach might also aid in understanding contributions from rain-on-snow events. Rain-on-snow produces some of the largest storm runoff events in the study region, but these are not explicitly investigated in this study. Because of the potential of rain-on-snow events to produce exceedingly high, and potentially damaging flow responses, this topic deserves further research especially in burned, mountainous watersheds.

In addition to the above suggestions related to storm runoff, there is a need for fundamental research into processes which contribute to fast hydrologic flow pathways in Canadian post-wildfire landscapes. This type of research has been done in the midwestern United States (among other places) and includes measurements of soil water repellency, infiltration, and the influence of burn severity on both of these properties. Further research is needed to determine if soil water repellency is as important in more northern, snow-dominated systems as it is elsewhere and how long-duration snow cover may affect the longevity and strength of soil water repellency.

In conclusion, this research found much higher net precipitation in burned subalpine forest stands than in unburned forest stands. However, despite the large increase in potential hydrologic forcing produced by fire, the effects on annual water yield were relatively small. Any additional snow accumulation in burned watersheds appeared to arrive earlier as snowmelt which is consistent with previous studies on wildfire and harvesting (e.g. Troendle and Bevenger 1996; Winkler et al. 2017). Moreover, while storm runoff appeared to be slightly elevated in burned watersheds, its magnitude was very low in both burned and reference watersheds. This 10-year study on post-wildfire hydrology represents an important contribution for consideration by municipalities, water supply managers and aquatic ecologists in Canadian Rocky Mountain environments particularly as the frequency, size, and severity of wildfires continue to increase.

References

Adams, MA (2013) Mega-fires, tipping points and ecosystem services: Managing forests and woodlands in an uncertain future. *Forest Ecology and Management*, **294**, 250-261. doi: http://dx.doi.org/10.1016/j.foreco.2012.11.039

ASRD (2006) Sustainable Resource Development, Government of Alberta. Wildfire perimeters for the years 2000-2005 vector digital data metadata file. Edmonton, Alberta.

Bates, CG (1921) First results in the streamflow experiment, Wagon Wheel Gap, Colorado. *Journal of Forestry*, **19**(4), 402-408.

Bazemore DE, Eshleman KN, Hollenbeck KJ (1994) The role of soil water in stormflow generation in a forested headwater catchment: synthesis of natural tracer and hydrometric evidence. *Journal of Hydrology* **162**, 47-75.

Beck HE, Zimmerman NE, McVicar TR, Vergopolan N, Berg A, Wood EF (2018) Present and future Köppen-Geiger climate classification maps at 1-km resolution. *Scientific Data* **5**, 180214. doi: 10.1038/sdata.2018.214

Benavides-Solorio J, MacDonald LH (2001) Post-fire runoff and erosion from simulated rainfall on small plots, Colorado Front Range. *Hydrological Processes* **15**, 2931-2952. doi: 10.1002/hyp.383

Beyene MT, Leibowitz SG, Pennino MJ (2021) Parsing weather variability and wildfire effects on the post-fire changes in daily stream flows: A quantile-based statistical approach and its application. *Water Resources Research* **57**(10). doi: 10.1029/2020WR028029

Bladon KD, Emelko MB, Silins U, Stone M (2014) Wildfire and the future of water supply. *Environmental Science and Technology* **48**(16), 8936-8943. doi: 10.1021/es500130g

Bladon KD, Silins U, Wagner MJ, Stone M, Emelko MB, Mendoza CA, Devito KJ, Boon S (2008) Wildfire impacts on nitrogen concentration and production from headwater streams in southern Alberta's Rocky Mountains. *Canadian Journal of Forest Research* **38**, 2359-2371. doi: 10.1139/X08-071

Bonell M, Fritsch JM (1997) Combining hydrometric-hydrochemistry methods: a challenge for advancing runoff generation process research. In *Hydrochemistry, Proceedings of the Rabat Symposium*, 165-184.

Boon, S (2009) Snow ablation energy balance in a dead forest stand. *Hydrological Processes: An International Journal*, **23**(18), 2600-2610. doi: https://doi.org/10.1002/hyp.7246

Bosch JM, Hewlett JD (1982) A review of catchment experiments to determine the effect of vegetation changes on water yield and evapotranspiration. *Journal of Hydrology* **55**, 3-23.

Brabender B (2005) Scaling leaf area index and rainfall interception in lodgepole pine. MSc. Thesis, University of Alberta. (Edmonton, AB)

Britton, DL (1991) Fire and the chemistry of a South African mountain stream. *Hydrobiologia*, **218**(3), 177-192.

Bruijnzeel LA (1989) (De)forestation and dry season flow in the tropics: A closer look. *Journal of Tropical Forest Science* **1**(3), 229-243. doi: 10.1016/j.agee.2004.01.015

Bruijnzeel LA (2004) Hydrological functions of tropical forests: not seeing the soil for the trees? *Agriculture, Ecosystems and Environment* **104**, 185-228.

Burles K, Boon S (2011) Snowmelt energy balance in a burned forest plot, Crowsnest Pass, Alberta, Canada. *Hydrological Processes* **25**(19), 3012-3029. doi: 10.1002/hyp.8067

Campbell RE, Baker, Jr. MB, Ffolliott PF, Larson FR, Avery CC (1977) Wildfire effects on a Ponderosa Pine ecosystem: An Arizona case study. U.S. Department of Agriculture, Forest Service Research Paper RM-191. Fort Collins, Colorado.

Cannon SH, Gartner JE, Wilson RC, Bowers JC, Laber JL (2008) Storm rainfall conditions for floods and debris flows from recently burned areas in southwestern Colorado and southern California. *Geomorphology* **96**, 250-269. doi:10.1016/j.geomorph.2007.03.019

Carlyle-Moses DE, Gash JHC (2011) Rainfall interception loss by forest canopies. In 'Forest Hydrology and Biogeochemistry: Synthesis of Past Research and Future Directions.' (Eds DF Levia, D Carlyle-Moses, T Tanaka.) pp. 407-423. (Springer: Dordrecht). doi: 10.1007/978-94-007-1363-5_20

Carlyle-Moses DE, Lishman CE, McKee AJ (2014) A preliminary evaluation of throughfall sampling techniques in a mature coniferous forest. *Journal of Forestry Research* **25**(2), 407-413. doi: 10.1007/s11676-014-0468-8

Carlyle-Moses DE, Iida S, Germer S, Llorens P, Michalzik B, Nanko K, Tischer A, Levia DF. (2018) Expressing stemflow commensurate with its ecohydrological importance. *Advances in Water Resources* **121**, 472-479. doi: 10.1016/j.advwatres.2018.08.015

Cayan, DR, Kammerdiener, SA, Dettinger, MD, Caprio, JM, Peterson, DH (2001) Changes in the onset of spring in the western United States. *Bulletin of the American Meteorological Society*, **82**(3), 399-416. doi: 10.1175/1520-0477(2001)082%3C0399:CITOOS%3E2.3.CO;2

Cerda, A, Doerr, SH (2005) Long-term soil erosion changes under simulated rainfall for different vegetation types following a wildfire in eastern Spain. *Journal of Wildland Fire*, **14**, 423-437.

Cerdà A, Robichaud PR (2009) Fire effects on soils and restoration strategies. In: Land Reconstruction and Management. Haigh MJ (ed). *Science Publishers*, Enfield, New Hampshire, USA.

Chang, M (2006) Forest hydrology: an introduction to water and forests. CRC press.

Cingolani AM, Poca M, Whitworth-Hulse JI, Giorgis MA, Vaieretti MV, Herrero L, Ramos SN, Renison D (2020) Fire reduces dry season low flows in a subtropical highland of central Argentina. *Journal of Hydrology* **590**, 125538. doi: 10.1016/j/jhydrol.2020.125538

Coogan, SC, Daniels, LD, Boychuk, D, Burton, PJ, Flannigan, MD. Gauthier, S, Kafka, V, Park, JS, Wotton, BM (2021) Fifty years of wildland fire science in Canada. *Canadian Journal of Forest Research*, **51**(2), 283-302. doi: 10.1139/cjfr-2020-0314

Coogan SCP, Robinne F-N, Jain P, Flannigan MD (2019) Scientists' warning on wildfire – a Canadian perspective. *Canadian Journal of Forest Research* **49,** 1015-1023. doi: 10.1139/cjfr-2019-0094

Cydzik K, Hogue TS (2009) Modeling postfire response and recovery using the Hydrologic Engineering Center hydrologic modeling system (HEC-HMS). *Journal of the American Water Resources Association* **45**(3), 702-714. doi: 10.1111/j.1752-1688.2009.00317.x

Debano LF (2000) The role of fire and soil heating on water repellency in wildland environments: a review. *Journal of Hydrology* **231–232**, 195–206.

Dennison PE, Brewer SC, Arnold JD, Moritz MA (2014) Large wildfire trends in western United States, 1984-2011. *Geophysical Research Letters* **41**, 2928-2933. doi: 10.1002/2014GL059576

Dixon D, Boon S (2012) Comparison of the SnowHydro snow sampler with existing snow tube designs. *Hydrological Processes* **26**, 2555-2562. doi:10.1002/hyp.9317

Dixon D, Boon S, Silins U (2014) Watershed-scale controls on snow accumulation in a small montane watershed, southwestern Alberta, Canada. *Hydrological Processes* **28**, 1294-1306. doi: 10.1002/hyp.9667

Doerr SH, Shakesby RA, Blake WH, Chafer CJ, Humphreys GS, Wallbrink PJ (2006) Effects of differing wildfire severities on soil wettability and implications for hydrological response. *Journal of Hydrology* **319**, 295-311. doi: 10.1016/j.jhydrol.2005.06.038

Doerr SH, Shakesby RA, Walsh RPD (2000) Soil water repellency: its causes, characteristics and hydro-geomorphological significance. *Earth-Science Reviews* **51**, 33-65.

Downing DJ, Pettapiece WW (2006) Natural regions and subregions of Alberta. Natural Regions Committee, Government of Alberta. Pub. No. T/852. (Edmonton, Alberta)

Dunkerley D (2020) How is the intensity of rainfall events best characterised? A brief critical review and proposed new rainfall intensity index for application in the study of landsurface processes. *Water* **12**, 929. doi: 10.3390/w12040929

Eaton BC, Moore RD, Giles TR (2010) Forest fire, bank strength and channel instability: the 'unusual' response of Fishtrap Creek, British Columbia. *Earth Surface Processes and Landforms* **35**, 1167-1183. doi: 10.1002/esp.1946

Ebel BA (2020) Temporal evolution of measured and simulated infiltration following wildfire in the Colorado Front Range, USA: Shifting thresholds of runoff generation and hydrologic hazards. *Journal of Hydrology* **585**, 124765. doi: 10.1016/j/jhydrol.2020.124765

Ebel BA, Martin DA (2017) Meta-analysis of field-saturated hydraulic conductivity recovery following wildland fire: Applications for hydrologic model parameterization and resilience assessment. *Hydrological Processes* **31**, 3682-3696. doi: 10.1002/hyp.11288

Ebel BA, Moody JA (2013) Rethinking infiltration in wildfire-affected soils. *Hydrological Processes* **27**, 1510-1514. doi:10.1002/hyp.9696.

Ebel BA, Hinckley ES, Martin DA (2012) Soil-water dynamics and unsaturated storage during snowmelt following wildfire. *Hydrology and Earth System Sciences* **16**, 1401-1417. doi: 10.5194/hess-16-1401-2012

Elder K, Rosenthal W, Davis RE (1998) Estimating the spatial distribution of snow water equivalence in a montane watershed. *Hydrological Processes* **12**, 1793-1808.

Elsenbeer H, Lack A, Cassel K (1995) Chemical fingerprints of hydrological compartments and flow paths at La Cuenca, western Amazonia. *Water Resources Research* **31**(12), 3051-3058.

Emelko MB, Silins U, Bladon KD, Stone M (2011) Implications of land disturbance on drinking water treatability in a changing climate: Demonstrating the need for "source water supply and protection" strategies. *Water Research* **45**, 461-72. doi: 10.1016/j.watres.2010.08.051

Emmerton CA, Cooke CA, Hustins S, Silins U, Emelko MB, Lewis T, Kruk MK, Taube N, Zhu D, Jackson B, Stone M, Kerr JG, Orwin JF (2020) Severe western Canadian wildfire affects water quality even at large basin scales. *Water Research* **183**, 116071. doi: 10.1016/j.watres.2020.116071

Fairman, TA, Nitschke, CR, Bennett, LT (2016) Too much, too soon? A review of the impacts of increasing wildfire frequency on tree demography and structure in temperate forests. *Int. J. Wildl. Fire*, **25**, 831-48. doi: http://dx.doi.org/10.1071/WF15010

Fang X, Pomeroy JW (2016) Impact of antecedent conditions on simulations of a flood in a mountain headwater basin. *Hydrological Processes* **30**, 2754-2772. doi: 10.1002/hyp.10910

Flannigan MD, Logan KA, Amiro BD, Skinner WR, Stocks BJ (2005) Future area burned in Canada. *Climatic Change* **72**, 1–16. doi:10.1007/s10584-005-5935-y

Frazer GW, Canham CD, Lertzman KP. (1999) Gap Light Analyzer (GLA), Version 2.0: Imaging software to extract canopy structure and gap light transmission indices from true-colour fisheye photographs, Users manual and program documentation. Burnaby: Simon Fraser University and Millbrook: Institute of Ecosystem Studies.

Gleason KE, Nolin AW, Roth TR (2013) Charred forests increase snowmelt: Effects of burned woody debris and incoming solar radiation on snow ablation. *Geophysical Research Letters* **40**, 4654–4661. doi:10.1002/grl.50896

Goeking SA, Tarboton DG (2020) Forests and water yield: A synthesis of disturbance effects on streamflow and snowpack in western coniferous forests. *Journal of Forestry*, 172-192. doi: 10.1093/jofore/fv069

Gluns DR (2001) Snowline pattern during the melt season: evaluation of the H60 concept. Watershed assessment in the southern Interior of British Columbia. DAA Toews and S. Chatwin (eds). BC Ministry of Forests, Research Branch, Victoria, BC Working Paper, (57), pp.68-93.

Gronsdahl S, Moore RD, Rosenfeld J, McCleary R, Winkler R (2019) Effects of forestry on summertime low flows and physical fish habitat in snowmelt-dominated headwater catchments of the Pacific Northwest. *Hydrological Processes* **33**, 3152-3168. doi: 10.1002/hyp.13580

Hallema DW, Sun G, Bladon KD, Norman SP, Caldwell PV, Liu Y, McNulty SG (2017) Regional patterns of postwildfire streamflow response in the Western United States: The importance of scale-specific connectivity. *Hydrological Processes* **31**, 2582-2598. doi: 10.1002/hyp.11208

Hanes CC, Wang X, Jain P, Parisien M-A, Little JM, Flannigan MD (2019) Fire-regime changes in Canada over the last half century. *Canadian Journal of Forest Research* **49**, 256-269. doi: 10.1139/cjfr-2018-0293

Harder P, Pomeroy JW, Westbrook CJ (2015) Hydrological resilience of a Canadian Rockies headwaters basin subject to changing climate, extreme weather, and forest management. *Hydrological Processes* **29**, 3905-3924. doi: 10.1002/hyp.10596

Harpold AA, Biederman JA, Condon K, Merino M, Korgaonkar Y, Nan T, Sloat LL, Ross M, Brooks PD (2014) Changes in snow accumulation and ablation following the Las Conchas Forest Fire, New Mexico, USA. *Ecohydrology* **7**, 440-452. doi:10.1002/eco.1363

Harvey BJ (2016) Human-caused climate change is now a key driver of forest fire activity in the western United States. *Proceedings of the National Academy of Sciences* **113**(42), 11649-11650.

Havel, A, Tasdighi, A, Arabi, M (2018) Assessing the hydrologic response to wildfires in mountainous regions. *Hydrology and Earth System Sciences*, **22**(4), 2527-2550. doi: https://doi.org/10.5194/hess-22-2527-2018

Hauer FR, Spencer CN (1998) Phosphorus and nitrogen dynamics in streams associated with wildfire: A study of immediate and longterm effects. *International Journal of Wildland Fire* **8**(4), 183-198.

Heath JT, Chafer DJ, van Ogtrop FF, Bishop TFA (2014) Post-wildfire recovery of water yield in the Sydney Basin water supply catchments: An assessment of the 2001/2002 wildfires. *Journal of Hydrology* **519**, 1428-1440. doi: 10.1016/j/jhydrol.2014.09.033

Hedstrom NR, Pomeroy JW (1998) Measurements and modeling of snow interception in the boreal forest. *Hydrological Processes* **12**, 1611–1625.

Helsel, DR, Hirsch, RM (2002) Statistical Methods in Water Resources Techniques of Water Resources Investigations, Book 4. *USDI, Geological Survey: Washington, DC*.

Helvey JD (1980) Effects of a north central Washington wildfire on runoff and sediment production. *Water Resources Bulletin* **16**(4), 627-634.

Hewlett JD, Bosch JM (1984). The dependence of storm flows on rainfall intensity and vegetal cover in South Africa. *Journal of Hydrology* **75**(1-4), 365-381. doi: 10.1016/0022-1694(84)90060-X

Hewlett JD, Hibbert AR (1967) Factors affecting the response of small watersheds to precipitation in humid areas. In: *International Symposium on Forest Hydrology* (Sopper WE, Lull HW, eds.), 275-290. Pergamon, Oxford, UK.

Herwitz SR, Slye RE (1995) Three-dimensional modeling of canopy tree interception of wind-driven rainfall. *Journal of Hydrology* **168**, 205-226.

Jordan, P (2015) Post-wildfire debris flows in southern British Columbia, Canada. *International journal of wildland fire*, **25**(3), 322-336. doi: https://doi.org/10.1071/WF14070

Jost G, Weiler M, Gluns DR, Alila Y (2007) The influence of forest and topography on snow accumulation and melt at the watershed-scale. *Journal of Hydrology* **347**, 101-115. doi: 10.1016/j.jhydrol.2007.09.006

Julian P, Helsel D (2021). NADA2: Data Analysis for Censored Environmental Data. R package version 1.0.2. https://github.com/SwampThingPaul/NADA2

Jung HY, Hogue TS, Rademacher LK, Meixner T (2009) Impact of wildfire on source water contributions in Devil Creek, CA: Evidence from end-member mixing analysis. Hydrological Processes 23, 183-200. doi: 10.1002/hyp.7132

Kaufmann MR, Edminster CB, Troendle CA (1982) Leaf area determinations for subalpine tree species in the central Rocky Mountains. U.S. Department of Agriculture, Forest Service Research Paper, RM-238. (Fort Collins, Colorado)

Kean JW, Staley DM, Cannon SH (2011) In situ measurements of post-fire debris flows in southern California: Comparisons of the timing and magnitude of 24 debris-flow events with rainfall and soil moisture conditions. *Journal of Geophysical Research* **116**, F04019. doi: 10.1029/2011JF002005

Keim RF, Skaugset AE (2003) Modelling effects of forest canopies on slope stability. *Hydrological Processes* **17**, 1457–1467. doi:10.1002/hyp.5121

Kienzle SW (2008) A new temperature based method to separate rain and snow. *Hydrological Processes* **22**, 5067–5085. doi:10.1002/hyp.7131

Kinoshita, AM, Hogue, TS (2011) Spatial and temporal controls on post-fire hydrologic recovery in Southern California watersheds. *Catena*, **87**(2), 240-252. doi: https://doi.org/10.1016/j.catena.2011.06.005

Kinoshita AM, Hogue TS (2015) Increased dry season water yield in burned watersheds in Southern California. *Environmental Research Letters* **10**, 014003. doi: 10.1088/1748-9326/10/1/014003

Kunze MD, Stednick JD (2006) Streamflow and suspended sediment yield following the 2000 Bobcat fire, Colorado. *Hydrological Processes* **20**, 1661-1681. doi: 10.1002/hyp.5954

Lane, PN, Sheridan, GJ, Noske, PJ (2006) Changes in sediment loads and discharge from small mountain catchments following wildfire in south eastern Australia. *Journal of Hydrology*, **331**(3-4), 495-510. doi:10.1016/j.jhydrol.2006.05.035

Larsen IJ, MacDonald LH, Brown E, Rough D, Welsh MJ, Pietraszek JH, Libohova Z, Benavides-Solorio JD, Schaffrath K (2009) Causes of post-fire runoff and erosion: Water repellency, cover, or soil sealing? *Soil Science Society of America Journal* **73**(4), 1393-1407. doi: 10.2136/sssaj2007.0432

Lehning M, Lowe H, Ryser M, Raderschall N (2008) Inhomogenous precipitation distribution and snow transport in steep terrain. *Water Resources Research* **44**, W07404, doi: 10.1029/2007WR006545.

Link TE, Unsworth M, Marks D (2004) The dynamics of rainfall interception by a seasonal temperate rainforest. *Agricultural and Forest Meteorology* **124**, 171-191. doi: 10.1016/j.agrformet.2004.01.010

Llorens P, Gallart F (2000) A simplified method for forest water storage capacity measurement. *Journal of Hydrology* **240**, 131-144.

Lundberg A, Halldin S (1994) Evaporation of intercepted snow: Analysis of governing factors. *Water Resources Research* **30**(9), 2587–2598.

MacDonald LH, Huffman EL (2004) Post-fire soil water repellency: Persistence and soil moisture thresholds. *Soil Science Society of America Journal* **68**, 1729-1734.

Mahat V, Anderson A (2013) Impacts of climate and catastrophic forest changes on streamflow and water balance in a mountainous headwater stream in Southern Alberta. *Hydrology and Earth System Science* **17**, 4941-4956. doi: 10.5194/hess-17-4941-2013

Mahat V, Silins U, Anderson A (2016) Effects of wildfire on the catchment hydrology in southwest Alberta. *Catena* **147**, 51-60. doi: 10.1016/j.catena.2016.06.040

Marks D, Kimball J, Tingey D, Link T (1998) The sensitivity of snowmelt processes to climate conditions and forest cover during rain-on-snow: a case study of the 1996 Pacific Northwest flood. *Hydrological Processes* **12**, 1569-1587.

Martens, AM, Silins, U, Proctor, HC, Williams, CHS, Wagner, MJ, Emelko, MB, Stone, M (2019) Long-term impact of severe wildfire and post-wildfire salvage logging on macroinvertebrate assemblage structure in Alberta's Rocky Mountains. *International Journal of Wildland Fire*, **28**(10), 738-749. doi: https://doi.org/10.1071/WF18177

Maxwell JD, Call A, Clair SBS (2019) Wildfire and topography impacts on snow accumulation and retention in montane forests. *Forest Ecology and Management* **432**, 256-263.

Mayor AG, Bautista S, Llovet J, Bellot J (2007) Post-fire hydrological and erosional responses of a Mediterranean landscape: Seven years of catchment-scale dynamics. *Catena* **71**, 68-75. doi: 10.1016/j.catena.2006.10.006

Melone F, Corradini C, Singh VP (2002) Lag prediction in ungauged basins: an investigation through actual data of the upper Tiber River valley. *Hydrological Processes* **16**, 1085-1094. doi: 10.1002/hyp.313

Mendiburu FD, Yaseen M (2020) Agricolae: Statistical procedures for agricultural research. R package version 1.4.0. https://myaseen208.github.io/agricolae/https://cran.r-project.org/package=agricolae

Micheletty PD, Kinoshita AM, Hogue TS (2014) Application of MODIS snow cover products: wildfire impacts on snow and melt in the Sierra Nevada. *Hydrology and Earth System Sciences* **18**, 4601-4615. doi: 10.5194/hess-18-4601-2014

Mitsudera M, Kamata Y, Nakane K (1984) Effect of fire on water and major nutrient budgets in forest ecosystems III. Rainfall interception by forest canopy. *Japanese Journal of Ecology* **34**, 15-25.

Moody JA (2012) An analytical method for predicting postwildfire peak discharges. U.S. Geological Survey, Scientific Investigations Report 2011-5236, 36 p.

Moody JA, Ebel BA (2012) Hyper-dry conditions provide new insights into the cause of extreme floods after wildfire. *Catena* **93**, 58-63. doi: 10.1016/j.catena.2012.01.006

Moody JA, Martin DA (2001) Post-fire, rainfall intensity-peak discharge relations for three mountainous watersheds in the Western USA. *Hydrological Processes* **15**, 2981–2993. doi:10.1002/hyp.386

Moody JA, Martin DA (2009) Synthesis of sediment yields after wildland fire in different rainfall regimes in the western United States. *International Journal of Wildland Fire* **18**, 96-115. doi: 10.1071/WF07162

Moody JA, Martin DA, Haire SL, Kinner DA (2008) Linking runoff response to burn severity after a wildfire. *Hydrological Processes* **22**, 2063-2074. doi: 10.1002/hyp.6806

Moody, JA, Shakesby, RA, Robichaud, PR, Cannon, SH, Martin, DA (2013) Current research issues related to post-wildfire runoff and erosion processes. *Earth-Science Reviews*, **122**, 10-37. doi: 10.1016/j.earscirev.2013.03.004

Moore D, Winkler R, Carlyle-Moses D, Spittlehouse D, Giles T, Phillips J, Leach J, Eaton B, Owens P, Petticrew E, Blake W, Heise B, Redding T (2008) Watershed response to the McLure Forest Fire: presentation summaries from the Fishtrap Creek workshop, March 2008. *Streamline Watershed Management Bulletin* **12**(1), 1–8.

Moore RD, Wondzell SM (2005) Physical hydrology and the effects of forest harvesting in the Pacific Northwest: A review. *Journal of the American Water Resources Association* **41**(4), 763-784. doi: 10.1111/j.1752-1688.2005.tb04463.x

Moreno HA, Gourley JJ, Pham TG, Spade DM (2020) Utility of satellite-derived burn severity to study short- and long-term effects of wildfire on streamflow at the basin scale. *Journal of Hydrology* **580**, 124244. doi: 10.1016/j.jhydrol.2019.124244

Neary DG, Ryan KC, DeBano LF, eds. (2005) Wildland fire in ecosystems: Effects of fire on soils and water. General Technical Report RMRS-GTR-42-vol.4. Ogden, UT. U.S. Department of Agriculture, Forest Service, Rocky Mountain Research Station. 250 p.

Neimeyer RJ, Bladon KD, Woodsmith RD (2020) Long-term hydrologic recovery after wildfire and post-fire forest management in the interior Pacific Northwest. *Hydrological Processes* **34**(5), 1182-1197. doi: 10.1002/hyp.13665.

Onodera, SI, Van Stan, JT (2011) Effect of forest fires on hydrology and biogeochemistry of watersheds. In *Forest hydrology and biogeochemistry* (pp. 599-621). Springer, Dordrecht. doi: 10.1007/978-94-007-1363-5_30

Owens PN, Giles TR, Petticrew EL, Leggat MS, Moore RD, Eaton BC (2013) Muted responses of streamflow and suspended sediment flux in a wildfire-affected watershed. *Geomorphology* **202**, 128-139. doi: 10.1016/j.geomorph.2013.01.001

Parker GG (1983) Throughfall and stemflow in the forest nutrient cycle. *Advances in Ecological Research* **13**, 57-133.

Peddle DR, Hall RJ, Jackson CD, Soenen SA, Gibb MR, Juhlin DT (2007) MFM canopy reflectance modeling and normalized burn ratio assessment of pre-fire overstory canopy structure and post-fire burn severity at the Lost Creek fire, Alberta Rocky Mountains. Our Common Borders – Safety, Security, and the Environment through Remote Sensing, October 28 – November 1 2007, Ottawa, Ontario, Canada.

Penna D, Tromp-van Meerveld HJ, Gobbi A, Borga M, Dalla Fontana G (2011) The influence of soil moisture on the threshold runoff generation processes in an alpine headwater catchment. *Hydrology and Earth System Sciences* **15**, 689-702. doi: 10.519/hess-15-689-2011

Pereira P, Jordán A, Cedrà A, Martin D (2015) Editorial: The role of ash in fire-affected ecosystems. *Catena* **135**, 337-339. doi: 10.1016/j.catena.2014.11.016

Perry TD, Jones JA (2017) Summer streamflow deficits from regenerating Douglas-fir forest in the Pacific Northwest, USA. *Ecohydrology,* **10**, e1790. doi: 10.1002/eco.1790

Philipsen LJ, Gill KM, Shepherd A, Rood SB (2018) Climate change and hydrology at the prairie margin: Historic and prospective future flows of Canada's Red Deer and other Rocky Mountain rivers. *Hydrological Processes* **32**, 2669-2684. doi: 10.1002/hyp.13180

Plamondon AP, Prevost M, Naud RC (1984) Rainfall interception in balsam fir stands, Montmorency forest. *Canadian Journal of Forest Research* **14**, 722-730.

Pomeroy JW, Gray DM (1995) Snowcover accumulation, relocation and management (Vol. 350). Saskatoon, Sask., Canada: National Hydrology Research Institute.

Pomeroy JW, Gray DM, Hedstrom NR, Janowicz JR (2002) Prediction of seasonal snow accumulation in cold climate forests. *Hydrological Processes* **16**, 3543-3558. doi: 10.1002/hyp.1228

Pomeroy J, Fang X, Ellis C (2012) Sensitivity of snowmelt hydrology in Marmot Creek, Alberta, to forest cover disturbance. *Hydrological Processes* **26**, 1891–1904. doi:10.1002/hyp.9248

Pomeroy JW, Parviainen J, Hedstrom N, Gray DM (1998) Coupled modelling of forest snow interception and sublimation. *Hydrological Processes* **12**, 2317–2337.

Pomeroy J, Schmidt RA (1993) The use of fractal geometry in modelling intercepted snow accumulation and sublimation. Proceedings of the 50th Annual Eastern Snow Conference. pp. 1-10.

Rakhmatulina E, Thompson S (2020) Freeze-thaw processes degrade post-fire water repellency in wet soils. *Hydrological Processes* **34**(26), 5229-5241. doi:10.1002/hyp.13931

Rantz SE *and others* (1982) Measurement and computation of streamflow: Volume 2. Computation of discharge. Geological Survey Water-Supply Paper 2175, U.S. Geological Survey, Washington, D.C.

Robichaud PR (2000) Fire effects on infiltration rates after prescribed fire in Northern Rocky Mountain forests, USA. *Journal of Hydrology* **231-232**, 220-229.

Robinne F-N, Bladon KD, Silins U, Emelko MB, Flannigan MD, Parisien M-A, Kiezle SW, Dupnt DP (2019) A regional-scale index for assessing the exposure of drinking-water sources to wildfires. *Forests* **10**, 384. doi: 10.3390/f10050384

Robinne F-N, Hallema DW, Bladon KD, Buttle JM (2020) Wildfire impacts on hydrologic ecosystem services in North American high-latitude forests: A scoping review. *Journal of Hydrology* **581**, 124360. doi: 10.1016/j.jhydrol.2019.124360

Rogeau M-P, Flannigan MD, Hawkes BC, Parisien M-A, Arthur R (2016) Spatial and temporal variations of fire regimes in the Canadian Rocky Mountains and Foothills of southern Alberta. *International Journal of Wildland Fire* **25**, 1117-1130. doi: 10.1071/WF15120

Rolland C (2003) Spatial and seasonal variations of air temperature lapse rates in alpine regions. *Journal of Climate* **16**, 1032-1046.

Rothacher J (1963) Net precipitation under a Douglas-Fir forest. *Forest Science* **9**(4), 423-429.

Rothwell R, Hillman G, Pomeroy JW (2016) Marmot Creek Experimental Watershed Study. *The Forestry Chronicle* **92**(1), 32-36.

RStudio Team (2021) RStudio: Integrated Development Environment for R. RStudio, PBC, Boston, MA URL http://www.rstudio.com/.

Rutter AJ, Morton AJ, Robins PC (1975) Predictive model of rainfall interception in forests II. Generalization of model and comparison with observations in some coniferous and hardwood stands. *Journal of Applied Ecology* **12**(1), 367-380.

Ryan SE, Dwire KA, Dixon MK (2011) Impacts of wildfire on runoff and sediment loads at Little Granite Creek, western Wyoming. *Geomorphology* **129**, 113-130. doi: 10.1016/j.geomorph.2011.01.017

Saxe S, Hogue TS, Hay L (2018) Characterization and evaluation of controls on post-fire streamflow response across western US watersheds. *Hydrology and Earth System Sciences* **22**, 1221-1237. doi: 10.5194/hess-22-1221-2018

Schellekens J, Scatena FN, Bruijnzeel LA, van Dijk AIJM, Groen MMA, van Hogezand RJP (2004) Stormflow generation in a small rainforest catchment in the Luquillo Experimental Forest, Puerto Rico. *Hydrological Processes* **18**, 505-530. doi: 10.1002/hyp.1335

Schmidt RA, Gluns DR (1991) Snowfall interception on branches of three conifer species. *Canadian Journal of Forest Research* **21**, 1262-1269.

Schindler DW, Newbury RW, Beaty KG, Prokopowich J, Ruszczynski T, Dalton JA (1980) Effects of a windstorm and forest fire on chemical losses from forested watersheds and on the quality of receiving streams. *Canadian Journal of Fisheries and Aquatic Sciences*, **37**(3), 328-334.

Schnorbus M, Alila Y (2004) Forest harvesting impacts on the peak flow regime in the Columbia Mountains of southeastern British Columbia: An investigation using long-term numerical modeling. *Water Resources Research* **40**, W05205. doi: 10.1029/2003WR002918

Scott DF (1993) The hydrological effects of fire in South African mountain catchments. *Journal of Hydrology* **150**, 409-432.

Scott DF, Van Wyk DB (1990) The effects of wildfire on soil wettability and hydrological behaviour of an afforested catchment. *Journal of Hydrology* **121**, 239-256.

Searcy JK (1959) Flow-duration curves. In: Manual of hydrology: Part 2. Low-flow techniques. Geological Survey Water-Supply Paper 1542-A. United States Government Printing Office, Washington. 33 p.

Seibert J, McDonnell JJ, Woodsmith RD (2010) Effects of wildfire on catchment runoff response: a modelling approach to detect changes in snow-dominated forested catchments. *Hydrology Research* **41**, 378–390. doi:10.2166/nh.2010.036.

Shakesby, RA (2011) Post-wildfire soil erosion in the Mediterranean: review and future research directions. *Earth-Science Reviews*, **105**(3-4), 71-100. doi:10.1016/j.earscirev.2011.01.001

Shakesby RA, Doerr SH (2006) Wildfire as a hydrological and geomorphological agent. *Earth-Science Reviews* **74**, 269-307. doi: 10.1016/j.earscirev.2005.10.006.

Silins U, Anderson A, Bladon KD, Emelko MB, Stone M, Spencer SA, Williams CHS, Wagner MJ, Martens AM, Hawthorn K (2016) Southern Rockies Watershed Project. *The Forestry Chronicle* **92**(1), 39-42.

Silins U, Bladon KD, Kelly EN, Esch E, Spence JR, Stone M, Emelko MB, Boon S, Wagner MJ, Williams CHS, Tichkowsky I (2014) Five-year legacy of wildfire and salvage logging impacts on nutrient runoff and aquatic plant, invertebrate, and fish productivity. *Ecohydrology* **7**, 1508-1523. doi: 10.1002/eco.1474

Silins U, Stone M, Emelko MB, Bladon KD (2009) Sediment production following severe wildfire and post-fire salvage logging in the Rocky Mountain headwaters of the Oldman River Basin, Alberta. *Catena* **79**, 189-197. doi: 10.1016/j.catena.2009.04.001

Skidmore PB (1994) Snow accumulation and ablation under fire-altered lodgepole pine forest canopies. MSc. Thesis, Montana State University. (Bozeman, Montana)

Sklash MG, Farvolden RN (1979) The role of groundwater in storm runoff. *Journal of Hydrology* **43**, 45-65.

Smith RS, Scherer RA, Dobson DA (2008) Snow cover extent during spring snowmelt in the south-central interior of British Columbia. *BC Journal of Ecosystems and Management* **9**(1), 57-70.

Soto B, Diaz-Fierros F (1997) Soil water balance as affected by throughfall in gorse (Ulex europaeus, L) shrubland after burning. *Journal of Hydrology* **195**, 218-231.

Spencer SA, Anderson A, Bladon KD (2016) Long-term watershed research in Alberta. *The Forestry Chronicle* **92**(1), 3-5

Spencer SA, Anderson AE, Silins U, Collins AL (2021) Hillslope and groundwater contributions to streamflow in a Rocky Mountain watershed underlain by glacial till and fractured sedimentary bedrock. *Hydrology and Earth System Sciences* **25**, 237-255. doi: 10.5194/hess-25-237-2021

Spencer SA, Silins U, Anderson AE (2019) Precipitation-runoff and storage dynamics in watersheds underlain by till and permeable bedrock in Alberta's Rocky Mountains. *Water Resources Research* **55**(12), 10690-10706. doi: 10.1029/2019WR025313

Spencer, SA, van Meerveld, HV (2016) Double funnelling in a mature coastal British Columbia forest: spatial patterns of stemflow after infiltration. *Hydrological Processes*, **30**(22), 4185-4201. doi: 10.1002/hyp.10936

Spittlehouse DL (1998) Rainfall interception in young and mature conifer forests in British Columbia. In, 'Proceedings of the 23rd conference on agriculture and forest meteorology, 2-6 Nov 1998, Albuquerque, NM.' *American Meteorological Society*, 171-174.

Stednick JD (1996) Monitoring the effects of timber harvest on annual water yield. *Journal of Hydrology* **176**, 79-95.

Stevens-Rumann, CS, Morgan, P (2019) Tree regeneration following wildfires in the western US: a review. *Fire Ecology*, **15**(1), 1-17. doi: https://doi.org/10.1186/s42408-019-0032-1

Stone M, Emelko MB, Droppo IG, Silins U (2011) Biostabilization and erodibility of cohesive sediment deposits in wildfire-affected streams. *Water Research* **45**, 521-534. doi: 10.1016/j.watres.2010.09.016

Stoof CR, Vervoort RW, Iwema J, van den Elsen E, Ferreira AJD, Ritsema CJ (2012) Hydrological response of a small catchment burned by experimental fire. *Hydrology and Earth System Sciences* **16**, 267-285. doi: 10.5194/hess-16-267-2012

Surfleet CG, Dietterick B, Skaugset A (2014) Change detection of storm runoff and sediment yield using hydrologic models following wildfire in a coastal redwood forest, California. *Canadian Journal of Forest Research* **44**, 572-581. doi: 10.1139/cjfr-2013-0328

Swanson RH, Golding DL, Rothwell RL, Bernier PY (1986) Hydrologic effects of clear-cutting at Marmot Creek and Streeter Watersheds, Alberta. Information Report NOR-X0278. Northern Forestry Centre, Canadian Forestry Service. 27 p.

Swanson RH, Hillman GR (1977) Predicted increased water yield after clearcutting in west—central Alberta. Northern Forest Research Centre, Edmonton, Alberta. IR NOR-X-198.

Tomkins KM, Humphreys GS, Gero AF, Shakesby RA, Doerr SH, Wallbrink PJ, Blake WH (2008) Postwildfire hydrological response in an El Niño-Southern Oscillation-dominated environment. *Journal of Geophysical Research* **113**, F02023. doi: 10.1029/2007JF000853

Tripler, CE, Kaushal, SS, Likens, GE, Todd Walter, M (2006) Patterns in potassium dynamics in forest ecosystems. *Ecology Letters*, **9**(4), 451-466. doi: 10.1111/j.1461-0248.2006.00891.x

Troendle, CA, Bevenger, GS (1996) Effect of fire on streamflow and sediment transport, Shoshone National Forest, Wyoming. *Ecological Implications of Fire in Greater Yellowstone. International Association of Wildland Fire, Fairfield, VA*, 43-45.

Valente F, David JS, Gash JHC (1997) Modelling interception loss for two sparse eucalypt and pine forests in central Portugal using reformulated Rutter and Gash analytical models. *Journal of Hydrology* **190**, 141-162.

Van Haveren BP (1988) A re-evaluation of the Wagon Wheel Gap Forest Watershed Experiment. *Forest Science* **34**(1), 208–214.

Van Stan JT, Levia DF (2010) Inter- and intraspecific variation of stemflow production from Fagus grandifolia Ehrh. (American beech) and Liriodendron tulipifera L. (yellow poplar) in relation to bark microrelief in the eastern United States. *Ecohydrology* **3**, 11-19. doi:10.1002/eco.83.

Varhola A, Coops NC, Weiler M, Moore RD (2010) Forest canopy effects on snow accumulation and ablation: An integrative review of empirical results. *Journal of Hydrology* **392**, 219–233. doi:10.1016/j.jhydrol.2010.08.009

Wagenbrenner JW, Ebel BA, Bladon KD, Kinoshita AM (2021) Post-wildfire hydrologic recovery in Mediterranean climates: A systematic review and case study to identify current knowledge and opportunities. *Journal of Hydrology* **602**, 126772. doi: 10.1016/j.jhydrol.2021.126772

Wagner, MJ, Bladon, KD, Silins, U, Williams, CHS, Martens, AM, Boon, S, MacDonald, RJ, Stone, M, Emelko, MB, Anderson, A (2014) Catchment-scale stream temperature response to land disturbance by wildfire governed by surface–subsurface energy exchange and atmospheric controls. *Journal of Hydrology*, **517**, 328-338. doi: 10.1016/j.jhydrol.2014.05.006

Wang X, Studens K, Parisien M-A, Taylor SW, Candau J-N, Boulanger Y, Flannigan MD (2020) Projected changes in fire size from daily spread potential in Canada over the 21st century. *Environmental Research Letters* **15**, 104048. doi: 10.1088/1748-9326/aba101

Westerling AL (2016) Increasing western US forest wildfire activity: sensitivity to changes in the timing of spring. *Philosphical Transactions B* **371**, 20150178. doi: 10.1098/rstb.2015.0178

Westerling AL, Hidalgo HG, Cayan DR, Swetnam TW (2006) Warming and earlier spring increase western US forest wildfire activity. *Science* **313**, 940-943

White AM (2015) Examining the impacts of wildfire on throughfall and stemflow chemistry and flux at plot and catchment scales. MSc. Thesis, University of Arizona. (Tucson, Arizona)

Williams CHS, Silins U, Spencer SA, Wagner MJ, Stone M, Emelko MB (2019) Net precipitation in burned and unburned subalpine forest stands after wildfire in the northern Rocky Mountains. *International Journal of Wildland Fire* **28**, 750-760. doi: 10.1071/WF18181

Wilson C, Kampf SK, Wagenbrenner JW, MacDonald LH (2018) Rainfall thresholds for post-fire runoff and sediment delivery from plot to watershed scales. *Forest Ecology and Management* **430**, 346-356. doi: 10.1016/j.foreco.2018.08.025

Wine, ML, Cadol, D (2016) Hydrologic effects of large southwestern USA wildfires significantly increase regional water supply: fact or fiction? *Environmental Research Letters*, **11**(8). doi: 10.1088/1748-9326/11/8/085006

Wine, ML, Makhnin, O, Cadol, D (2018) Nonlinear long-term large watershed hydrologic response to wildfire and climatic dynamics locally increases water yields. *Earth's Future*, **6**(7), 997-1006. doi: 10.1029/2018EF000930

Winkler R (2011) Changes in snow accumulation and ablation after a fire in south-central British Columbia. *Streamline Watershed Management Bulletin* **14**(2), 1–7.

Winkler RD, Allen DM, Giles TR, Heise BA, Moore RD, Redding TE, Spittlehouse DL, Wei X (2021) Approaching four decades of forest watershed research at Upper Penticton Creek, British Columbia: A synthesis. *Hydrological Processes* **35**(5), e14123. doi: 10.1002/hyp.14123

Winkler R, Spittlehouse D, Boon S (2017) Streamflow response to clear-cut logging on British Columbia's Okanagan Plateau. *Ecohydrology* **10**(2), e1836. doi:.10.1002/eco.1836

Winkler RD, Spittlehouse DL, Golding DL (2005) Measured differences in snow accumulation and melt among clearcut, juvenile, and mature forests in southern British Columbia. *Hydrological Processes* **19**, 51-62. doi: 10.1002/hyp.5757

Wohlgemuth PM (2016) Long-term hydrologic research on the San Dimas Experimental Forest, southern California: Lessons learned and future directions. In: Stringer CE, Krauss KW, Latimer JS, eds. (2016) Headwaters to estuaries: advances in watershed science and management - Proceedings of the Fifth Interagency Conference on Research in the Watersheds. March 2-5, 2015, North Charleston, South Carolina. e-General Technical Report SRS-211. Asheville, NC: U.S. Department of Agriculture Forest Service, Southern Research Station. 6 p.

Woods SW, Balfour VN (2010) The effects of soil texture and ash thickness on the post-fire hydrological response from ash-covered soils. *Journal of Hydrology* **393**, 274-286. doi: 10.1016/j.jhydrol.2010.08.025

Wortmann M, Bolch T, Menz C, Tong J, Krysanova V (2018) Comparison and correction of high-mountain precipitation data based on glaci-hydrological modeling in the Tarim River headwaters (High Asia). *American Meteorological Society* **19**, 777-801. doi: 10.1175/JHM-D-17-0106.1

Wotton BM, Nock CA, Flannigan MD (2010) Forest fire occurrence and climate change in Canada. *International Journal of Wildland Fire* **19**, 253-271. doi: 10.1071/WF09002

Wright KH, Rice RM, Thomas RB (1990) Logging effects on streamflow: storm runoff at Caspar Creek in Northwestern California. *Water Resources Research* **26**(7), 1657-1667.

Yue S, Pilon P, Phinney B, Cavadias G (2002) The influence of autocorrelation on the ability to detect trend in hydrological series. *Hydrological Processes* **16**, 1807-1829. doi: 10.1002/hyp.1095

Zégre, N, Skaugset, AE, Som, NA, McDonnell, JJ, Ganio, LM (2010) In lieu of the paired catchment approach: Hydrologic model change detection at the catchment scale. *Water Resources Research*, **46**(11). doi: 10.1029/2009WR008601

Zhao, F, Zhang, L, Xu, Z, Scott, DF (2010) Evaluation of methods for estimating the effects of vegetation change and climate variability on streamflow. *Water Resources Research*, **46**(3). doi: 10.1029/2009WR007702